TMDs at Small x

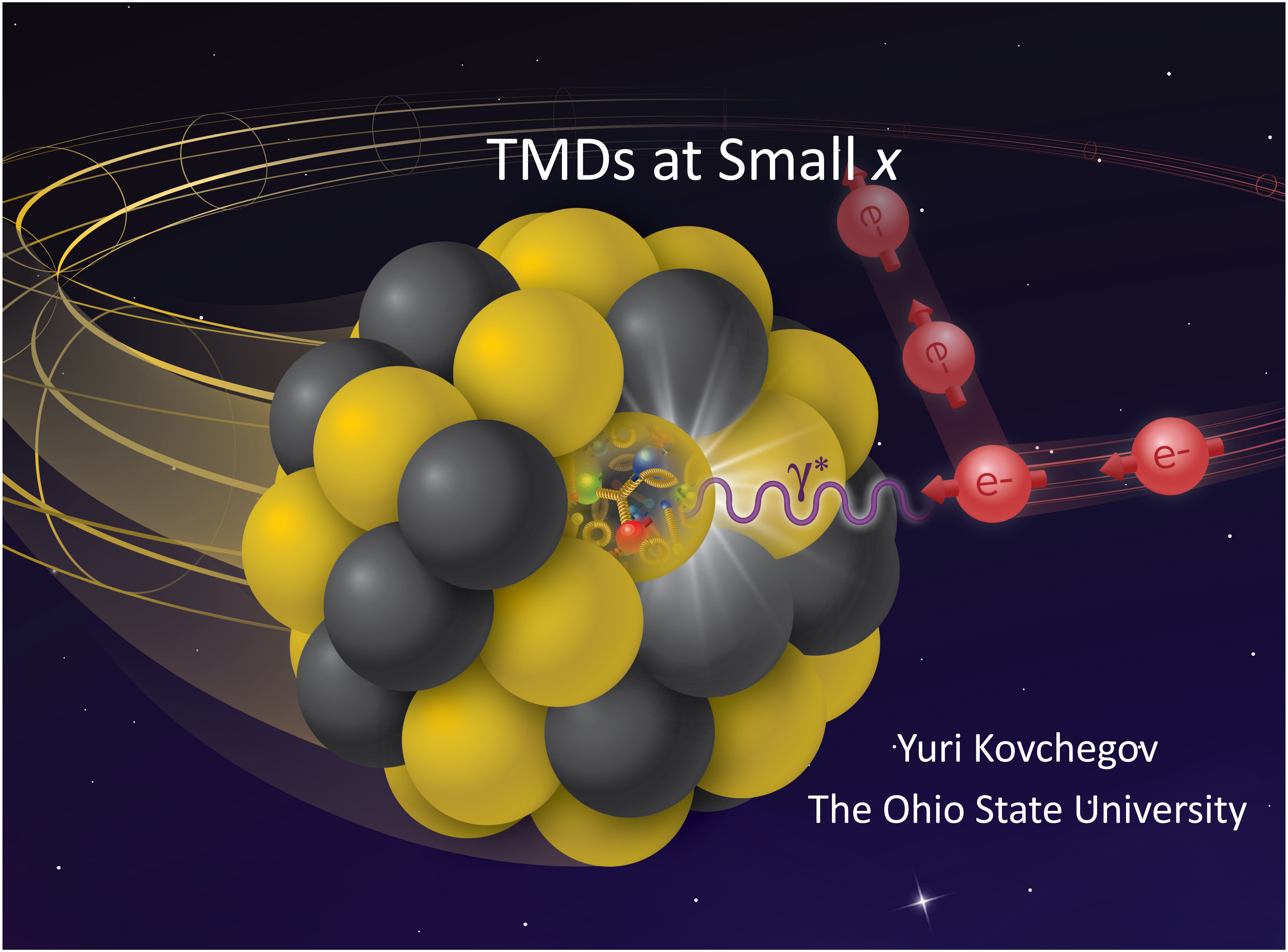

Yuri Kovchegov

The Ohio State University

Outline

- Classical small-*x* physics:
  - DIS in the dipole picture, Glauber-Gribov-Mueller formula
  - Black disk limit, parton saturation, saturation scale
  - McLerran-Venugopalan model, saturation scale for a nucleus, WW gluon TMD
- Nonlinear small-*x* evolution:
  - Non-linear BK and JIMWLK evolution equations
  - Solution of BK and JIMWLK equations, unitarity, energy dependence of the saturation scale, geometric scaling
  - Map of high-energy QCD
- TMDs at small *x*:
  - Eikonal TMDs: Unpolarized TMDs, the Sivers function
  - Sub-eikonal TMDs: quark and gluon helicity
  - Sub-sub-eikonal TMDs: transversity
- Conclusions

General Concepts

Running of QCD Coupling Constant

- QCD coupling constant $\alpha_s = \frac{g^2}{4\pi}$ changes with the momentum scale involved in the interaction

$$\alpha_s = \alpha_s(Q)$$

Asymptotic Freedom!

Gross and Wilczek, Politzer, ca '73

Physics Nobel Prize 2004!

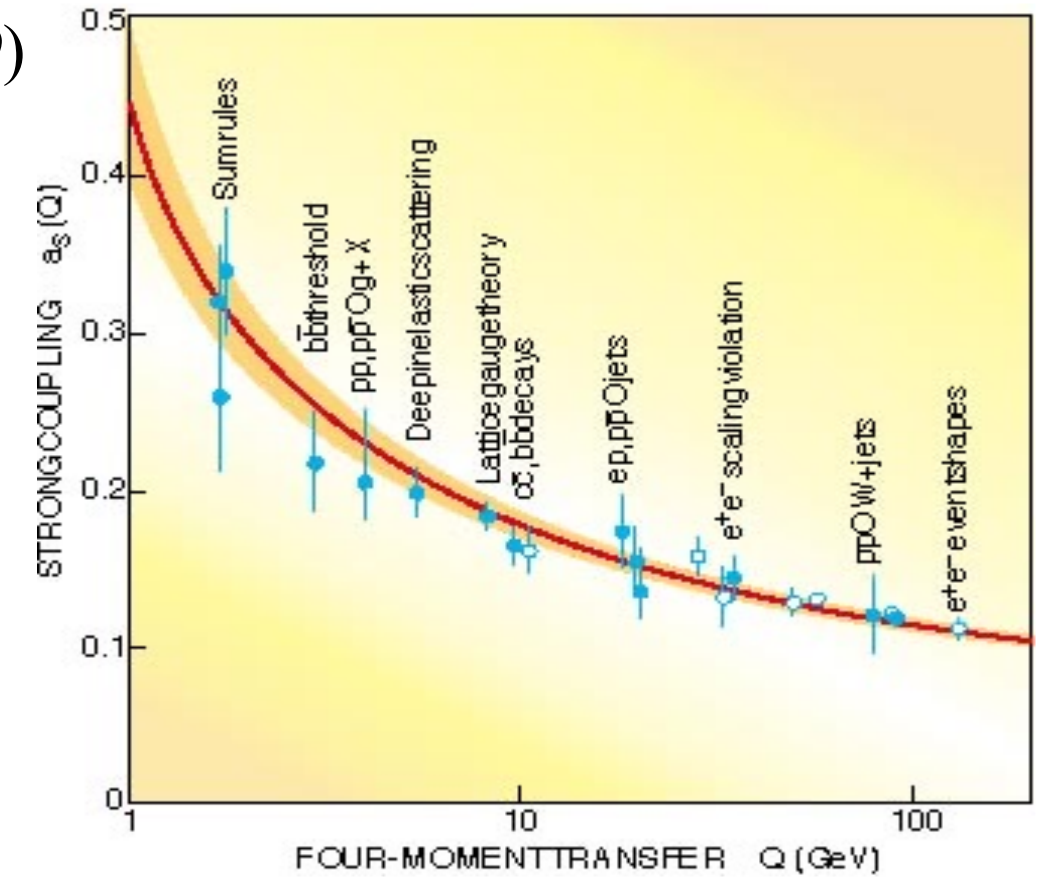

For short distances x < 0.2 fm, or, equivalently, large momenta k > 1 GeV the QCD coupling is small $\alpha_s << 1$ and interactions are weak.

What sets the scale of running QCD coupling in high energy collisions?

- "Optimist": $$\alpha_S = \alpha_S\left(\sqrt{s}\right) << 1$$
- Pessimist: $\alpha_S = \alpha_S\left(\Lambda_{QCD}\right) \sim 1$ we simply can not tackle high energy scattering in QCD.
- pQCD: only study high-p_T particles such that
$$\alpha_S = \alpha_S\left(p_T\right) << 1$$

But: what about total cross section? bulk of particles?

What sets the scale of running QCD coupling in high energy collisions?

- Saturation physics is based on the existence of a large internal momentum scale Q_S which grows with both energy s and nuclear atomic number A

$$Q_S^2 \sim A^{1/3} \, s^{\lambda}$$

such that $\alpha_S = \alpha_S(Q_S) << 1$

and we can calculate total cross sections, particle spectra and multiplicities, etc, from first principles.

The main principle

- Saturation physics is based on the existence of a large internal transverse momentum scale Q_S which grows with both decreasing Bjorken *x* and with increasing nuclear atomic number A

$$Q_s^2 \sim A^{1/3} \left(\frac{1}{x}\right)^{\lambda}$$

such that

$$\alpha_S = \alpha_S(Q_S) << 1$$

and we can use perturbation theory to calculate total cross sections, particle spectra and multiplicities, correlations, etc, from first principles.

Quasi-classical approximation

A. Glauber-Mueller Rescatterings

Kinematics of DIS

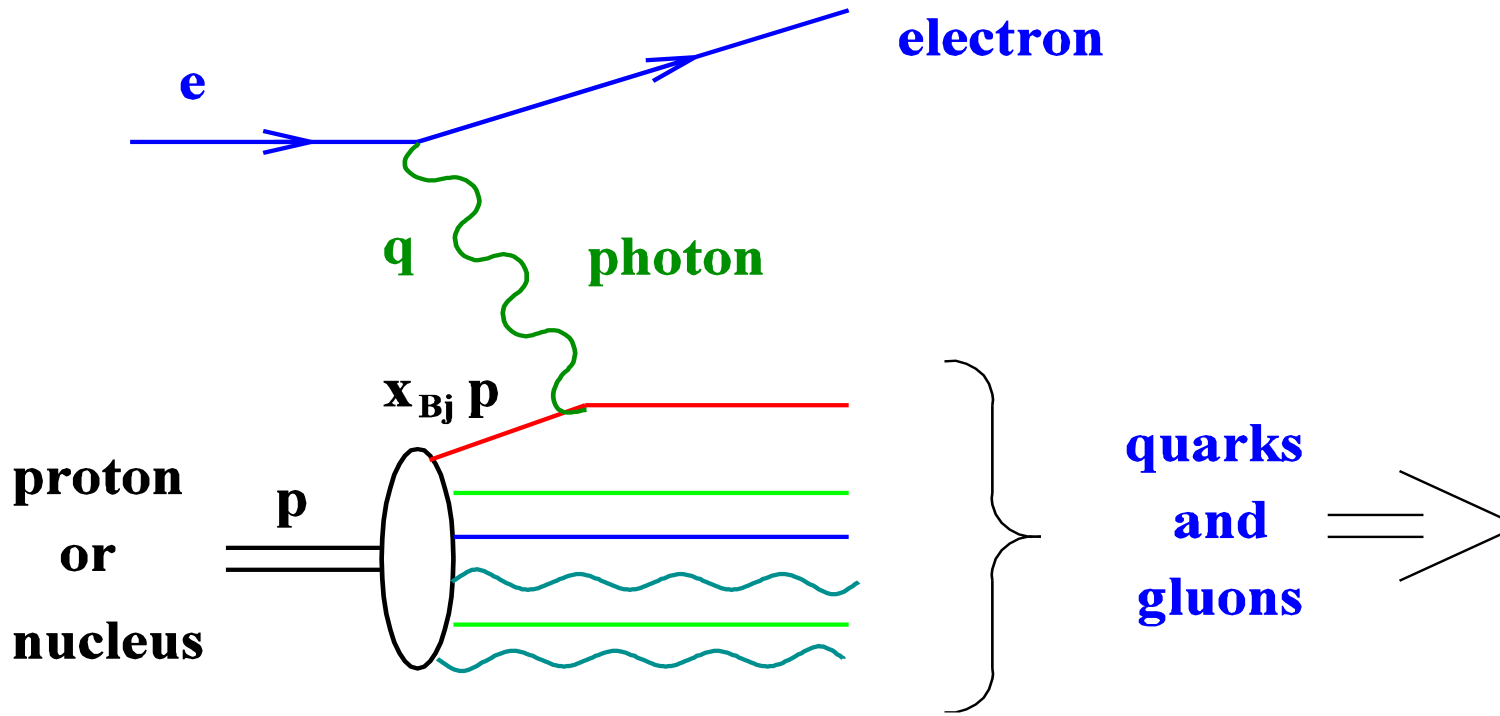

➢ Photon carries 4-momentum q_μ , its virtuality is

$$Q^2 = -q_\mu \, q^\mu$$

➢ Photon hits a quark in the proton carrying momentum $x_{Bj} p$ with p being the proton's momentum. Parameter x_{Bj} is the Bjorken *x* variable.

Dipole picture of DIS

- At small x, the dominant contribution to DIS structure functions does not come from the handbag diagram.

- Instead, the dominant terms comes from the dipole picture of DIS, where the virtual photon splits into a quark-antiquark pair, which then interacts with the target.

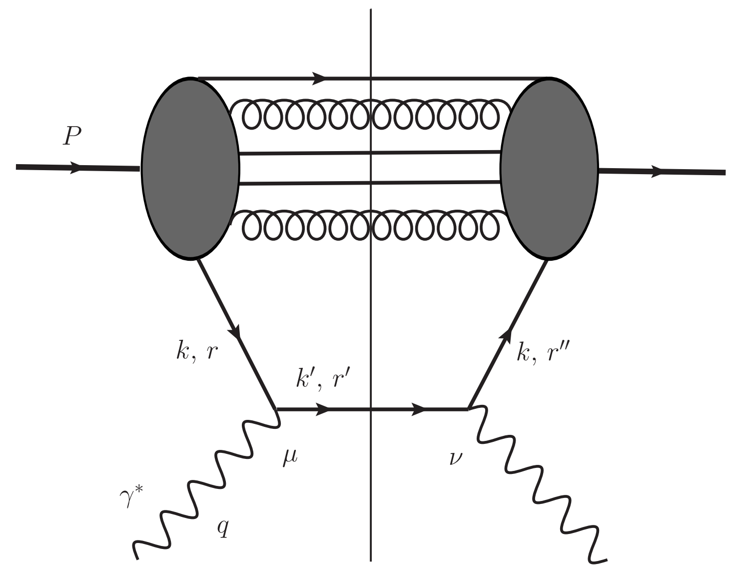

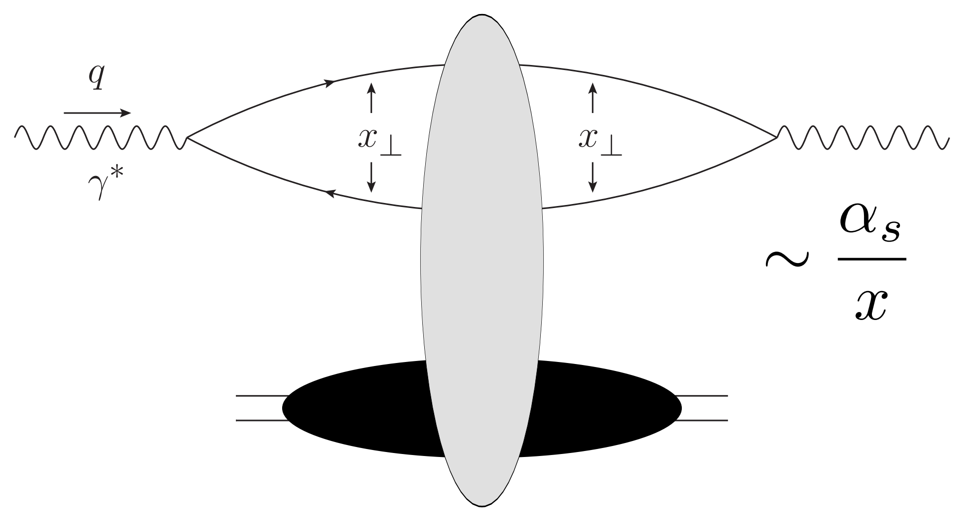

Dipole Amplitude

- The total DIS cross section is expressed in terms of the (Im part of the) forward quark dipole amplitude N:

$$\sigma_{tot}^{\gamma^* A} = \int \frac{d^2 x_\perp}{2\,\pi}\, d^2 b_\perp \int\limits_0^1 \frac{dz}{z\,(1-z)}\, |\Psi^{\gamma^* \to q\bar{q}}(\vec{x}_\perp, z)|^2\; N(\vec{x}_\perp, \vec{b}_\perp, Y)$$

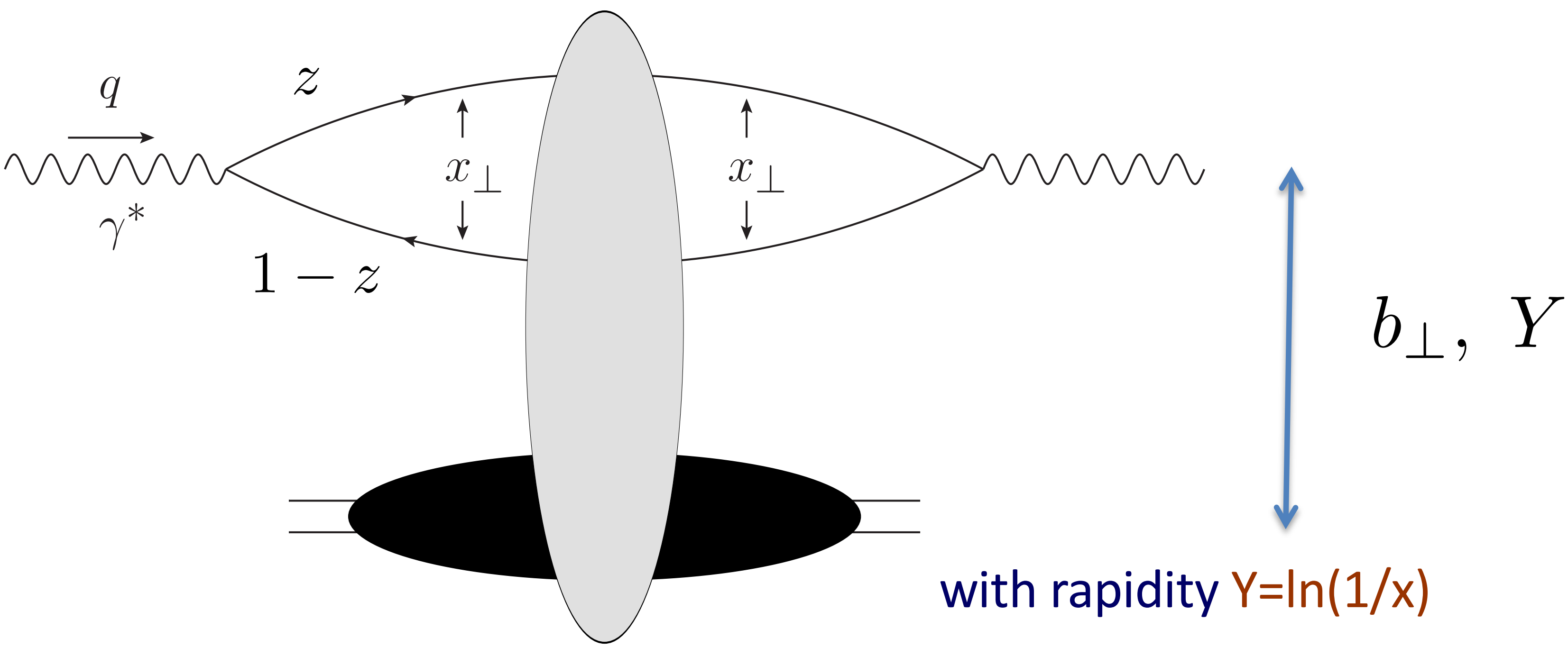

with rapidity Y=ln(1/x)

DIS in the Classical Approximation

The DIS process in the rest frame of the target nucleus is shown below.

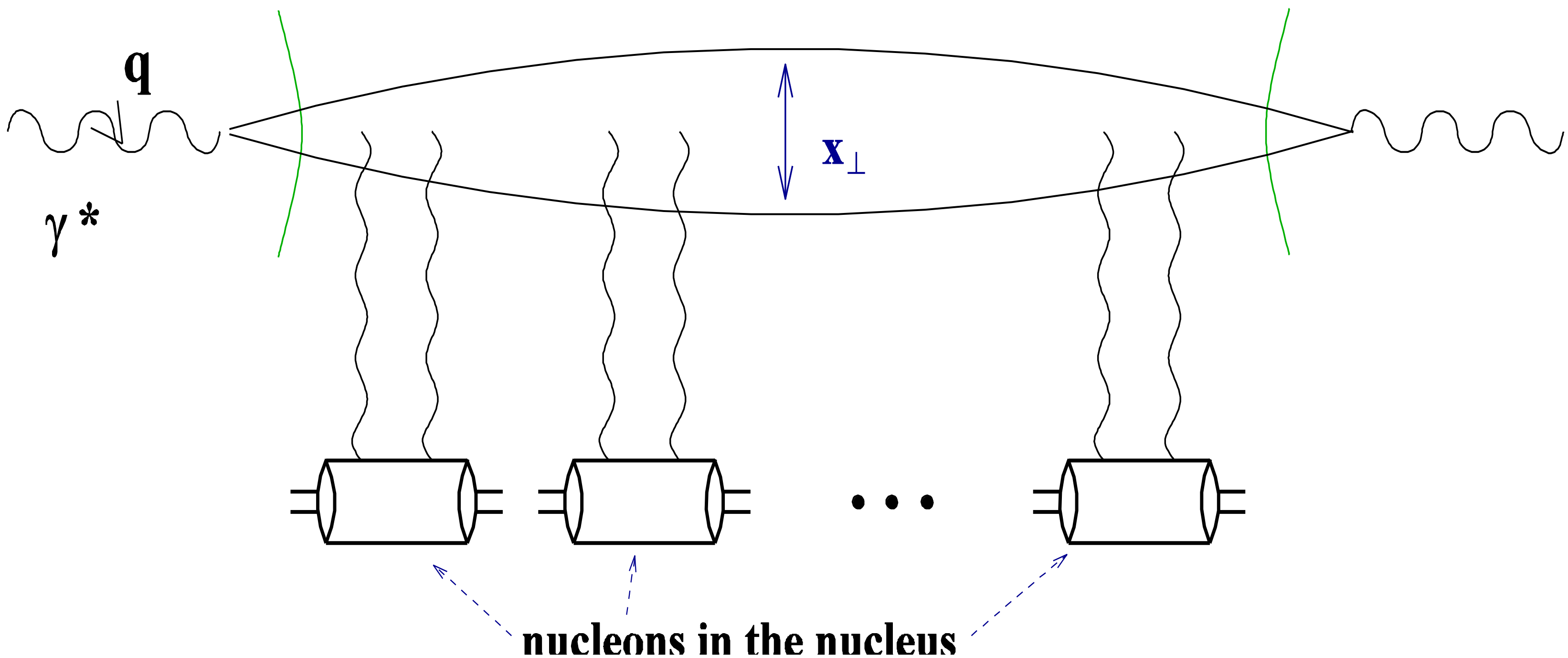

$$\sigma_{tot}^{\gamma * A}(x_{Bj}, Q^2) = |\Psi^{\gamma * \to q\bar{q}}|^2 \otimes N(x_\perp, Y = \ln 1/x_{Bj})$$

with rapidity Y=ln(1/x)

Dipole Amplitude

- The quark dipole amplitude is defined by

$$N(\underline{x}_1, \underline{x}_2) = 1 - \frac{1}{N_c} \left\langle \text{tr} \left[V(\underline{x}_1) \, V^\dagger(\underline{x}_2) \right] \right\rangle$$

- Here we use the Wilson lines along the light-cone direction

$$V(\underline{x}) = \text{P} \exp \left[i \, g \int\limits_{-\infty}^{\infty} dx^+ \, A^-(x^+, x^- = 0, \underline{x}) \right]$$

- In the classical Glauber-Mueller/McLerran-Venugopalan approach the dipole amplitude resums multiple rescatterings:

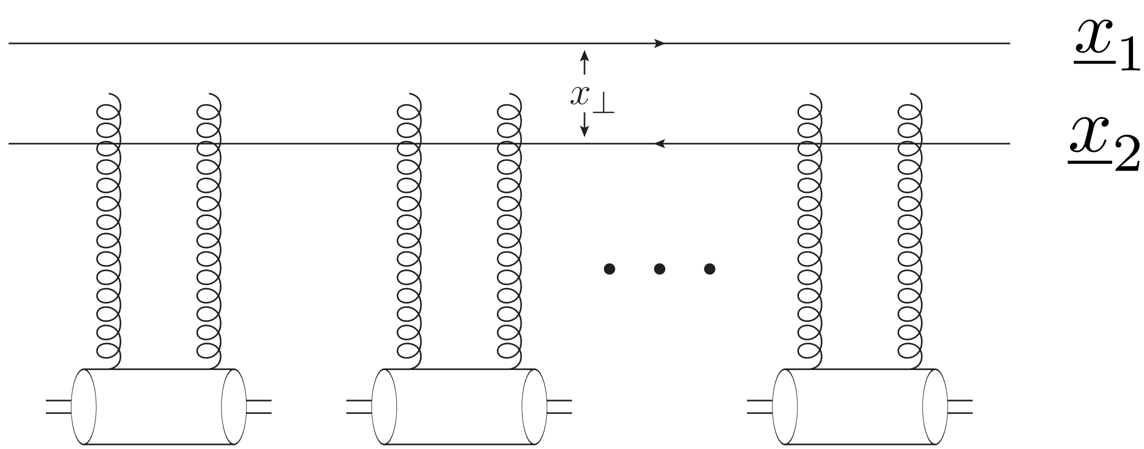

Quasi-classical dipole amplitude

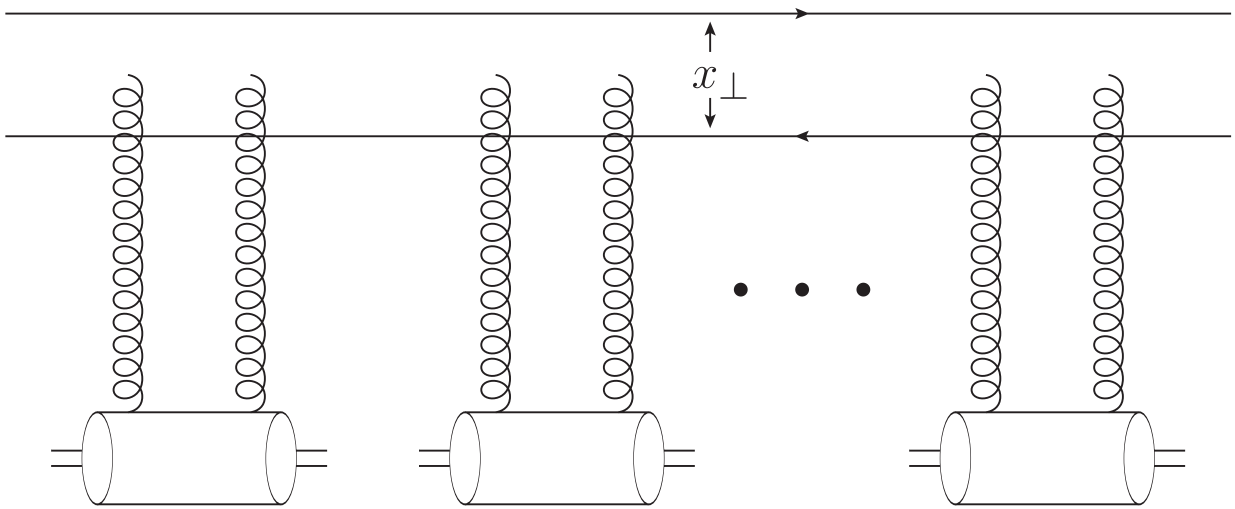

A.H. Mueller, ‘90

Lowest-order interaction with each nucleon – two gluon exchange – lead to the following resummation parameter:

$$\alpha_s^2\, A^{1/3}$$

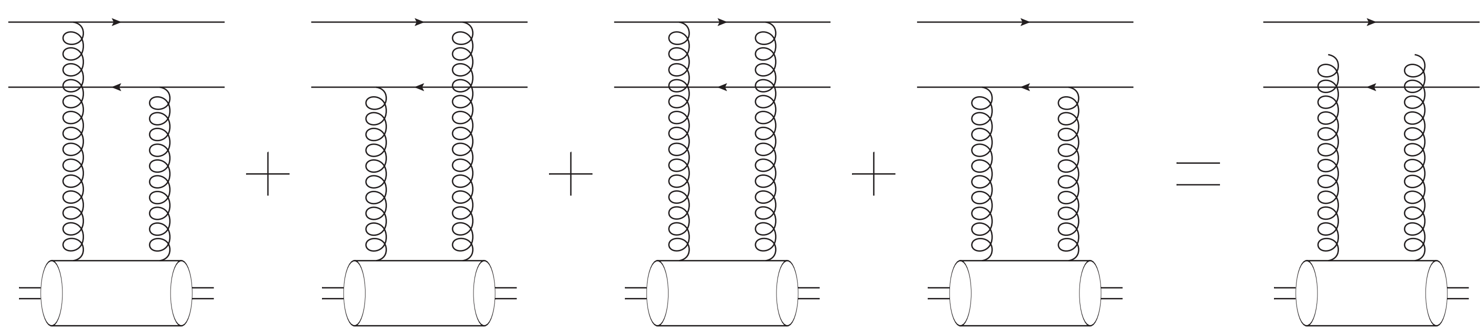

Quasi-classical dipole amplitude

- To resum multiple rescatterings, note that the nucleons are independent of each other and rescatterings on the nucleons are also independent.

- One then writes an equation (Mueller '90)

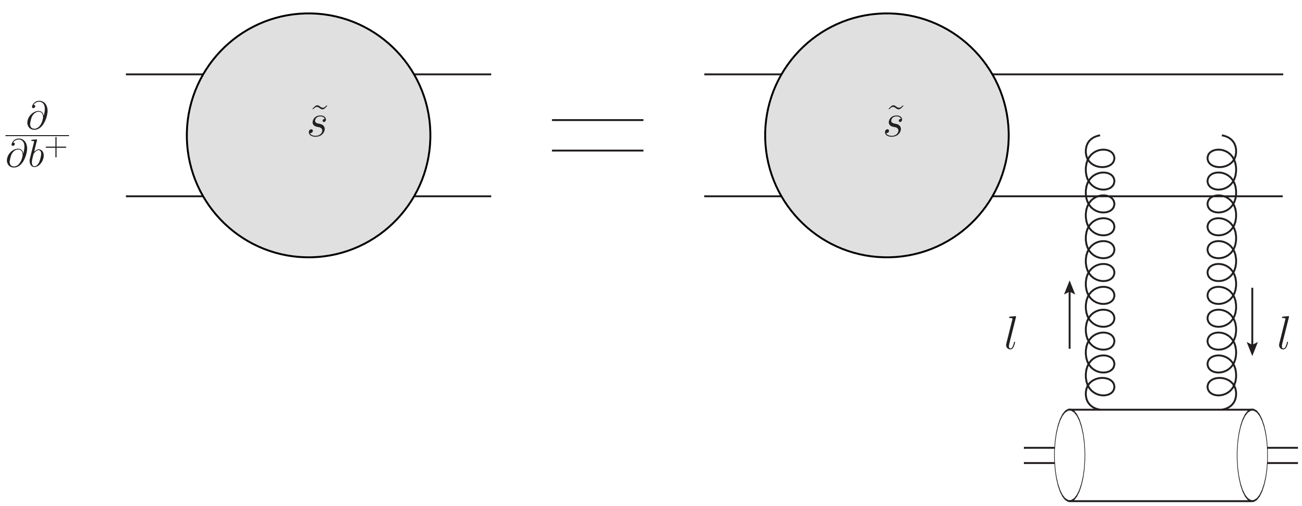

Each scattering!

$$N(x_\perp, Y) = 1 - \exp\left[-\frac{x_\perp^2 Q_s^2}{4} \ln \frac{1}{x_\perp \Lambda}\right]$$

DIS in the Classical Approximation

The dipole-nucleus amplitude in the classical approximation is

$$\sigma^{q\bar{q}A} = 2 \int d^2b\, N(x_\perp, b_\perp, Y)$$

$$N(x_\perp, Y) = 1 - \exp\left[-\frac{x_\perp^2 Q_s^2}{4} \ln \frac{1}{x_\perp \Lambda}\right]$$

A.H. Mueller, '90

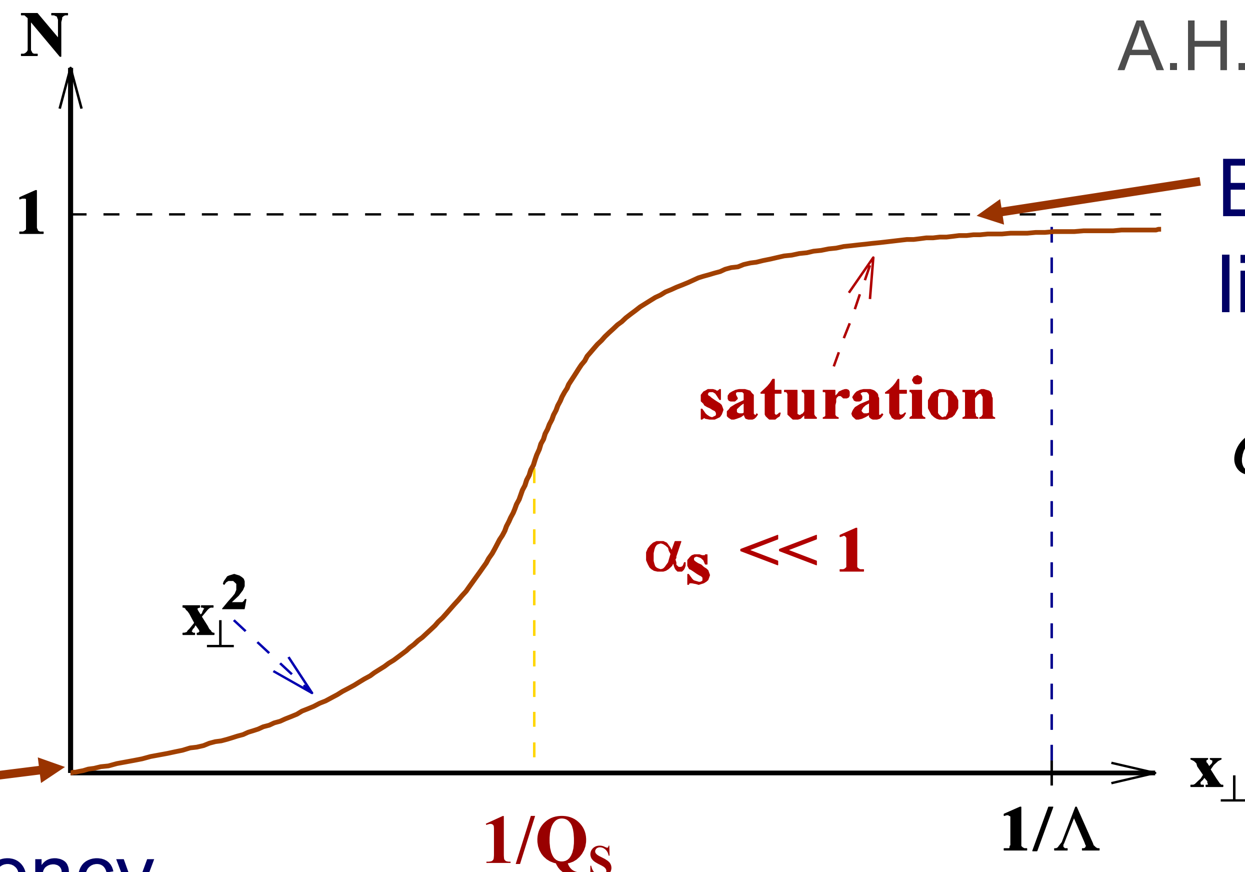

Black disk limit,

$$\sigma_{tot} < 2\pi R^2$$

Color transparency

$Q_S^2 \sim A^{1/3}$

B. McLerran-Venugopalan Model

Gluons at Small-x

- There is a large number of small-x gluons (and quarks) in a proton:

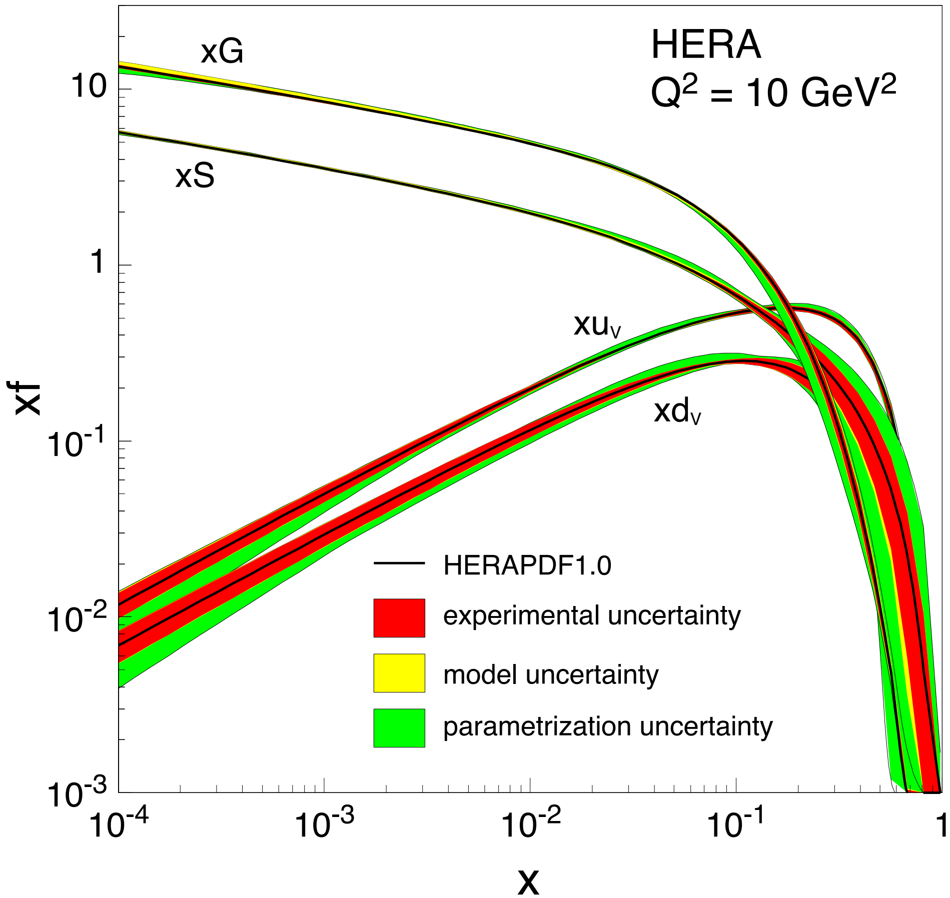

- $G(x, Q^2)$, $q(x, Q^2)$ = gluon and quark number densities (q=u,d, or S for sea).

McLerran-Venugopalan Model

- The wave function of a single nucleus has many small-x quarks and gluons in it.
- In the transverse plane the nucleus is densely packed with gluons and quarks.

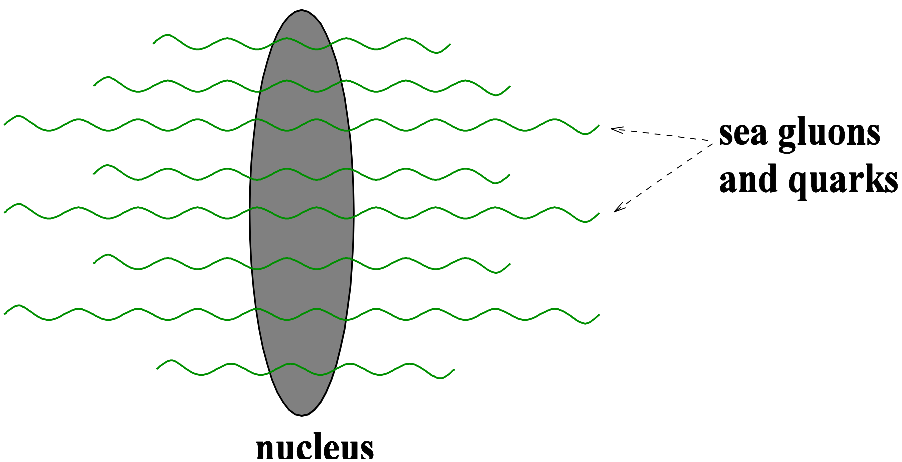

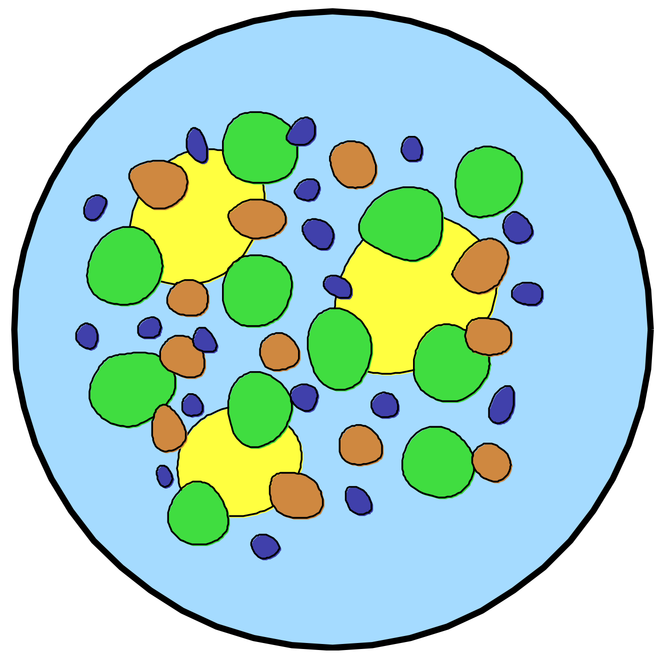

Large occupation number ⇨ Classical Field

McLerran-Venugopalan Model

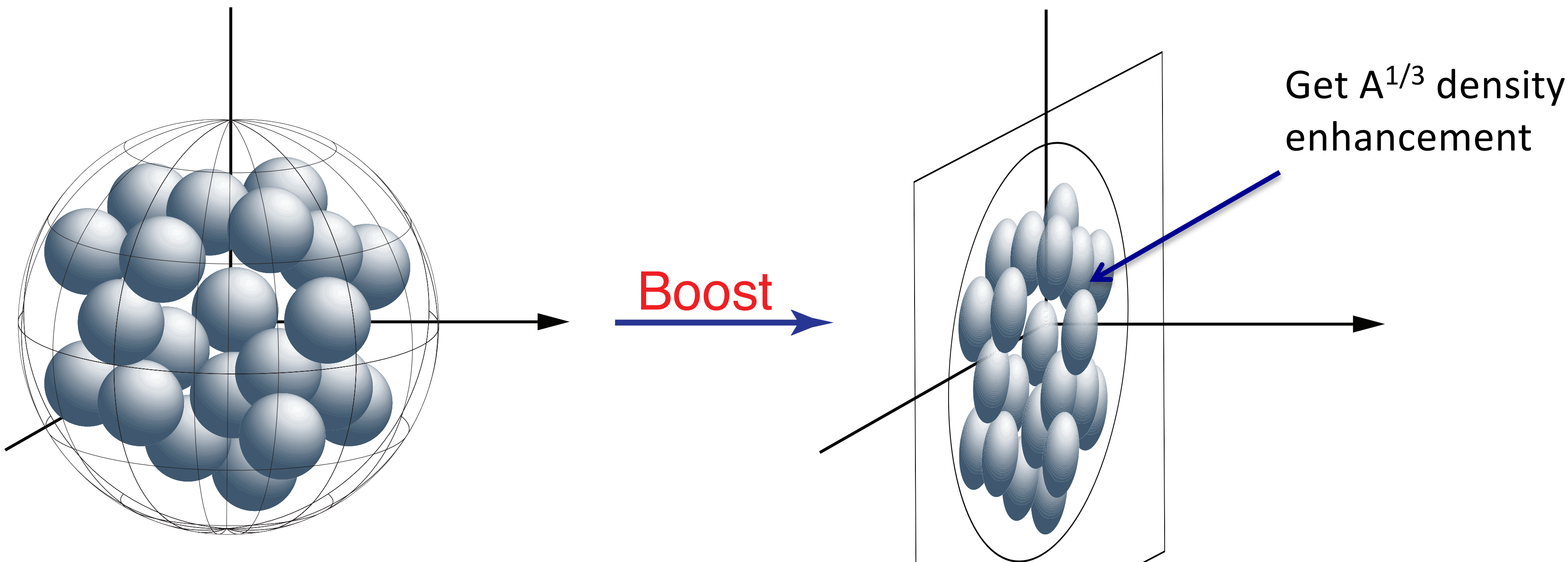

$$M = \rho V = \rho \frac{4}{3}\pi R^3 \sim A \quad \Rightarrow \quad R \sim A^{1/3}$$

$$Q_S^2 \sim A^{1/3}$$

- Large gluon density gives a large momentum scale Q_s (the saturation scale): Q_s^2 ~ # gluons per unit transverse area ~ $A^{1/3}$ (nuclear oomph).
- For Q_s >> Λ_{QCD}, get a theory at weak coupling $\alpha_s(Q_s^2) \ll 1$ and the leading gluon field is <u>classical</u>.

Color Charge Density

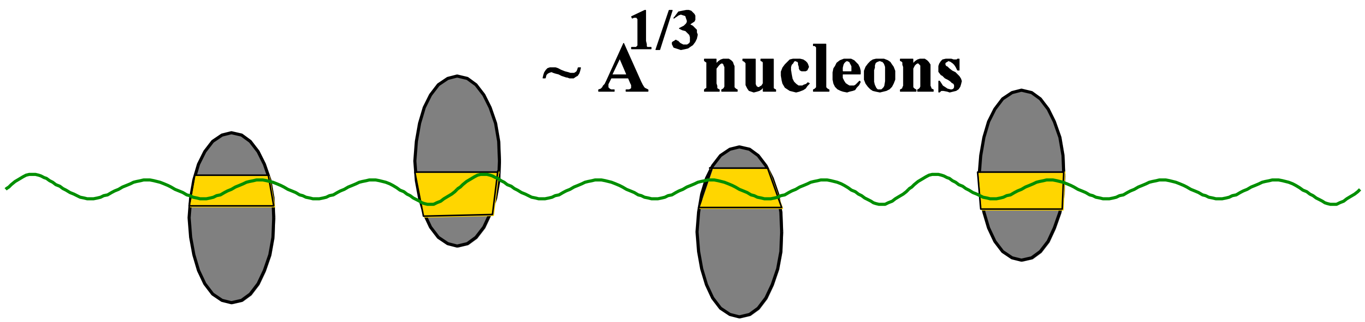

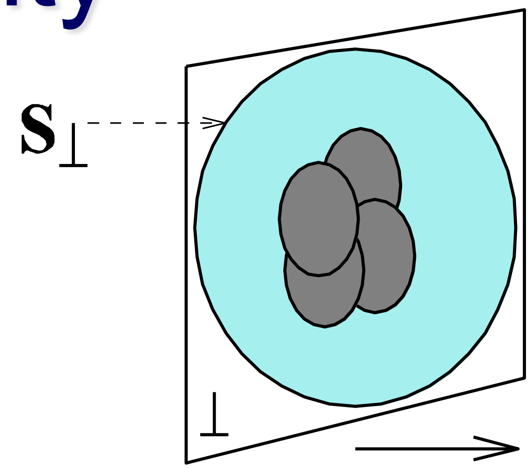

Small-x gluon "sees" the whole nucleus coherently in the longitudinal direction! It "sees" many color charges which form a net effective color charge Q = g (# charges)$^{1/2}$, such that $Q^2 = g^2$ #charges (random walk).

Define color charge density

$$\mu^2 = \frac{Q^2}{S_\perp} = \frac{g^2\ \#\,charges}{S_\perp} \propto g^2\,\frac{A}{S_\perp} \propto A^{1/3}$$

McLerran Venugopalan '93-'94

such that for a large nucleus (A>>1)

$$\mu^2 \propto \Lambda_{QCD}^2\, A^{1/3} \gg \Lambda_{QCD}^2 \quad \Longrightarrow \quad \alpha_s(\mu^2) \ll 1$$

Nuclear small-x wave function is perturbative! $\mu = Q_s$

Saturation Scale

To argue that $Q_s^2 \sim A^{1/3}$ let us consider an example of a particle scattering on a nucleus. As it travels through the nucleus it bumps into nucleons. Along a straight line trajectory it encounters $\sim R \sim A^{1/3}$ nucleons, with R the nuclear radius and A the atomic number of the nucleus.

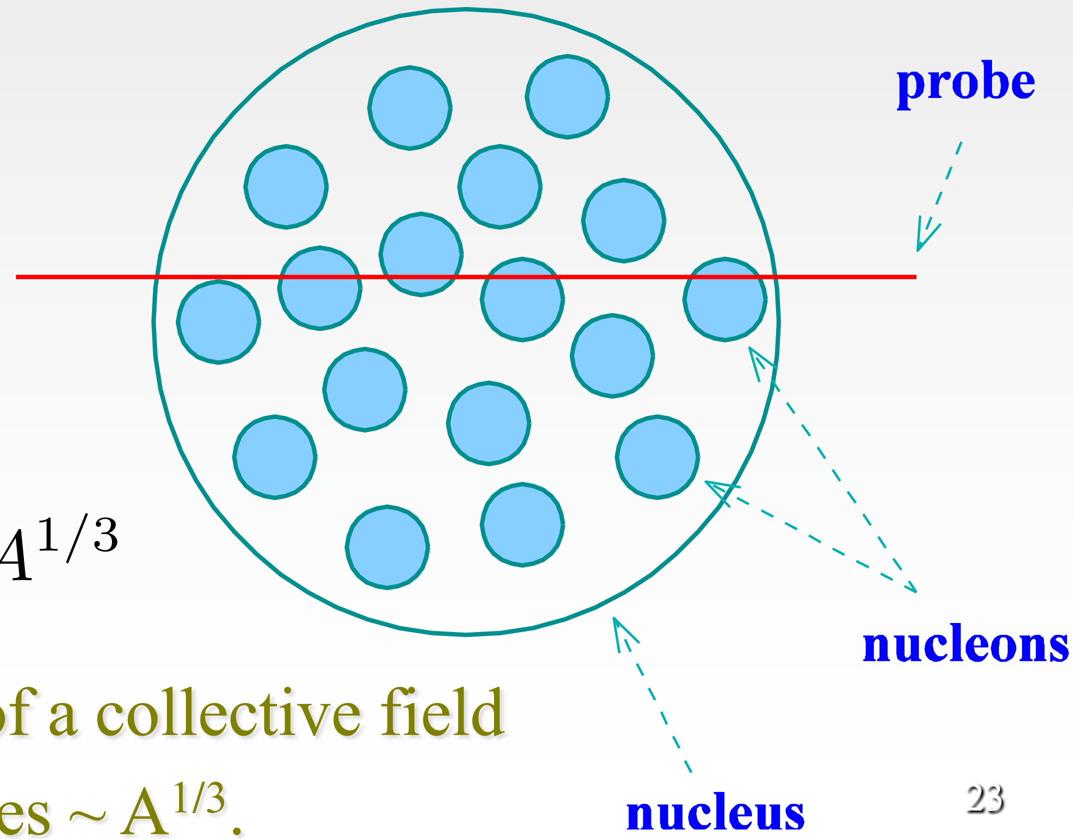

The particle receives $\sim A^{1/3}$ random kicks. Its momentum gets broadened by

$$\Delta k \sim \sqrt{A^{1/3}} \Rightarrow (\Delta k)^2 \sim A^{1/3}$$

Saturation scale, as a feature of a collective field of the whole nucleus also scales $\sim A^{1/3}$.

McLerran-Venugopalan Model

- To find the classical gluon field A_μ of the nucleus one has to solve the non-linear analogue of Maxwell equations – the Yang-Mills equations, with the nucleus as a source of the color charge:

$$\mathcal{D}_\nu F^{\mu\nu} = J^\mu$$

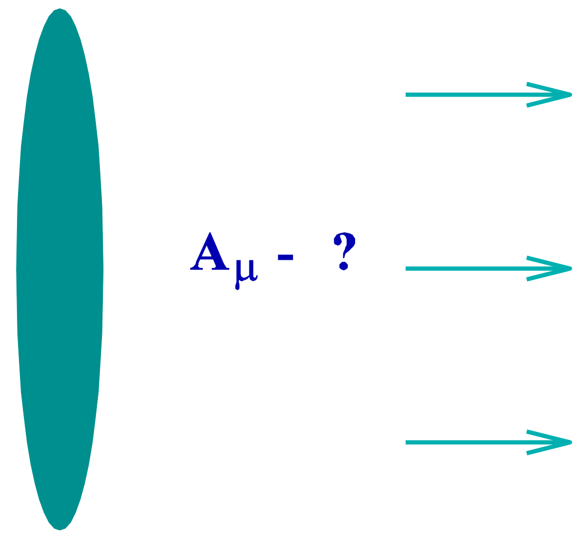

nucleus is Lorentz contacted into a pancake

Yu. K. ’96; J. Jalilian-Marian et al, ‘96

Classical Field of a Nucleus

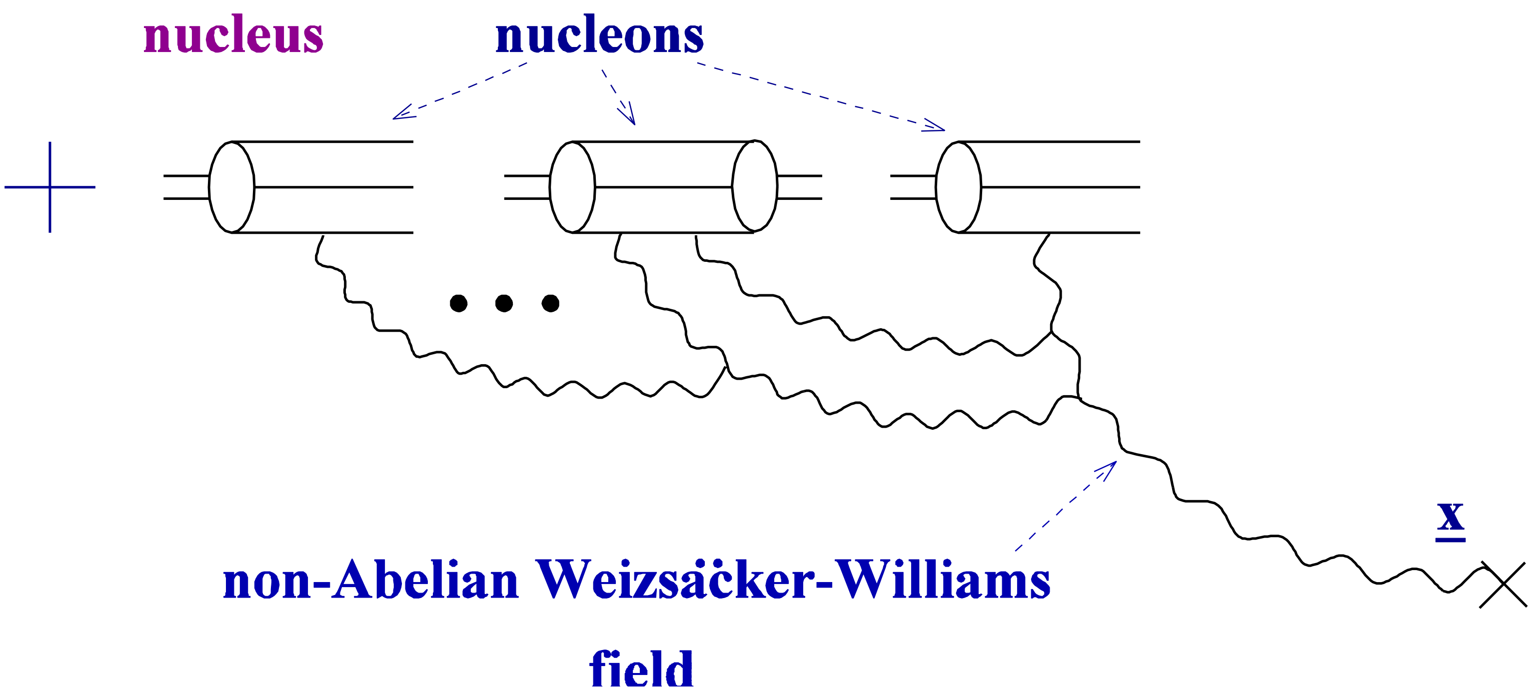

Here's one of the diagrams showing the non-Abelian gluon field of a large nucleus.

The resummation parameter is $\alpha_S{}^2 A^{1/3}$, corresponding to two gluons per nucleon approximation.

Unpolarized WW Gluon TMD

- One can calculate the unpolarized gluon TMD with, say, the forward-pointing (SIDIS) Wilson line staple

$$f^G(x, k_T^2) = \frac{2}{xP^+(2\pi)^3} \int dx^- d^2 x_\perp \, e^{ixP^+ x^- - i\vec{k}_T \cdot \vec{x}_\perp} \left\langle P \middle| \mathrm{tr}\left[F^{+i}(0)\, \mathcal{U}^{[+]}[0,x]\, F^{+i}(x^-, \vec{x}_\perp) \right] \middle| P \right\rangle$$

- In A^+=0 gauge, one can choose a sub-gauge eliminating the Wilson line staple (making it 1), and, since $F^{+i} = \partial_- A^i$, one obtains

$$f^G(x, k_T^2) = \frac{2xP^+}{(2\pi)^3} \int dx^- d^2 x_\perp \, e^{ixP^+ x^- - i\vec{k}_T \cdot \vec{x}_\perp} \left\langle P \middle| \mathrm{tr}\left[A^i(0)\, A^i(x^-, \vec{x}_\perp) \right] \middle| P \right\rangle$$

- Since the classical (Weizsacker-Williams) A^i field is known exactly from solving the Yang-Mills equations, one can directly calculate the gluon TMD in the classical limit.
- This is the WW gluon TMD.

Classical Gluon Field of a Nucleus

Using the obtained classical gluon field one can construct corresponding gluon distribution function (gluon WW TMD):

$$\phi_A(x, k^2) \sim \left\langle \underline{A}(-k) \cdot \underline{A}(k) \right\rangle$$

with the field in the $A^+=0$ gauge

$$\phi(x, k_T^2) = x\,\pi\, f^G(x, k_T^2)$$

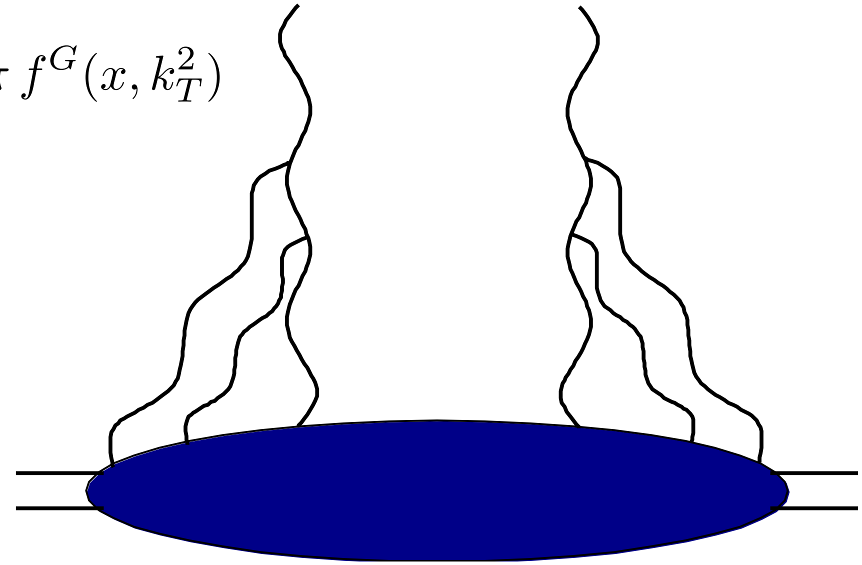

$$\phi_A(x, k_T^2) = \frac{C_F}{\alpha_s\,\pi} \int \frac{d^2 x_\perp}{x_\perp^2}\, e^{i\,\underline{k}\cdot\underline{x}} \left[1 - \exp\left(-\frac{x_\perp^2\, Q_s^2}{4} \ln \frac{1}{x_\perp\,\Lambda}\right)\right]$$

J. Jalilian-Marian et al, ' 97; Yu. K. and A. Mueller, '98

⇨ $Q_S=\mu$ is the saturation scale $\quad Q_S^2 \sim A^{1/3}$

⇨ Note that $\phi \sim \langle A_\mu A_\mu \rangle \sim 1/\alpha$ such that $A_\mu \sim 1/g$, which is what one would expect for a classical field.

$$\phi_A(x,k_T^2) = \frac{C_F}{\alpha_s\,\pi}\int \frac{d^2x_\perp}{x_\perp^2}\, e^{i\,\underline{k}\cdot\underline{x}}\left[1-\exp\left(-\frac{x_\perp^2\,Q_s^2}{4}\,\ln\frac{1}{x_\perp\,\Lambda}\right)\right]$$

⇨ In the UV limit of k→∞,

x_T is small and one obtains

$$\phi_A(x,k_T^2) \sim \int d^2x_\perp\, e^{i\,\underline{k}\cdot\underline{x}}\, Q_s^2\,\ln\frac{1}{x_\perp\,\Lambda} \;\propto\; \frac{Q_s^2}{k_T^2}$$

which is the usual LO result.

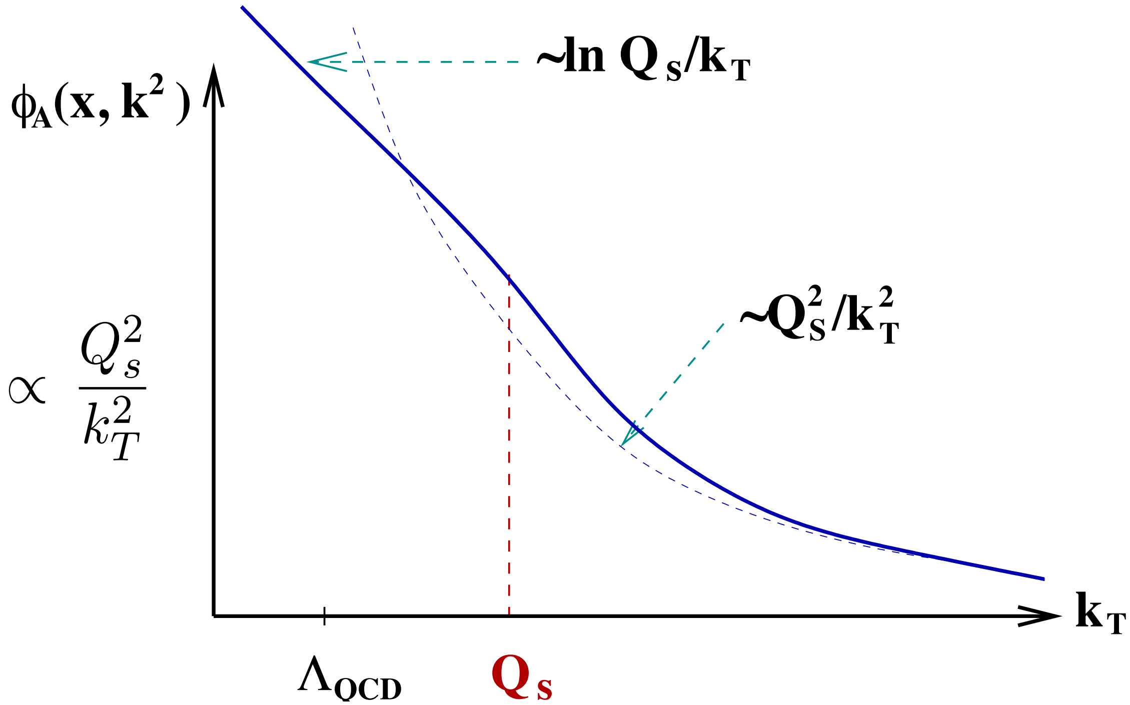

⇨ In the IR limit of small k_T,

x_T is large and we get

$$\phi_A(x,k_T^2) \approx \frac{C_F}{\alpha_s\,\pi}\int_{1/Q_s}\frac{d^2x_\perp}{x_\perp^2}\,e^{i\,\underline{k}\cdot\underline{x}} \;\propto\; \ln\frac{Q_s}{k_T}$$

SATURATION !

Divergence is regularized.

Classical Gluon Distribution

A good object to plot is the classical gluon TMD distribution multiplied by the phase space k_T:

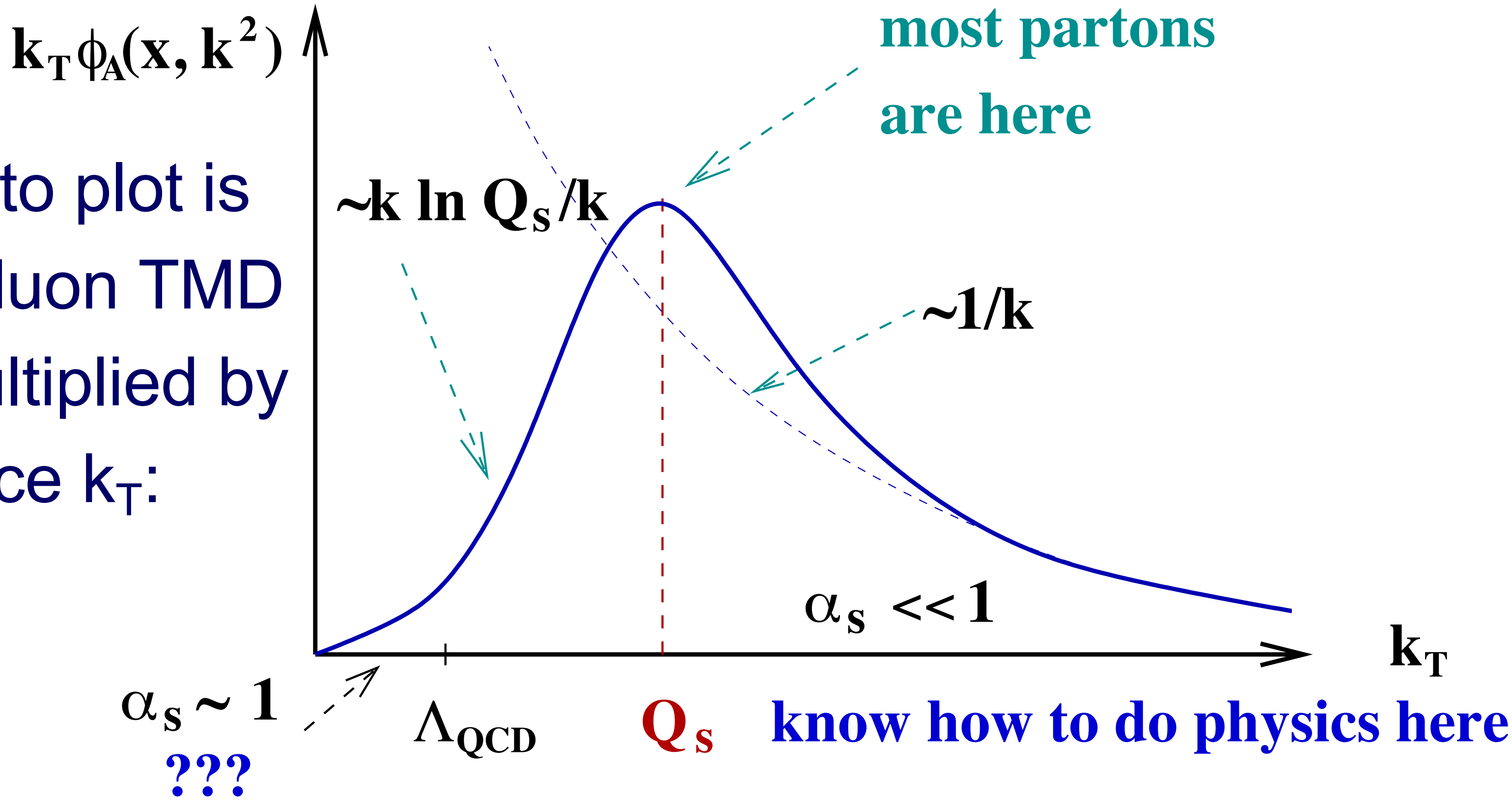

⇨ Most gluons in the nuclear wave function have transverse momentum of the order of $k_T \sim Q_S$ and $Q_S^2 \sim A^{1/3}$

⇨ We have a small coupling description of the whole wave function in the classical approximation.

Summary

- We applied the quasi-classical small-*x* approach to DIS in the dipole picture, obtaining Glauber-Mueller formula for multiple rescatterings of a dipole in a nucleus.
- We saw that onset of saturation ensures that unitarity (the black disk limit) is not violated. Saturation is a consequence of unitarity!
- We have reviewed the McLerran-Venugopalan model for the small-*x* wave function of a large nucleus.
- We saw the onset of gluon saturation and the appearance of a large transverse momentum scale – the saturation scale:

$$Q_s^2 \sim A^{1/3}$$

Small-x evolution equations

A. Birds-Eye View

Why Evolve?

- No energy or rapidity dependence in classical field and resulting cross sections.
- Energy/rapidity-dependence comes in via quantum corrections.
- Quantum corrections are included through "evolution equations".


BFKL Equation

Balitsky, Fadin, Kuraev, Lipatov '78


Start with N gluons in the proton's wave function. As we increase the energy a new gluon can be emitted by either one of the N gluons. The number of newly emitted particles is proportional to N.

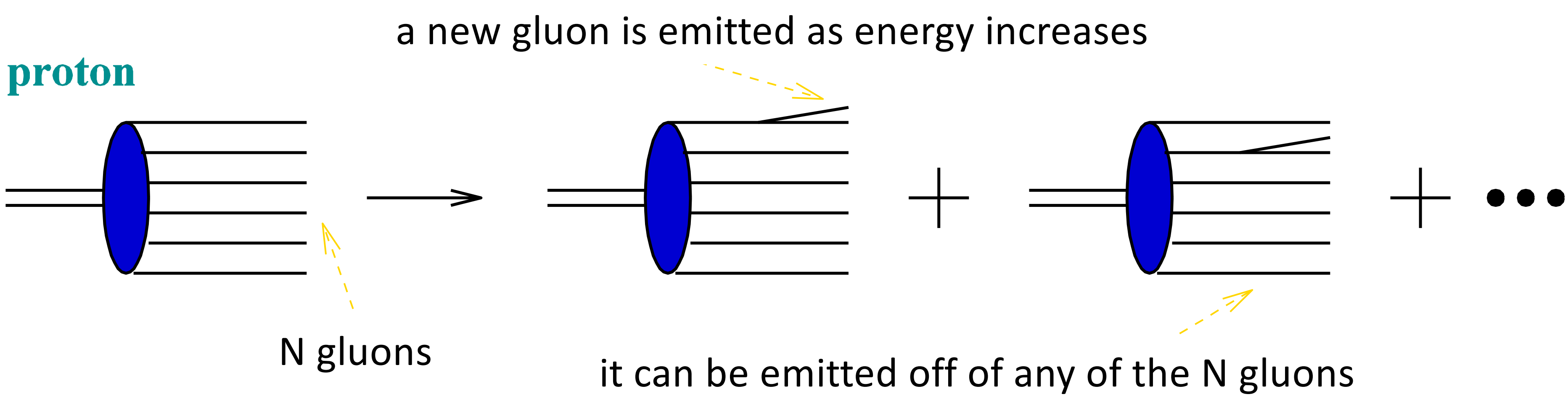

The BFKL equation for the number of gluons N reads:

$$\frac{\partial}{\partial \ln(1/x)} N(x,Q^2) = \alpha_S K_{BFKL} \otimes N(x,Q^2)$$

BFKL Equation as a High Density Machine

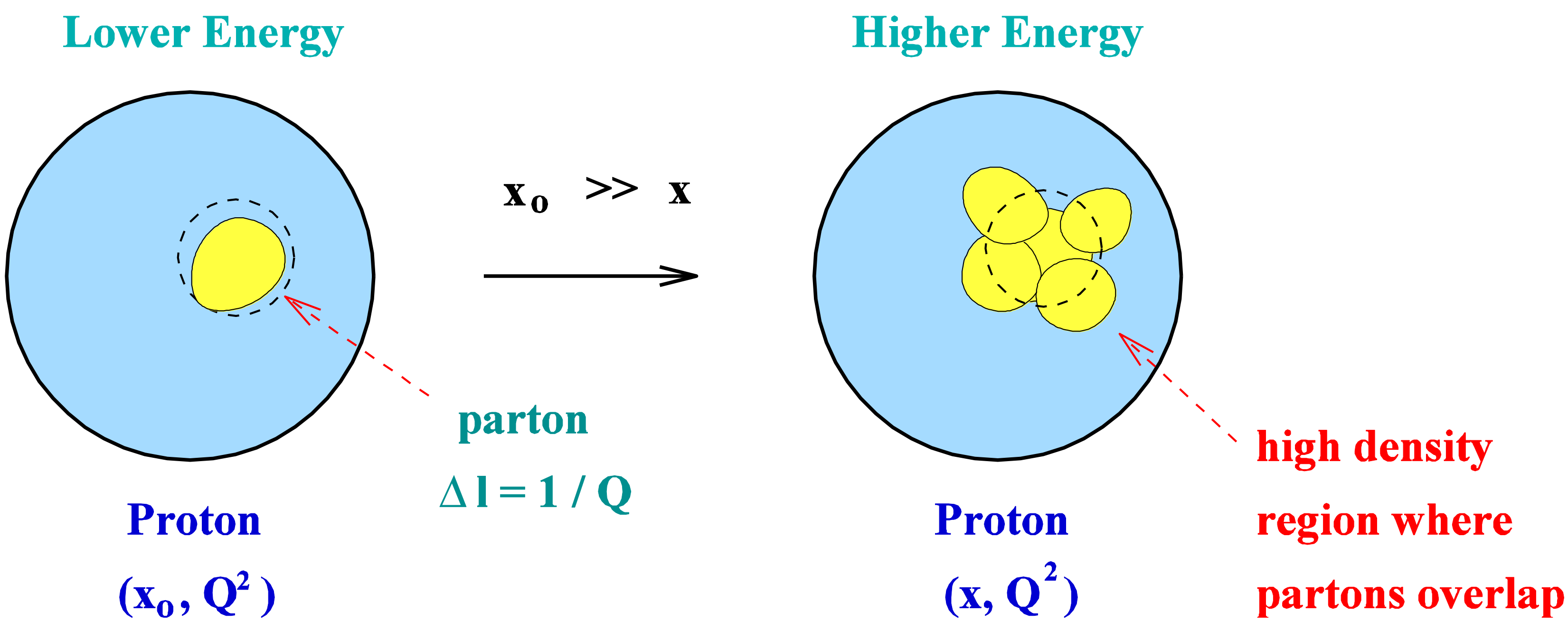

- As energy increases BFKL evolution produces more gluons, roughly of the same size. The gluons overlap each other creating areas of very high density.

- Number density of gluons, along with corresponding cross sections grows as a power of 1/x or, equivalently, of energy (s)

$$N \sim e^{\Delta \ln(1/x)} = \left(\frac{1}{x}\right)^{\Delta} \sim s^{\Delta}$$

BFKL Equation as a High Density Machine

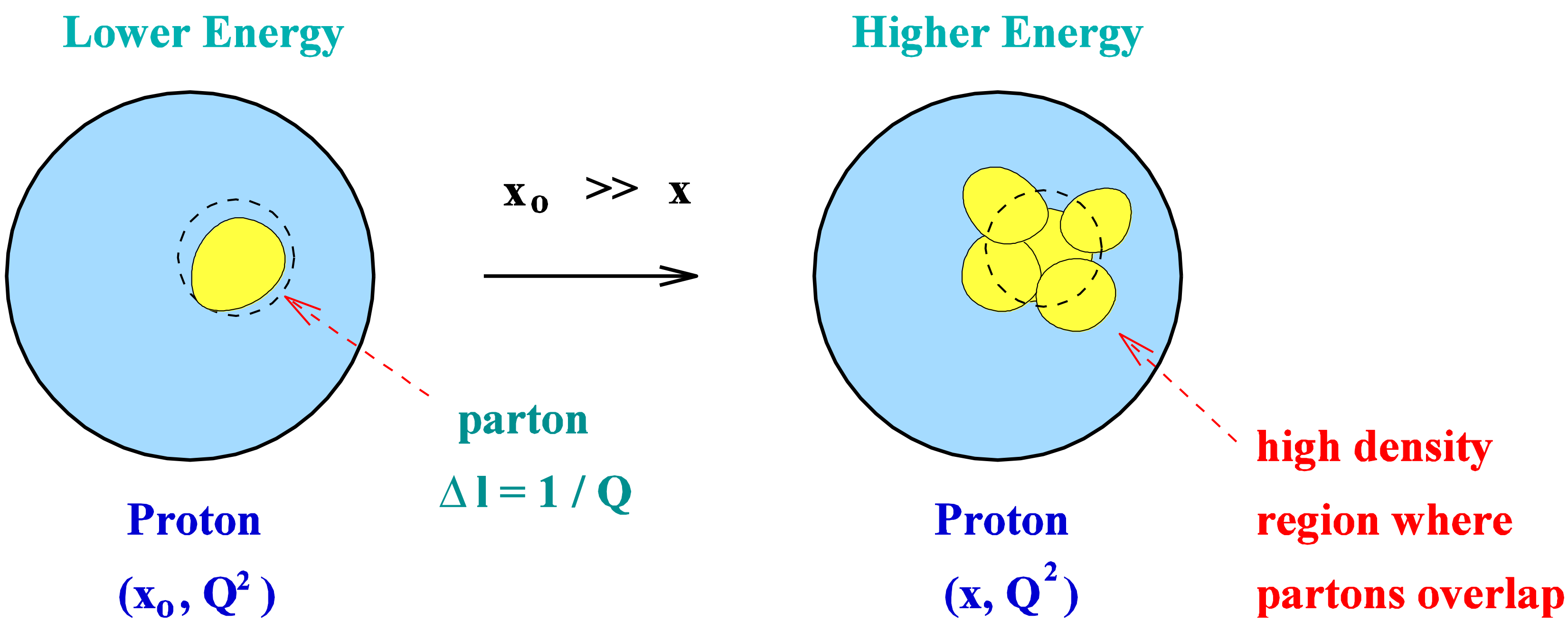

- But can parton densities rise forever? Can gluon fields be infinitely strong? Can the cross sections rise forever?
- No! There exists a black disk limit for cross sections, which we know from Quantum Mechanics: for high-energy scattering on a disk of radius R the total cross section is bounded by

$$\sigma_{tot} \leq 2\pi R^2$$

Nonlinear Equation

At very high energy gluon recombination becomes important. As energy (rapidity) increases, gluons not only split into more gluons, but also recombine. Recombination reduces the number of gluons in the wave function. Here Y~ln s~ln 1/x is rapidity, s is cms energy squared.

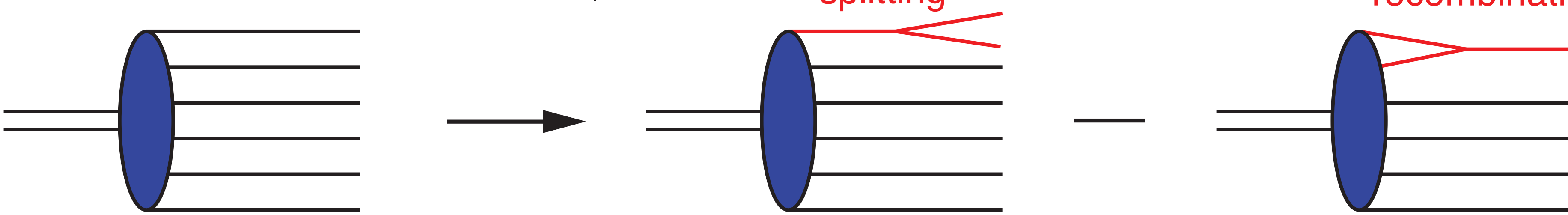

$$\frac{\partial}{\partial Y} N(x, k_T^2) = \alpha_s \, K_{BFKL} \otimes N(x, k_T^2) - \alpha_s \, [N(x, k_T^2)]^2$$

I. Balitsky '96, Yu. K. '99 (large N_c)

Number of gluon pairs ~ N^2

$$Y = \ln \frac{1}{x}$$

Nonlinear Equation: Saturation

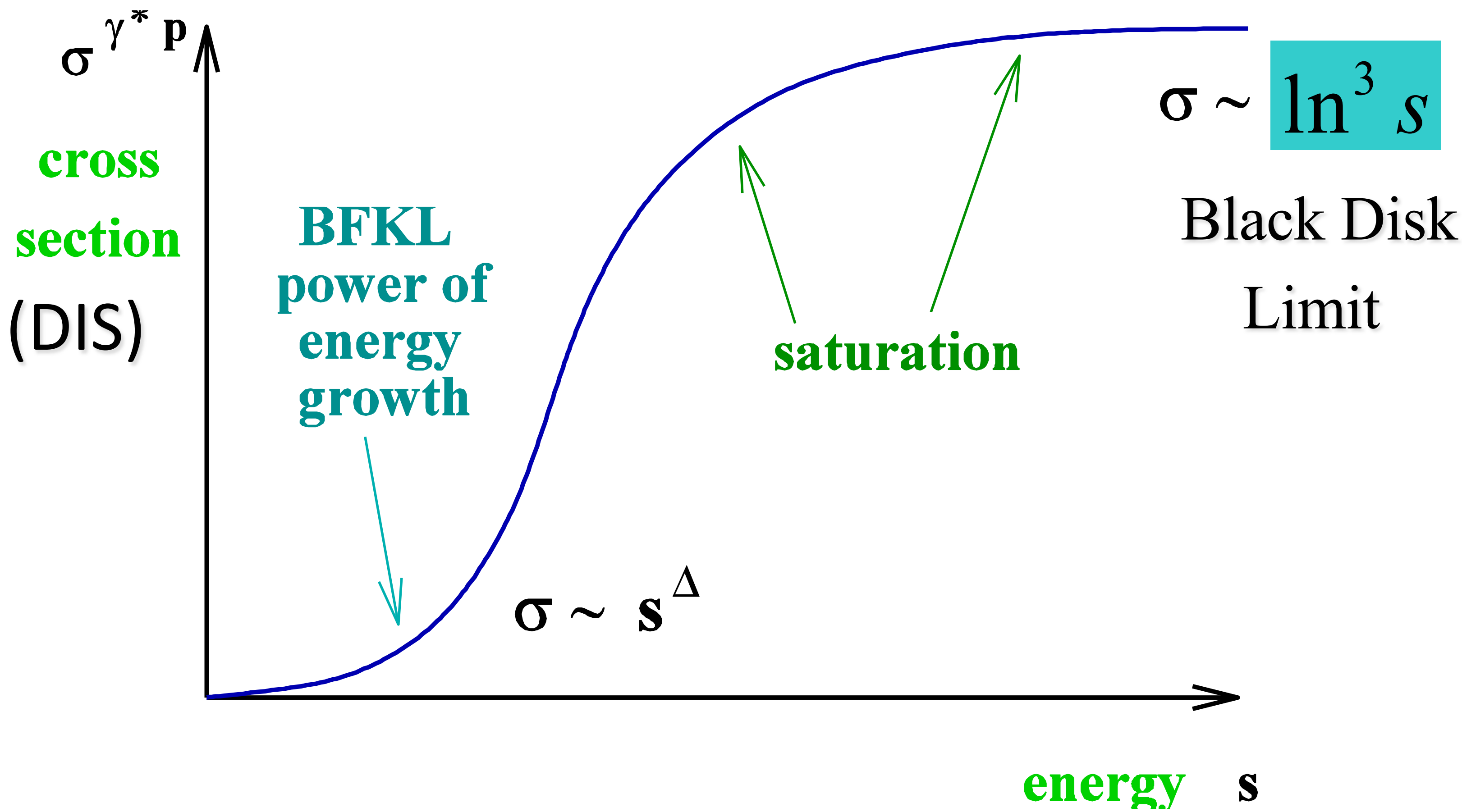

Gluon recombination tries to reduce the number of gluons in the wave function. At very high energy recombination begins to compensate gluon splitting. Gluon density reaches a limit and does not grow anymore. Ditto for the total DIS cross sections. Black disk limit and unitarity are restored!

B. In-Depth Discussion

Quantum Evolution

- The energy dependence comes in through the long-lived s-channel gluon corrections (higher Fock states):

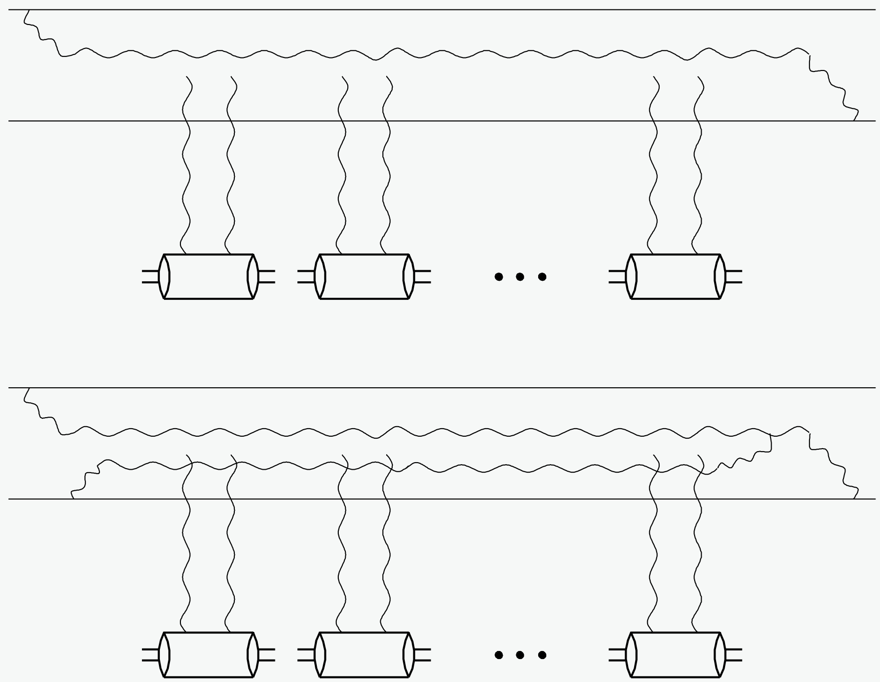

$$\alpha_s \ln s \sim \alpha_s Y \sim 1$$

These extra gluons bring in powers of $\alpha_s \ln s$, such that when $\alpha_s \ll 1$ and $\ln s \gg 1$ this parameter is $\alpha_s \ln s \sim 1$ (leading logarithmic approximation, LLA).

Mueller's Dipole Model

To include the quantum evolution in a dipole amplitude one can use the approach developed by A. H. Mueller in '93-'94.

Emission of a small-x gluon taken in the large-N_C limit would split the original color dipole in two:

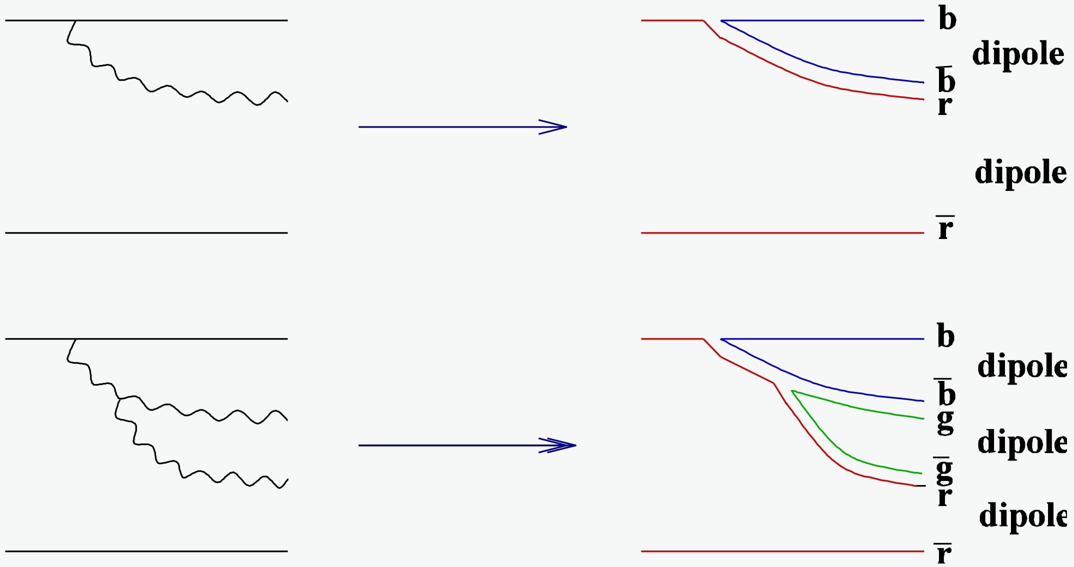

$$3 \otimes \bar{3} = 1 \oplus 8 \quad \Rightarrow \quad N_c \otimes \bar{N}_c = 1 \oplus (N_c^2 - 1) \approx N_c^2 - 1$$

Re-summing gluon cascade

- At large N_c the gluon cascade turns into a dipole cascade. We need to resum the dipole cascade, with each dipole interacting with the target independently.

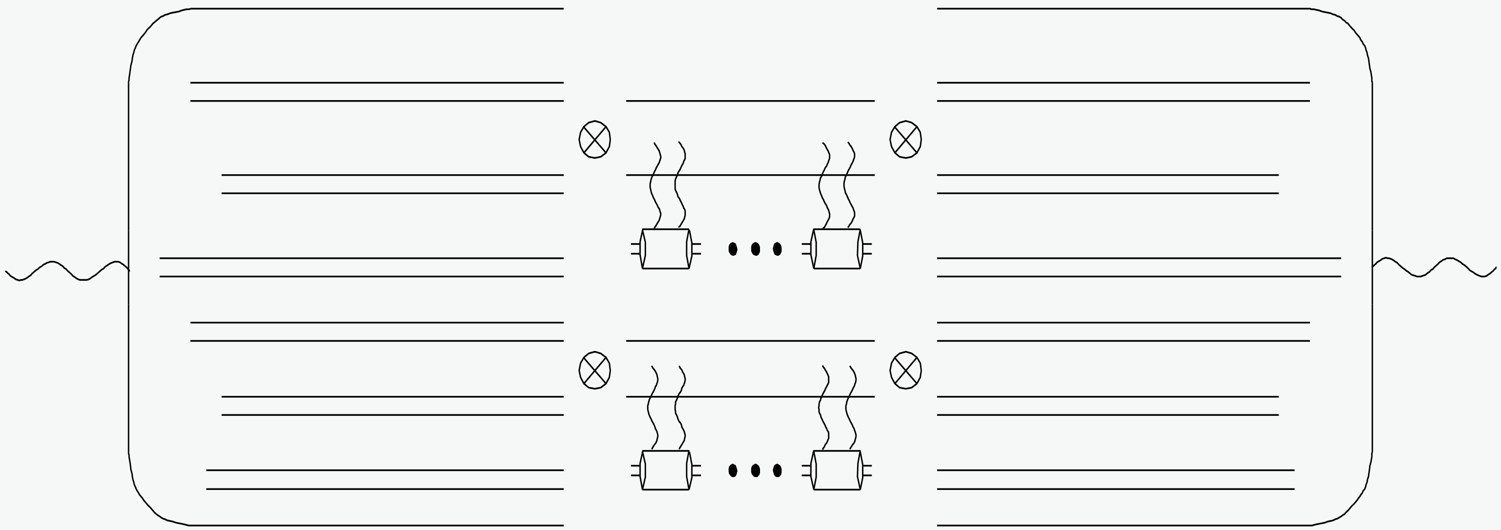

Notation (Large-N_c)

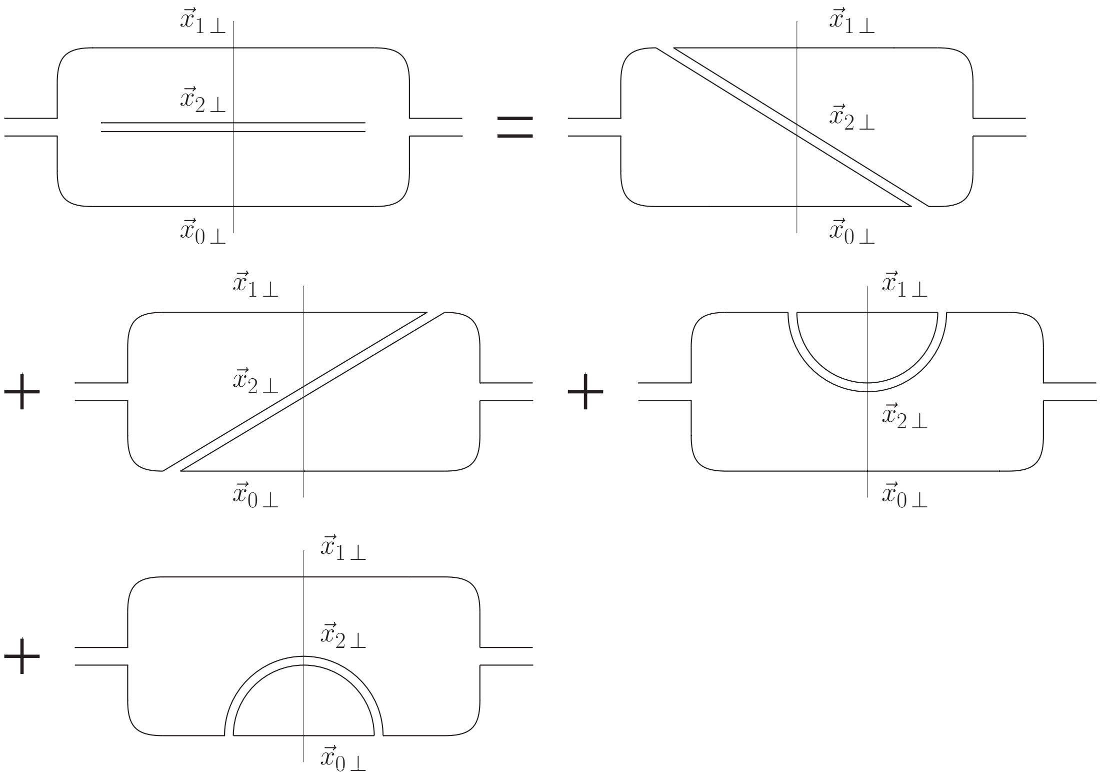

Real emissions in the amplitude squared

(dashed line – all Glauber-Mueller exchanges at light-cone time =0)

Virtual corrections in the amplitude (wave function)

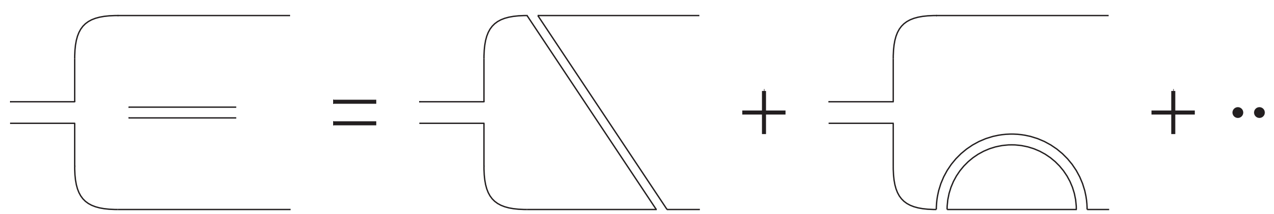

Nonlinear Evolution

To sum up the gluon cascade at large-N_C we write the following equation for the dipole S-matrix:

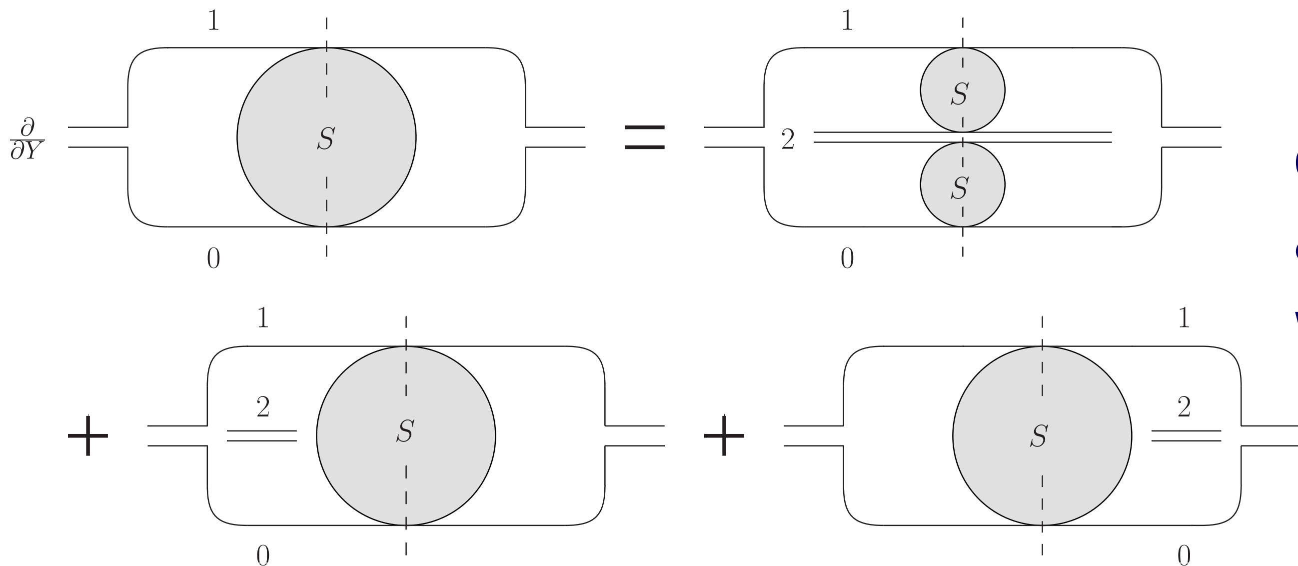

dashed line = all interactions with the target

$$\partial_Y S_{\mathbf{x}_0,\mathbf{x}_1}(Y) = \frac{\alpha_s N_c}{2\pi^2} \int d^2 x_2 \frac{x_{01}^2}{x_{02}^2 \, x_{21}^2} \left[S_{\mathbf{x}_0,\mathbf{x}_2}(Y) \, S_{\mathbf{x}_2,\mathbf{x}_1}(Y) - S_{\mathbf{x}_0,\mathbf{x}_1}(Y) \right]$$

Remembering that S= 1-N we can rewrite this equation in terms of the dipole scattering amplitude N.

Nonlinear evolution at large N_c

As N=1-S we write

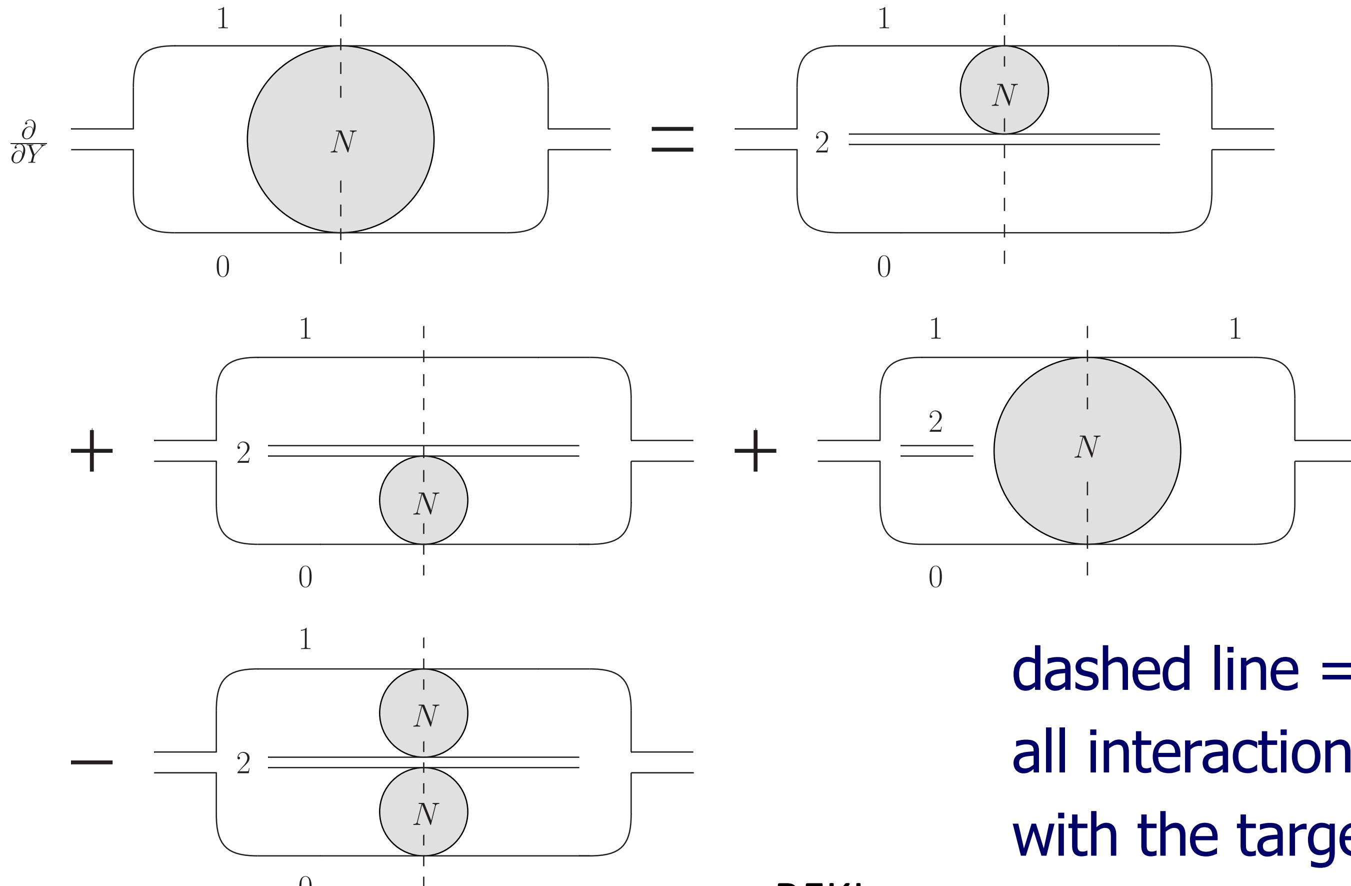

dashed line = all interactions with the target

BFKL

$$\partial_Y N_{\mathbf{x}_0,\mathbf{x}_1}(Y) = \frac{\alpha_s\, N_c}{2\,\pi^2} \int d^2x_2\, \frac{x_{01}^2}{x_{02}^2\, x_{21}^2}\, [N_{\mathbf{x}_0,\mathbf{x}_2}(Y) + N_{\mathbf{x}_2,\mathbf{x}_1}(Y) - N_{\mathbf{x}_0,\mathbf{x}_1}(Y) - N_{\mathbf{x}_0,\mathbf{x}_2}(Y)\, N_{\mathbf{x}_2,\mathbf{x}_1}(Y)]$$

Balitsky ‘96, Yu.K. ‘99

Nonlinear Evolution Equation

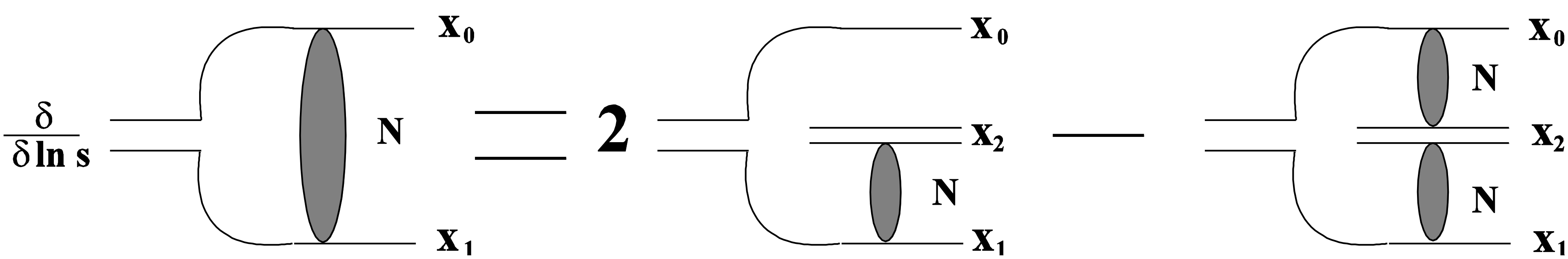

We can resum the dipole cascade

$$\frac{\partial N(x_{01},Y)}{\partial Y}=\frac{\alpha_S N_C}{\pi^2}\int d^2x_2\left[\frac{x_{01}^2}{x_{02}^2\,x_{12}^2}-2\pi\,\delta^2(\underline{x}_{01}-\underline{x}_{02})\ln\left(\frac{x_{01}}{\rho}\right)\right]N(x_{02},Y)$$

$$-\frac{\alpha_S N_C}{2\pi^2}\int d^2x_2\,\frac{x_{01}^2}{x_{02}^2\,x_{12}^2}\,N(x_{02},Y)\,N(x_{12},Y)$$

I. Balitsky, ’96, HE effective lagrangian
Yu. K., ’99, large N_C QCD

$$N(x_\perp,Y)=1-\exp\left[-\frac{x_\perp^2\,Q_s^2}{4}\,\ln\frac{1}{x_\perp\,\Lambda}\right]$$

← initial condition

⇨ Linear part is BFKL, quadratic term brings in damping

Resummation parameter

- BK equation resums powers of

$$\alpha_s \, N_c \, Y$$

- The Galuber-Mueller/McLerran-Venugopalan initial conditions for it resum powers of

$$\alpha_s^2 \, A^{1/3}$$

- Beyond the large-N_c limit: use the JIMWLK functional evolution equation (Iancu, Jalilian-Marian, Kovner, Leonidov, McLerran and Weigert, 1997-2002)

JIMWLK: derivation outline

A.H. Mueller, 2001

- Start by introducing a weight functional, $W_Y[\alpha]$. Here $\alpha = A^+$ is the gluon field of the target proton or nucleus. $\alpha(x^-, \vec{x}) \equiv A^+(x^+ = 0, x^-, \vec{x})$
- The functional is used to generate expectation values of gluon-field dependent operators in the target state:

$$\langle \hat{O}_\alpha \rangle_Y = \int \mathcal{D}\alpha \; \hat{O}_\alpha \, W_Y[\alpha]$$

- Imagine that we know small-x evolution for some operator O:

$$\partial_Y \, \langle \hat{O}_\alpha \rangle_Y = \langle \mathcal{K}_\alpha \otimes \hat{O}_\alpha \rangle_Y = \int \mathcal{D}\alpha \, \left[\mathcal{K}_\alpha \otimes \hat{O}_\alpha \right] W_Y[\alpha]$$

- On the other hand, we can differentiate the first equation above,

$$\partial_Y \, \langle \hat{O}_\alpha \rangle_Y = \int \mathcal{D}\alpha \; \hat{O}_\alpha \; \partial_Y \, W_Y[\alpha]$$

- Comparing the last two equations and integrating by parts in the second to last equation, we will arrive at and equation for the weight functional $W_Y[\alpha]$.

JIMWLK: derivation outline

- As a test operator, take a pair of Wilson lines (not a dipole!):

$$\hat{O}_{\vec{x}_{1\perp},\vec{x}_{0\perp}} = V_{\vec{x}_{1\perp}} \otimes V^{\dagger}_{\vec{x}_{0\perp}}$$

- Construct the evolution of this operator by summing the following familiar diagrams:

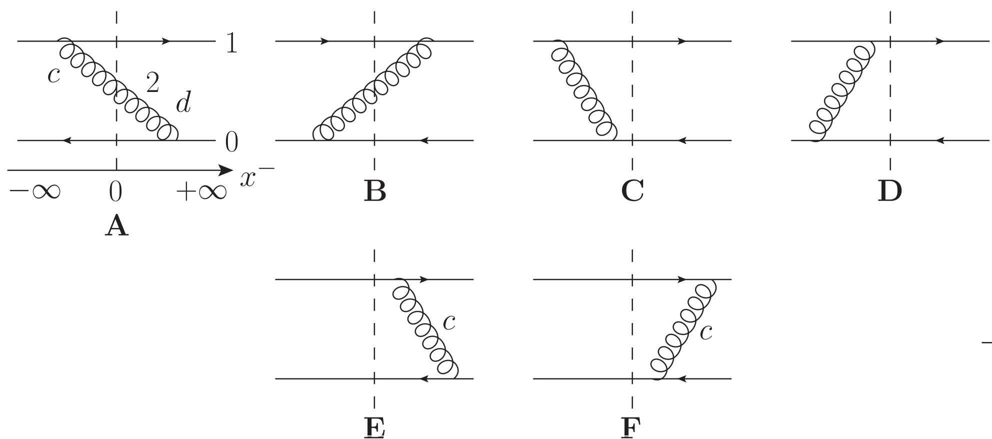

real

virtual

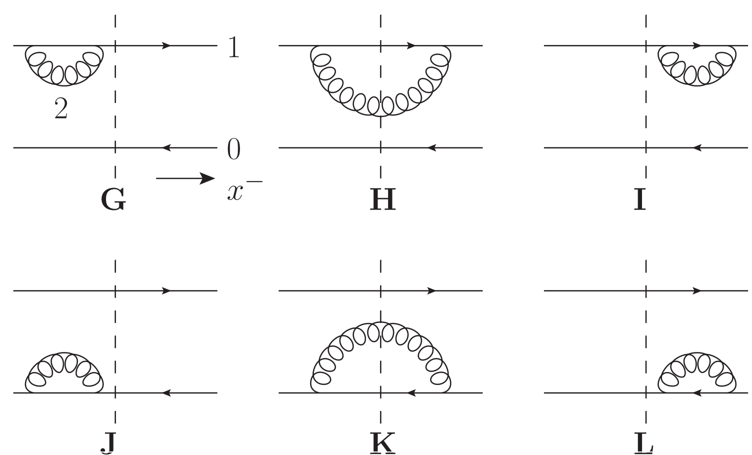

JIMWLK Equation

- In the end one arrive at the JIMWLK evolution equation (1997-2002):

$$\partial_Y W_Y[\alpha] = \alpha_s \left\{ \frac{1}{2} \int d^2x_\perp\, d^2y_\perp\, \frac{\delta^2}{\delta\alpha^a(x^-, \vec{x}_\perp)\,\delta\alpha^b(y^-, \vec{y}_\perp)} \left[\eta^{ab}_{\vec{x}_\perp \vec{y}_\perp} W_Y[\alpha]\right] - \int d^2x_\perp \frac{\delta}{\delta\alpha^a(x^-, \vec{x}_\perp)} \left[\nu^a_{\vec{x}_\perp} W_Y[\alpha]\right] \right\}$$

with

$$\eta^{ab}_{\vec{x}_{1\perp}\vec{x}_{0\perp}} = \frac{4}{g^2\,\pi^2} \int d^2x_2\, \frac{\vec{x}_{21}\cdot\vec{x}_{20}}{x_{21}^2\, x_{20}^2} \left[\mathbf{1} - U_{\vec{x}_{1\perp}} U^\dagger_{\vec{x}_{2\perp}} - U_{\vec{x}_{2\perp}} U^\dagger_{\vec{x}_{0\perp}} + U_{\vec{x}_{1\perp}} U^\dagger_{\vec{x}_{0\perp}}\right]^{ab}$$

$$\nu^a_{\vec{x}_{1\perp}} = \frac{i}{g\,\pi^2} \int \frac{d^2x_2}{x_{21}^2}\, \mathrm{Tr}\left[T^a U_{\vec{x}_{1\perp}} U^\dagger_{\vec{x}_{2\perp}}\right]$$

- Here U is the adjoint Wilson line on a light cone,

$$U_{\vec{x}_\perp} = \mathrm{P}\exp\left\{ i\,g \int\limits_{-\infty}^{\infty} dx^-\, \mathcal{A}^+(x^+ = 0, x^-, \vec{x}_\perp) \right\}$$

JIMWLK Equation

- JIMWLK equation can be used to construct any-N_C small-x evolution of any operator made of infinite light-cone Wilson lines (in any representation), such as color-dipole, color-quadrupole, etc., and other operators.

- Since

$$\Box \alpha(x^-, \vec{x}) \, = \, \rho(x^-, \vec{x})$$

  JIMWLK evolution can be re-written in terms of the color density ρ in the kernel.

- JIMWLK approach sums up powers of $\alpha_s \, Y$ and $\alpha_s^2 \, A^{1/3}$

Solving JIMWLK

- The JIMWLK equation was solved on the lattice by K. Rummukainen and H. Weigert '04 (and others since).
- For the dipole amplitude $N(x_0,x_1, Y)$, the **relative** corrections to the large-N_C limit BK equation are **< 0.001 !** Not the naïve $1/N_C^2 \sim 0.1$! (For realistic rapidities/energies.)
- The reason for that is dynamical and is largely due to saturation effects suppressing the bulk of the potential $1/N_C^2$ corrections (Yu.K., J. Kuokkanen, K. Rummukainen, H. Weigert, '08).
- There are other objects at small x, quadrupoles, double-trace operators, etc. Some (linear combinations) of them are subleading-N_c, and one has to use JIMWLK to describe their evolution.

Solution of the nonlinear equation

Solution of BK equation

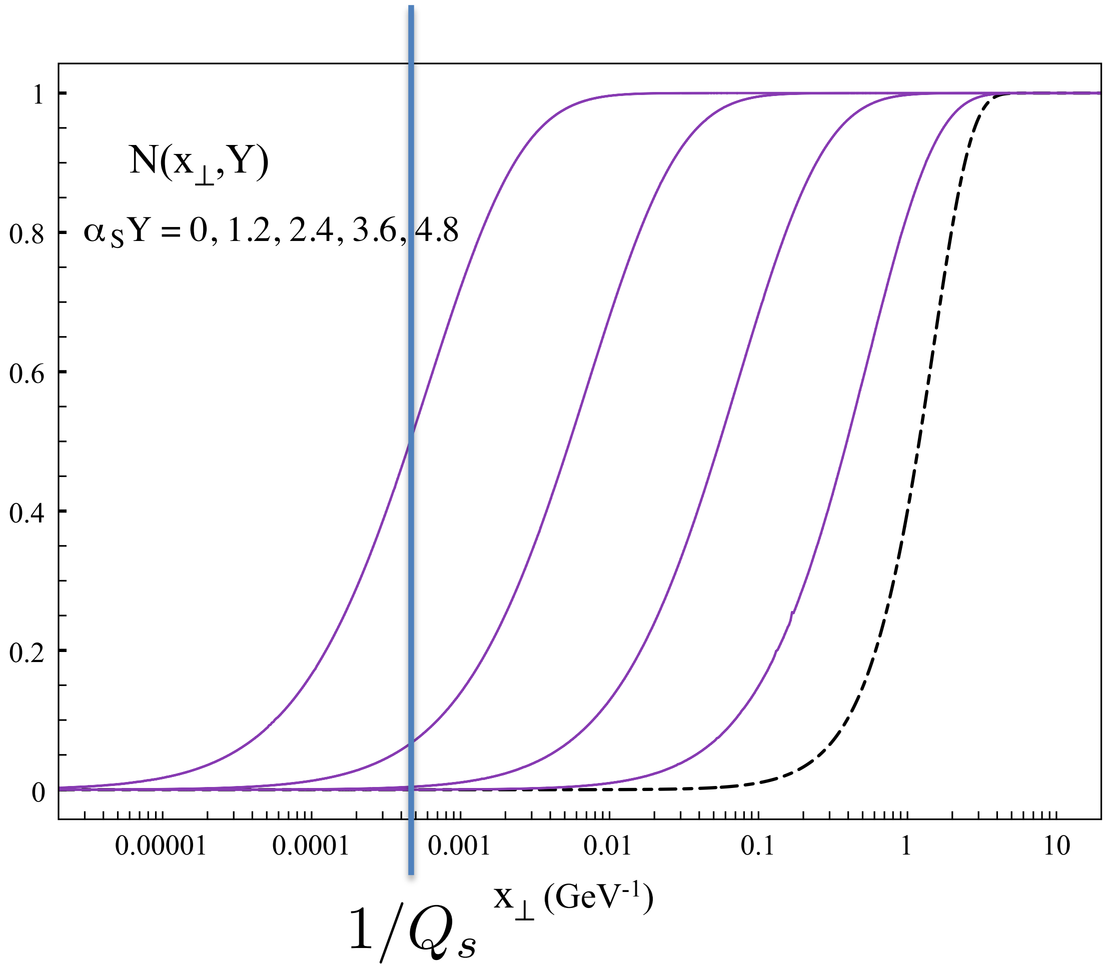

numerical solution by J. Albacete '03 (earlier solutions were found numerically by Golec-Biernat, Motyka, Stasto, by Braun, and by Lublinsky et al in '01)

BK solution preserves the black disk limit, N<1 always (unlike the linear BFKL equation)

$$\sigma^{q\bar{q}A} = 2 \int d^2b\, N(x_\perp, b_\perp, Y)$$

Saturation scale

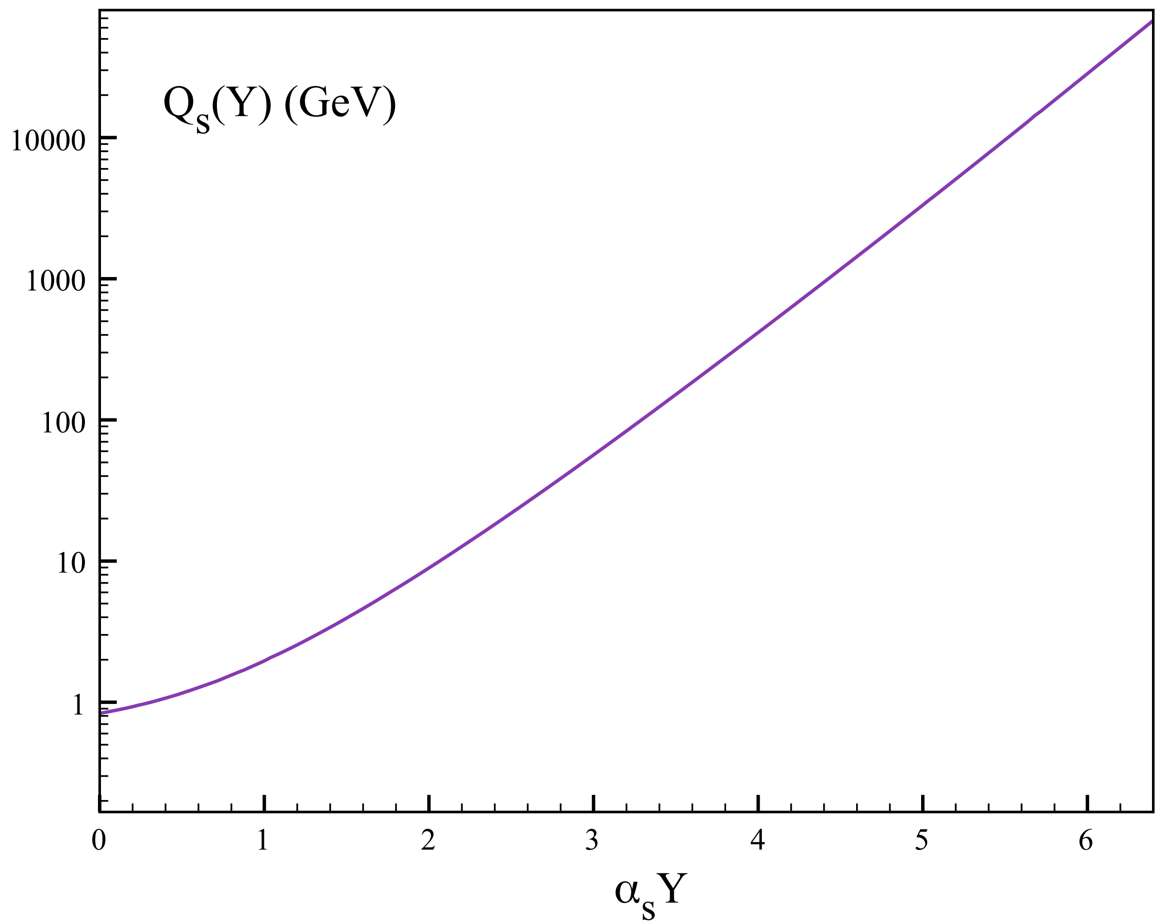

numerical solution by J. Albacete (ca. 2006)

BK Solution

- Preserves the black disk limit, N<1 always.

$$\sigma^{q\bar{q}A} = 2 \int d^2b\, N(x_\perp, b_\perp, Y)$$

- Avoids the IR problem of BFKL evolution due to the saturation scale screening the IR:

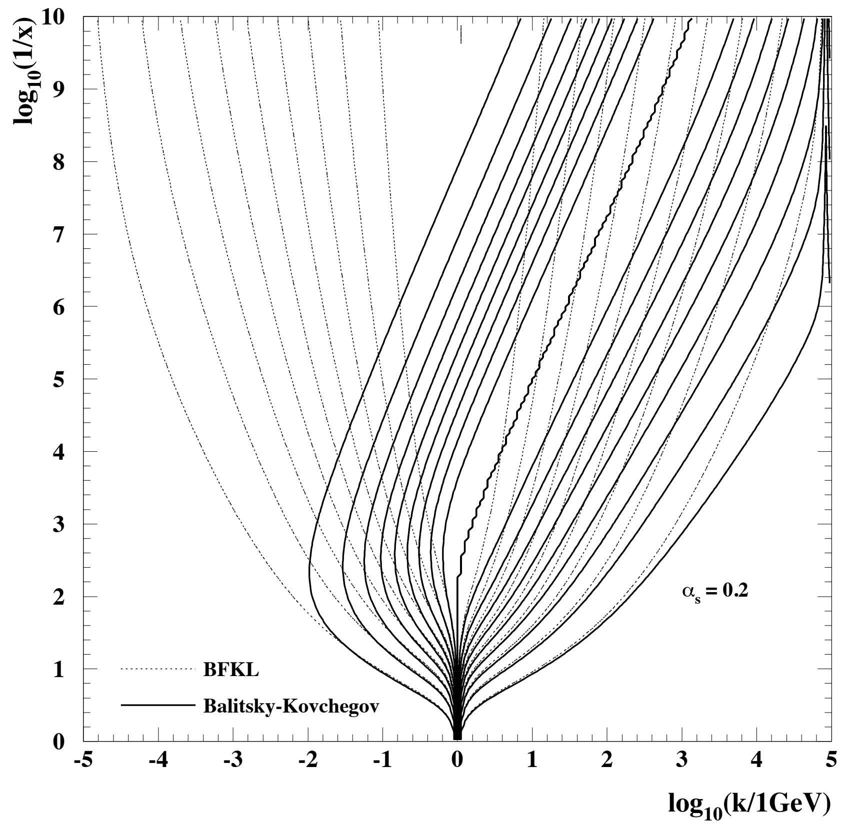

Golec-Biernat, Motyka, Stasto ‘02

The BFKL Equation

- The Balitsky, Fadin, Kuraev, Lipatov (BFKL) equation was derived in 1977-78.
- One starts with a two-gluon exchange diagram (left) and "dresses" it by radiative corrections.
- The leading high-energy contribution can be drawn as a ladder diagram, with the t-channel gluons being the special "reggeized" gluons and the thick dots representing effective Lipatov vertices.

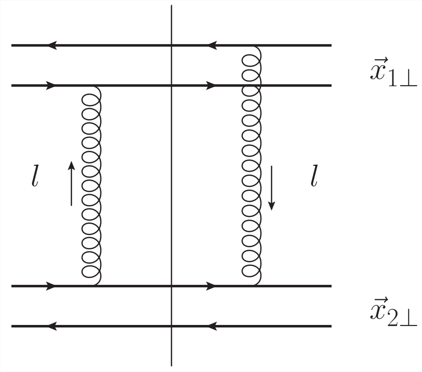

$$\frac{\partial f}{\partial \ln s} = \alpha_s \, K_{BFKL} \otimes f$$

The BFKL equation.
K_{BFKL} is an integral kernel.

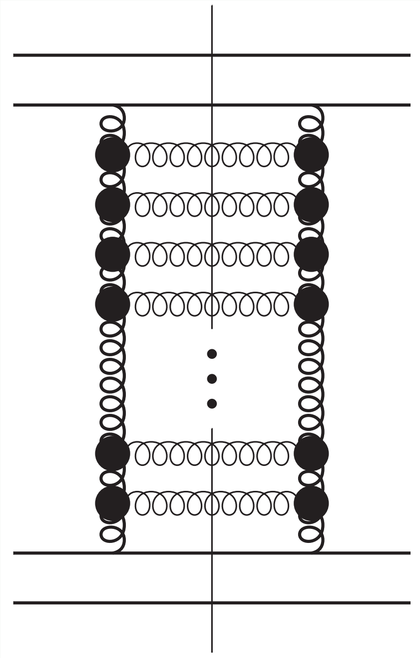

BFKL Equation

In the conventional Feynman diagram picture the BFKL equation can be represented by a ladder graph shown here. Each rung of the ladder brings in a power of $\alpha \ln s$.

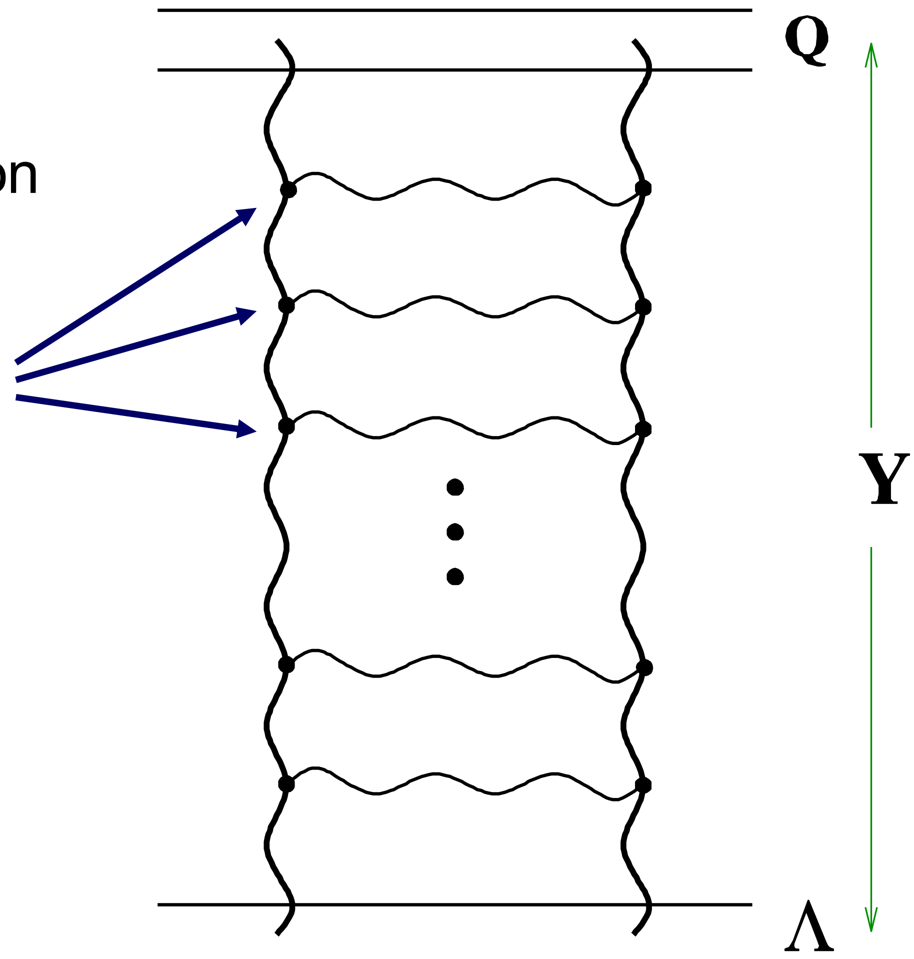

The resulting dipole amplitude grows as a power of energy

$$N \sim s^{\Delta}$$

violating Froissart unitarity bound

$$\sigma_{tot} \leq const \ln^2 s$$

GLR-MQ Equation

Gribov, Levin and Ryskin ('81) proposed summing up "fan" diagrams:

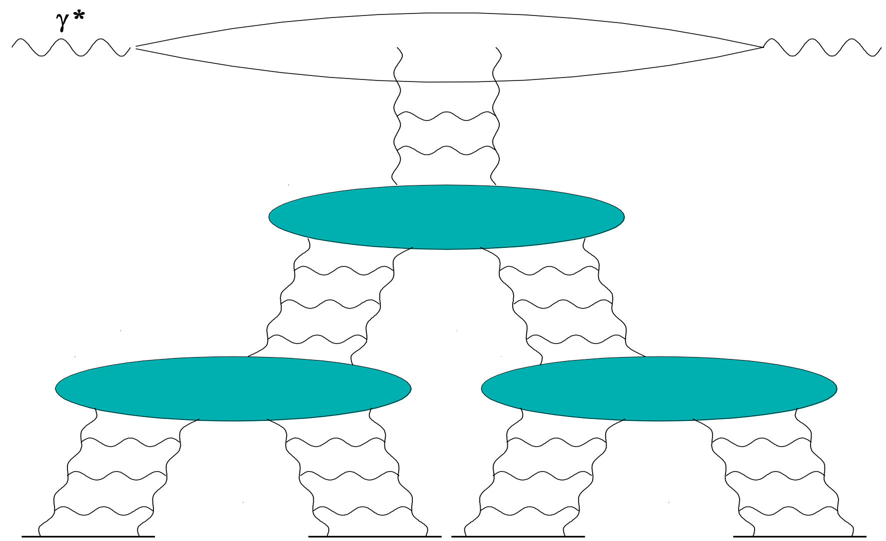

Mueller and Qiu (' 85) summed "fan" diagrams for large Q^2.

The GLR-MQ equation reads:

$$\frac{\partial}{\partial \ln 1/x} \phi(x, k_T^2) = \alpha_s K_{BFKL} \otimes \phi(x, k_T^2) - \alpha_s [\phi(x, k_T^2)]^2$$

GLR-MQ equation has the same principle of recombination as BK and JIMWLK. GLR-MQ equation was thought about as the first nonlinear correction to the linear BFKL evolution. An AGL (Ayala, Gay Ducati, Levin '96) equation was suggested to resum higher-order nonlinear corrections.

BK/JIMWLK derivation showed that for the dipole amplitude N (!) there are no more terms in the large-N_C limit and obtained the correct kernel for the non-linear term (compared to GLR suggestion).

Energy Dependence of the Saturation Scale

Single BFKL ladder gives scattering amplitude of the order

$$N \sim \frac{\Lambda}{k_T} s^{\Delta}$$

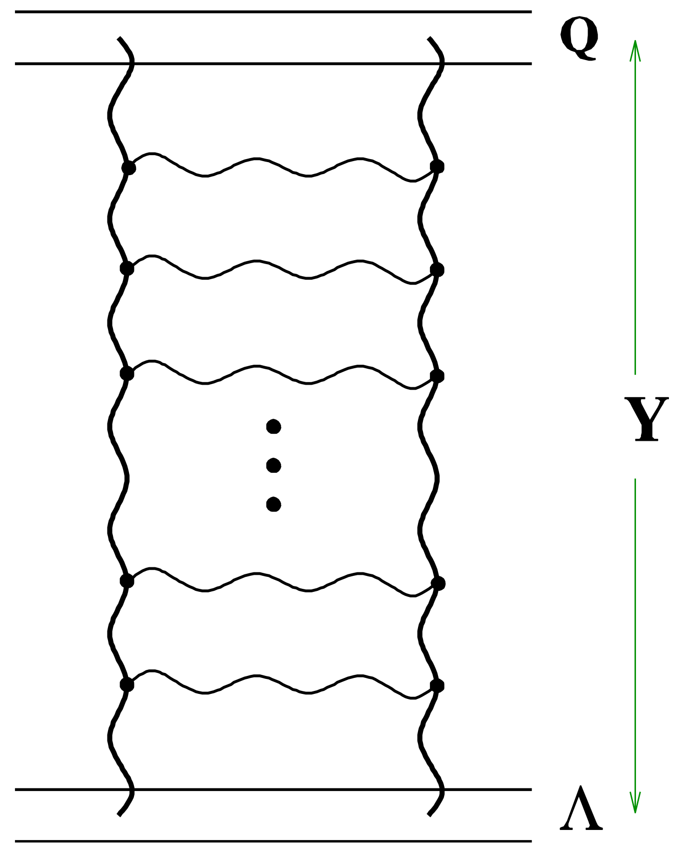

Nonlinear saturation effects become important when N ~ N^2 ⇨ N ~ 1. This happens at

$$k_T = Q_s \sim \Lambda\, s^{\Delta}$$

Saturation scale grows with energy!

Typical partons in the wave function have $k_T \sim Q_S$, so that their characteristic size is of the order $r \sim 1/k_T \sim 1/Q_S$.

⇨ Typical parton size decreases with energy!

Saturation scale

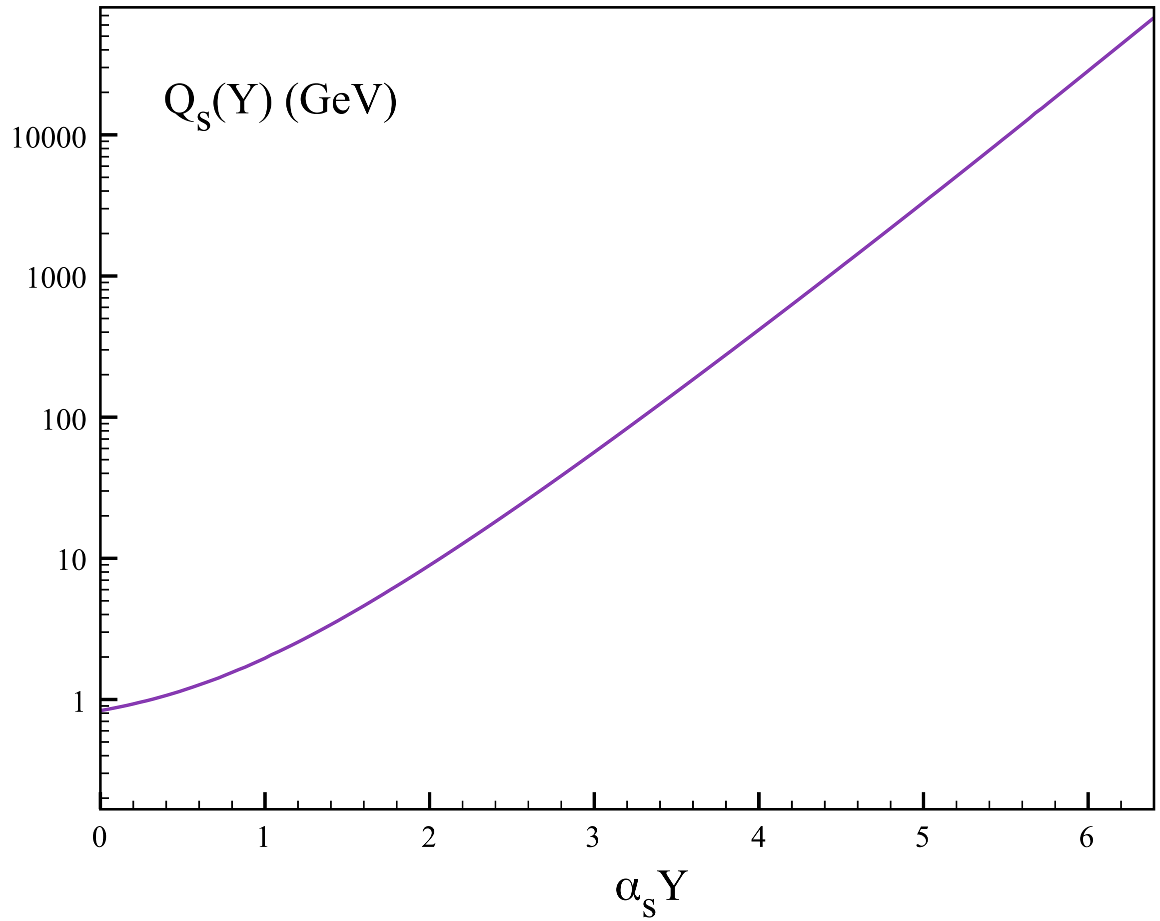

numerical solution by J. Albacete

High Density of Gluons

- High number of gluons populates the transverse extent of the proton or nucleus, leading to a very dense saturated wave function known as the Color Glass Condensate (CGC):

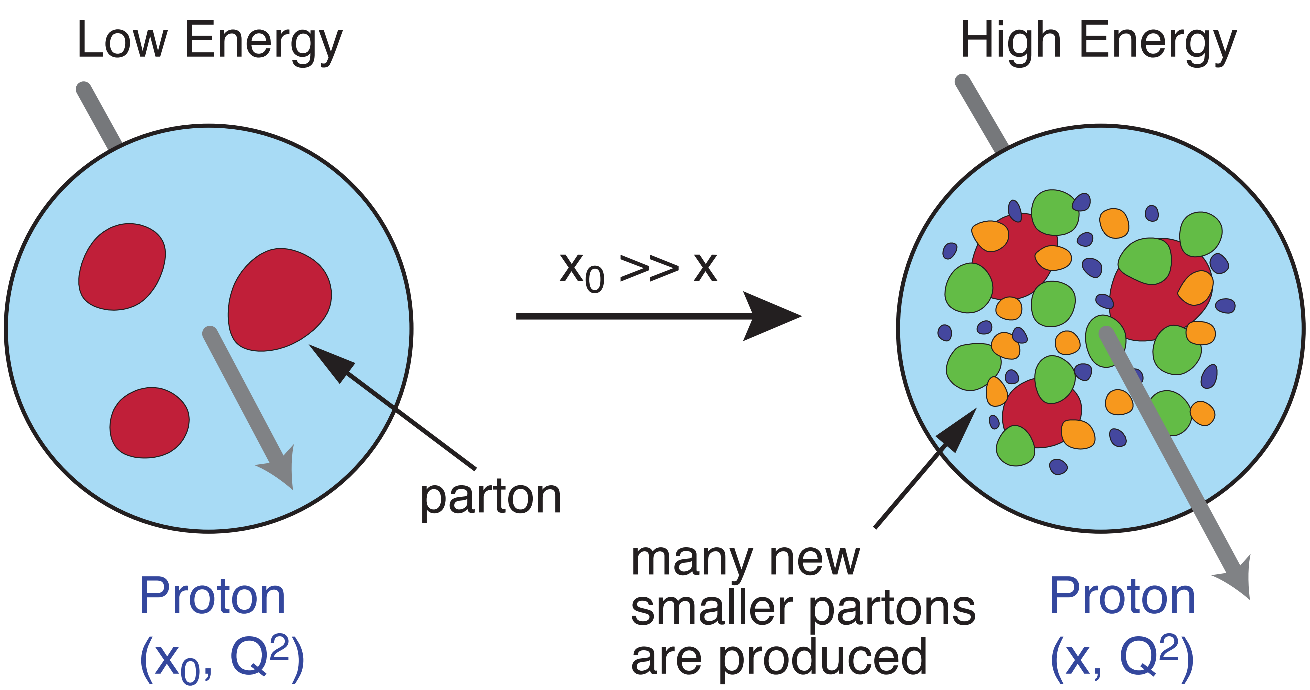

"Color Glass Condensate"

Map of High Energy QCD

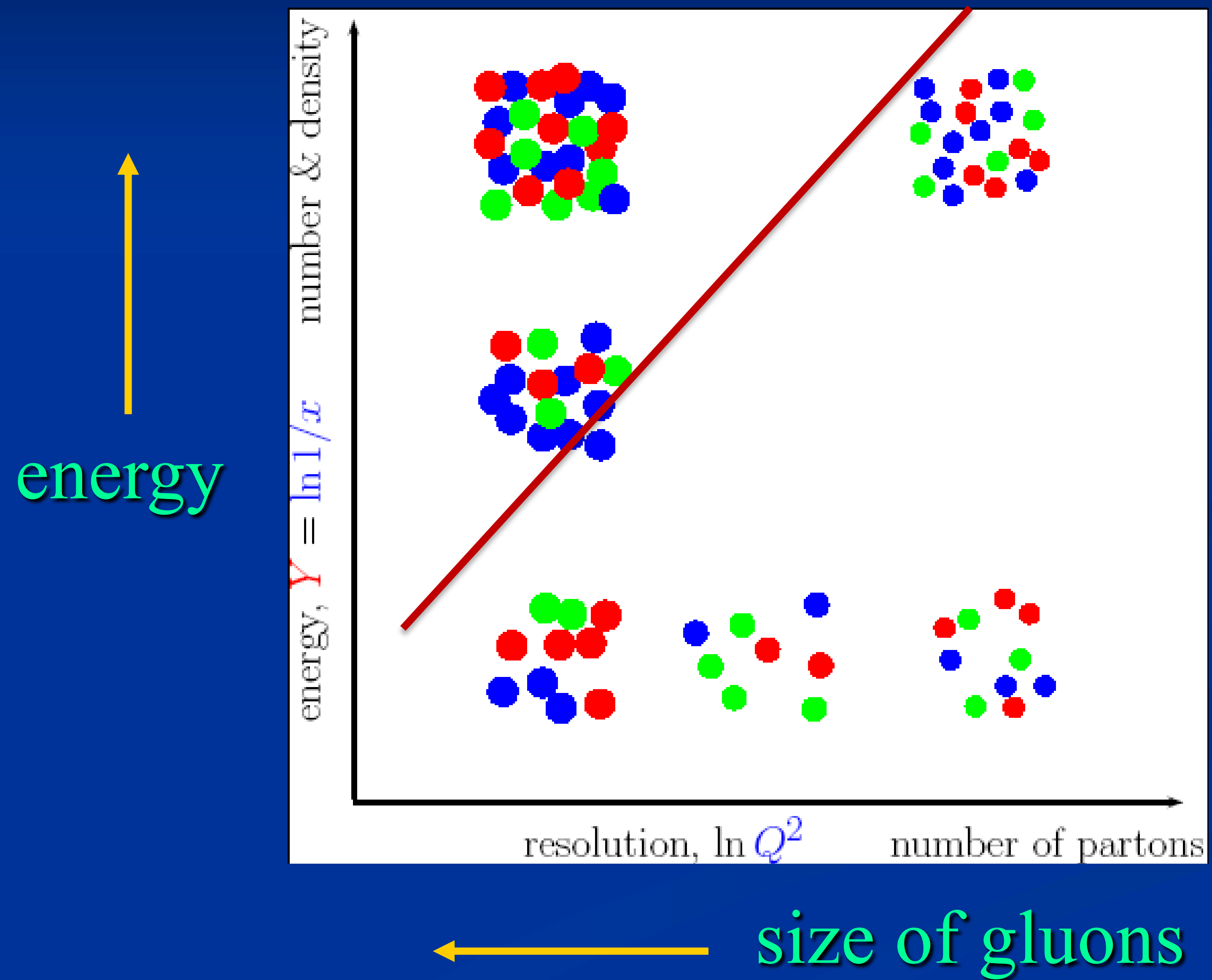

Map of High Energy QCD

energy

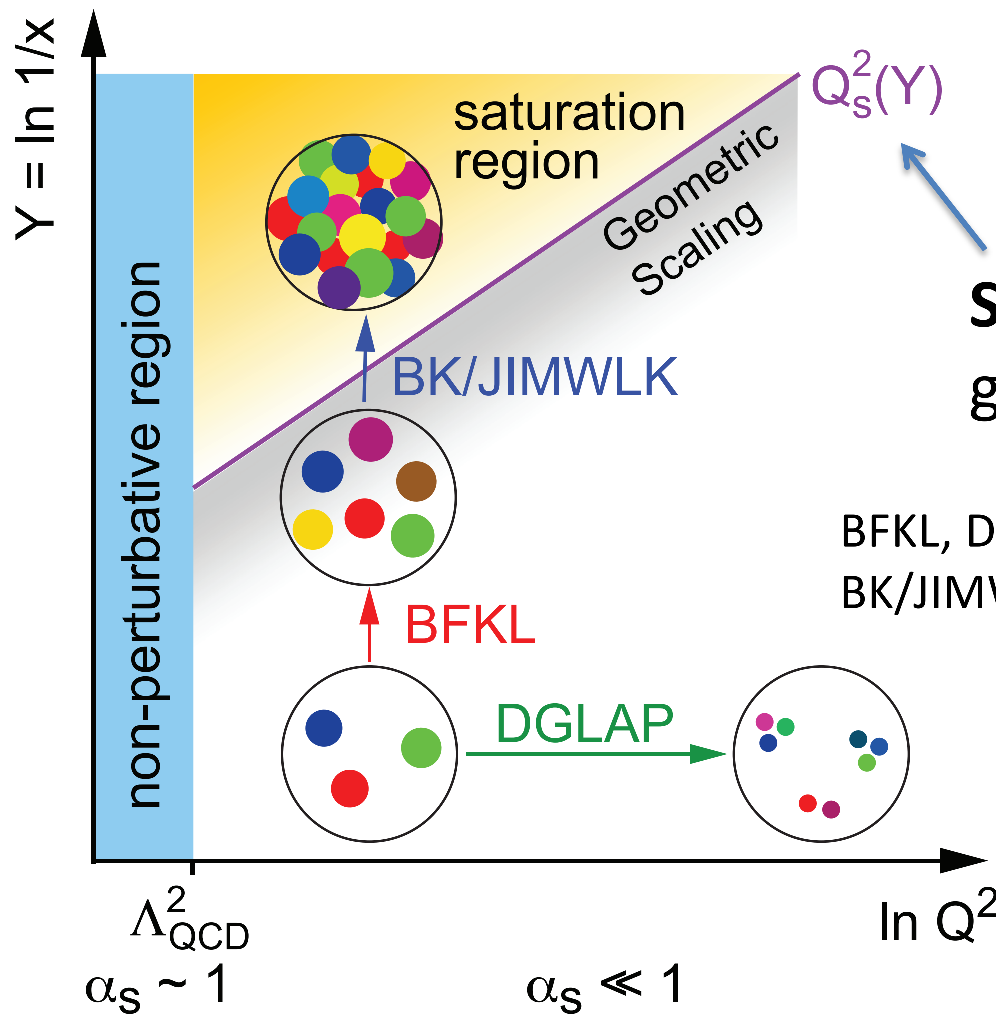

size of gluons

$$Q_s^2 \sim \left(\frac{1}{x}\right)^\lambda$$

Saturation Scale
grows with energy

BFKL, DGLAP – linear equations
BK/JIMWLK – nonlinear

Nonlinear Evolution at Work

✓ First partons are produced overlapping each other, all of them about the same size.

✓ When some critical density is reached no more partons of given size can fit in the wave function. The proton starts producing smaller partons to fit them in.

Proton

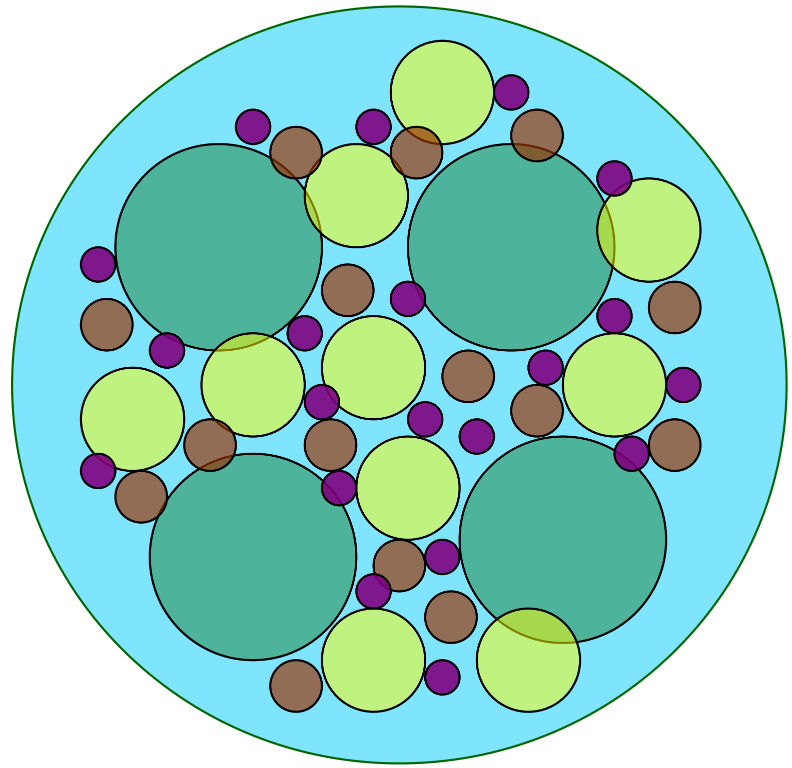

Color Glass Condensate

Map of High Energy QCD

Saturation physics allows us to study regions of high parton density in the small coupling regime, where calculations are still under control!

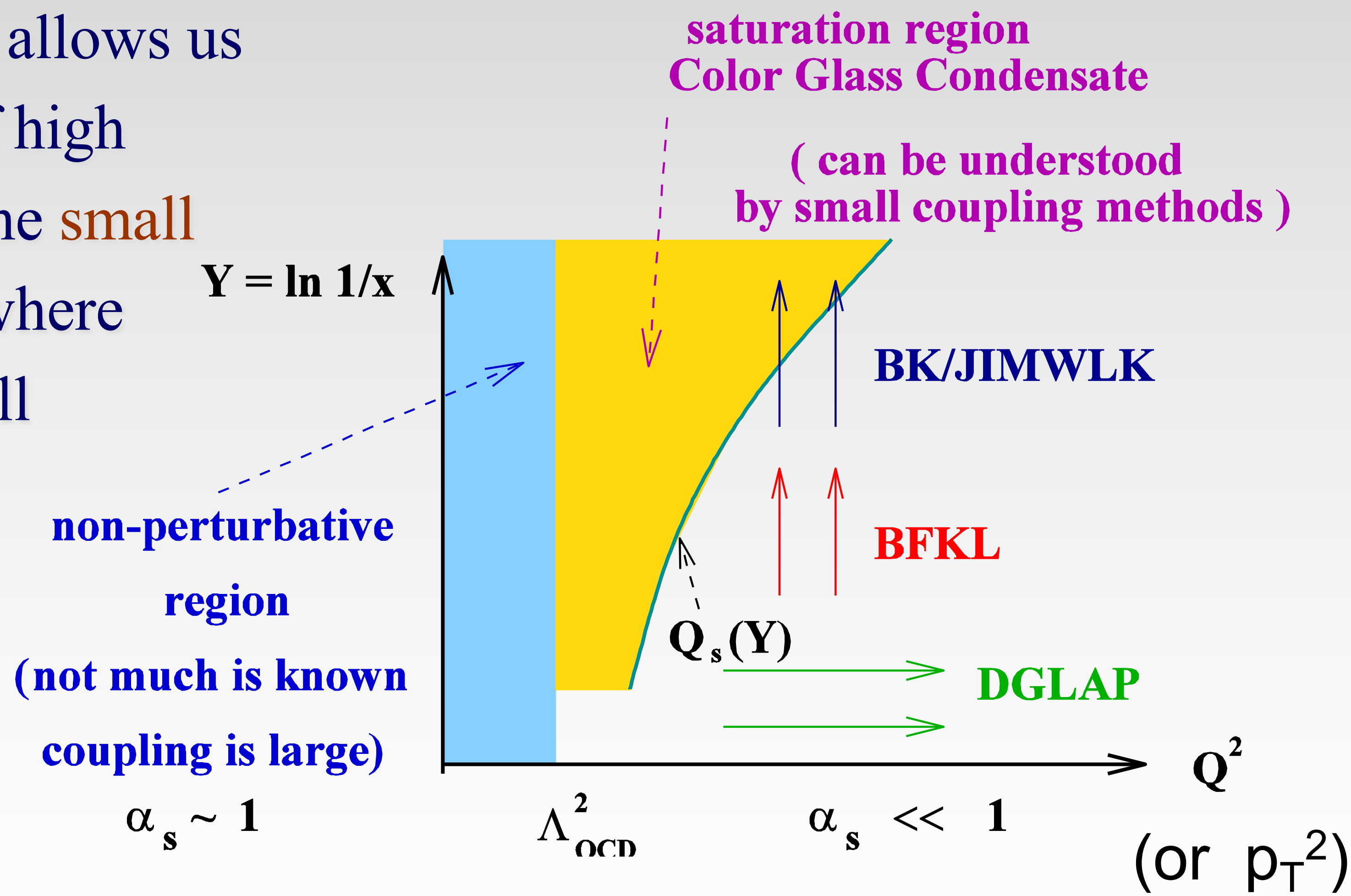

Transition to saturation region is characterized by the saturation scale

$$Q_S^2 \sim A^{1/3} \left(\frac{1}{x} \right)^{\lambda}$$

Geometric Scaling

- One of the predictions of the JIMWLK/BK evolution equations is geometric scaling:

  DIS cross section should be a function of one parameter:

$$\sigma_{DIS}(x, Q^2) = \sigma_{DIS}(Q^2 / Q_S^2(x))$$

(Levin, Tuchin ' 99; Iancu, Itakura, McLerran ' 02)

Geometric Scaling

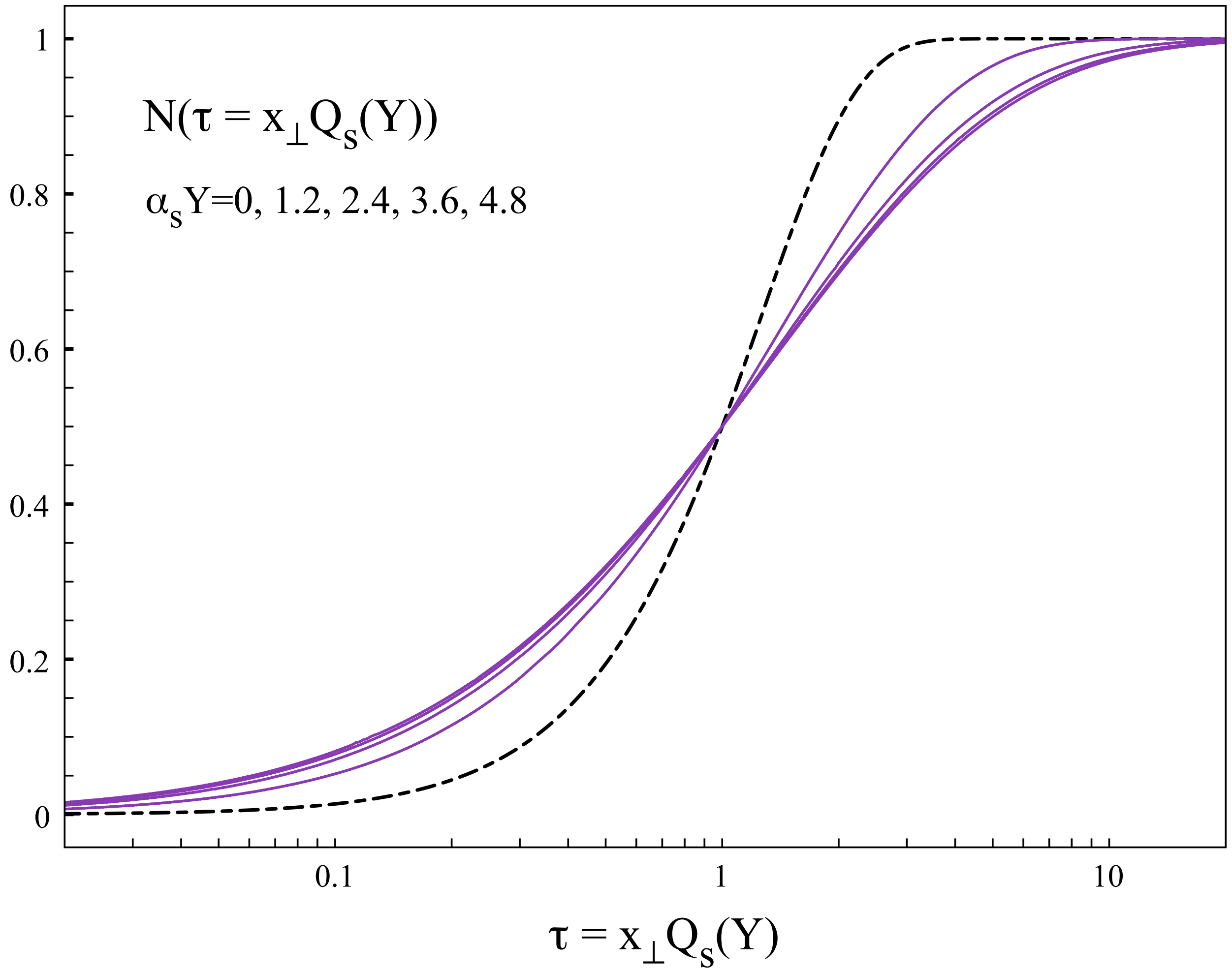

numerical solution by J. Albacete

Geometric Scaling in DIS

Geometric scaling has been observed in DIS data by
Stasto, Golec-Biernat, Kwiecinski in ’00.

Here they plot the total DIS cross section, which is a function of 2 variables - Q^2 and x, as a function of just <u>one</u> variable:

$$\tau = \frac{Q^2}{Q_s^2}$$

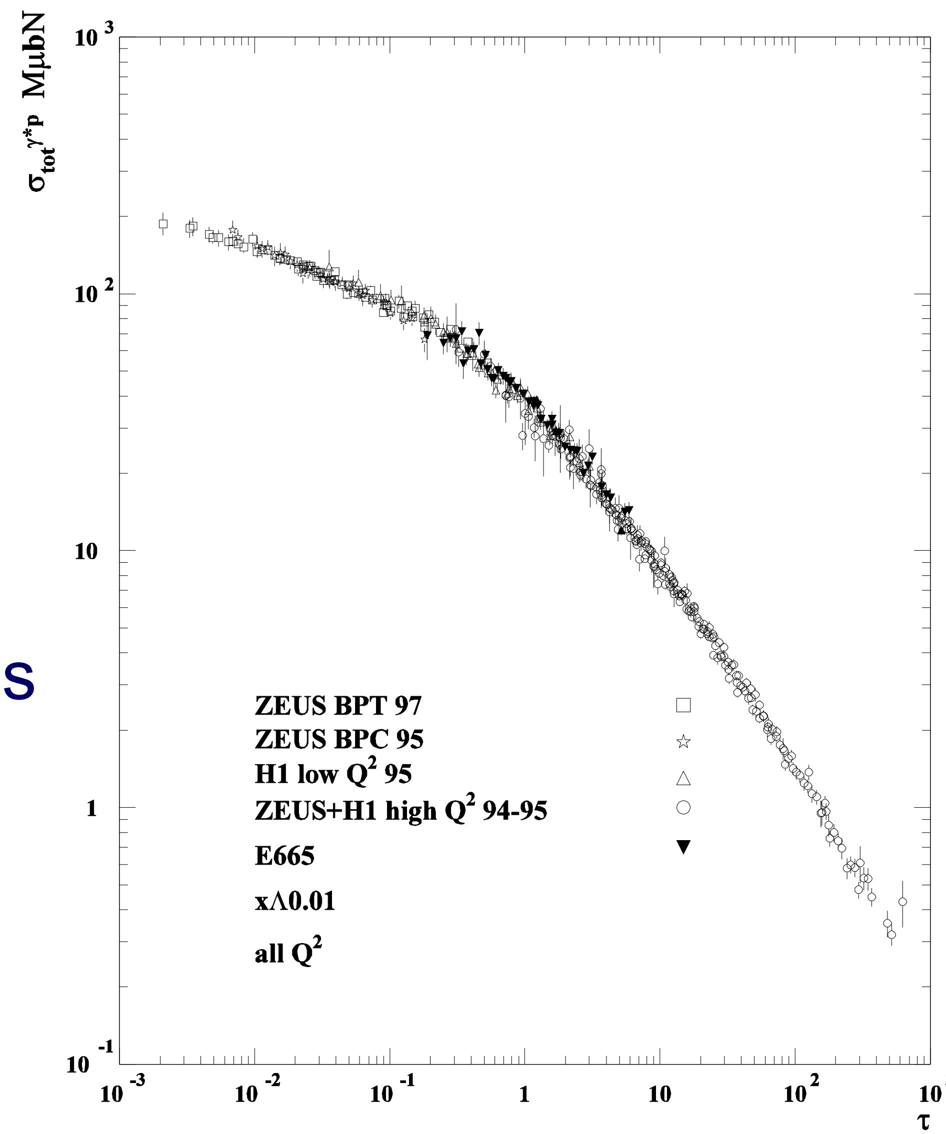

Map of High Energy QCD

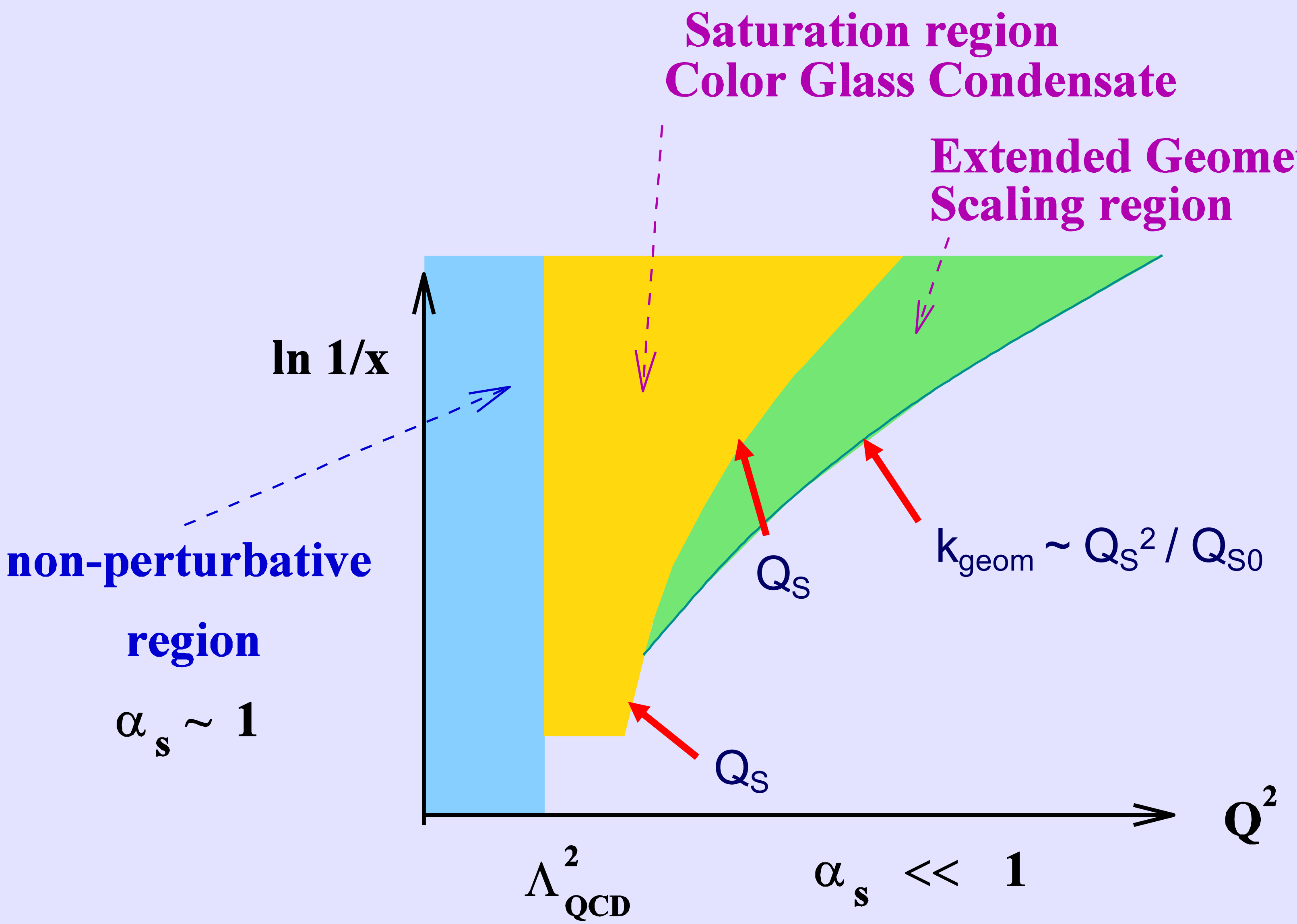

Saturation Scale

To summarize, saturation scale is an increasing function of both energy (1/x) and A:

$$Q_s^2 \sim \left(\frac{A}{x}\right)^{1/3}$$

Gold nucleus provides an enhancement by $197^{1/3}$, which is equivalent to doing scattering on a proton at 197 times smaller x / higher s!

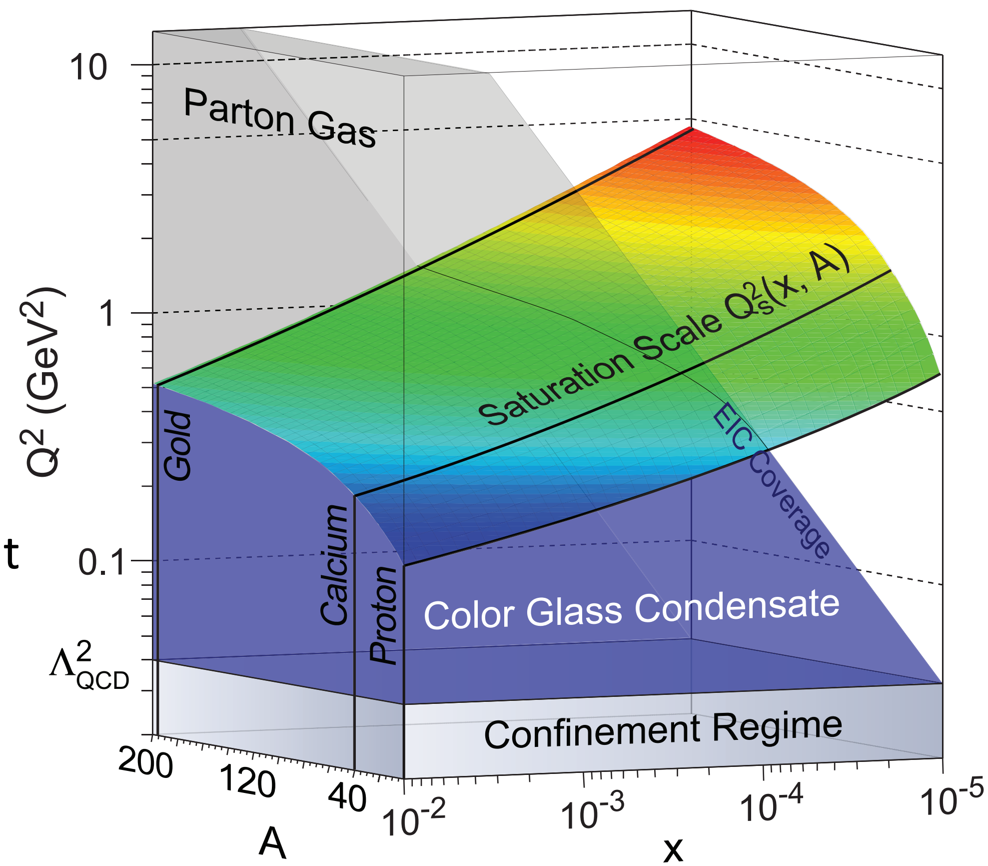

References

- E.Iancu, R.Venugopalan, hep-ph/0303204.
- H.Weigert, hep-ph/0501087
- J.Jalilian-Marian, Yu.K., hep-ph/0505052
- F. Gelis et al, arXiv:1002.0333 [hep-ph]
- J.L. Albacete, C. Marquet, arXiv:1401.4866 [hep-ph]
- and…

References

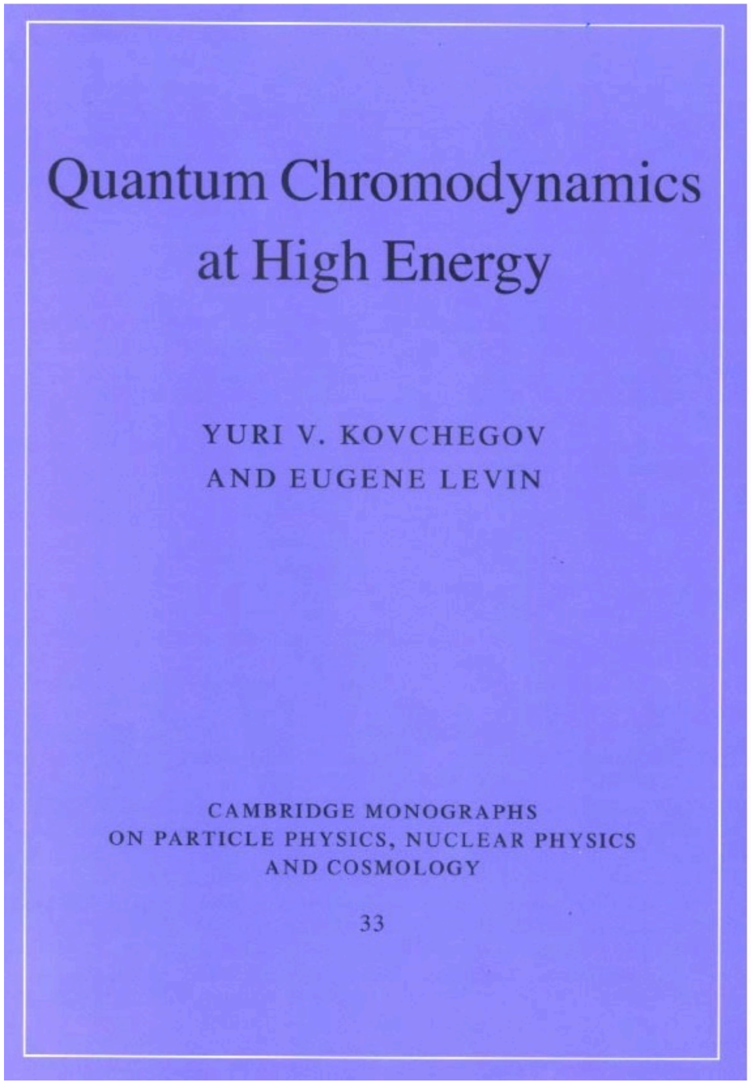

Published in September 2012
by Cambridge U Press

Summary

- We have constructed nuclear/hadronic wave function in the quasi-classical approximation (MV model), and studied DIS in the same approximation
- We included small-*x* evolution corrections into the DIS process, obtaining nonlinear BK/JIMWLK evolution equations
- We found the saturation scale justifying the whole procedure.

$$Q_S^2 \sim A^{1/3} \left(\frac{1}{x}\right)^{\lambda}$$

- Saturation/CGC physics predicts geometric scaling observed experimentally at HERA.

TMDs at Small *x*

Our goal here

- The above machinery can be used to <u>predict</u> the small-x asymptotics of the quark (and gluon) TMDs.

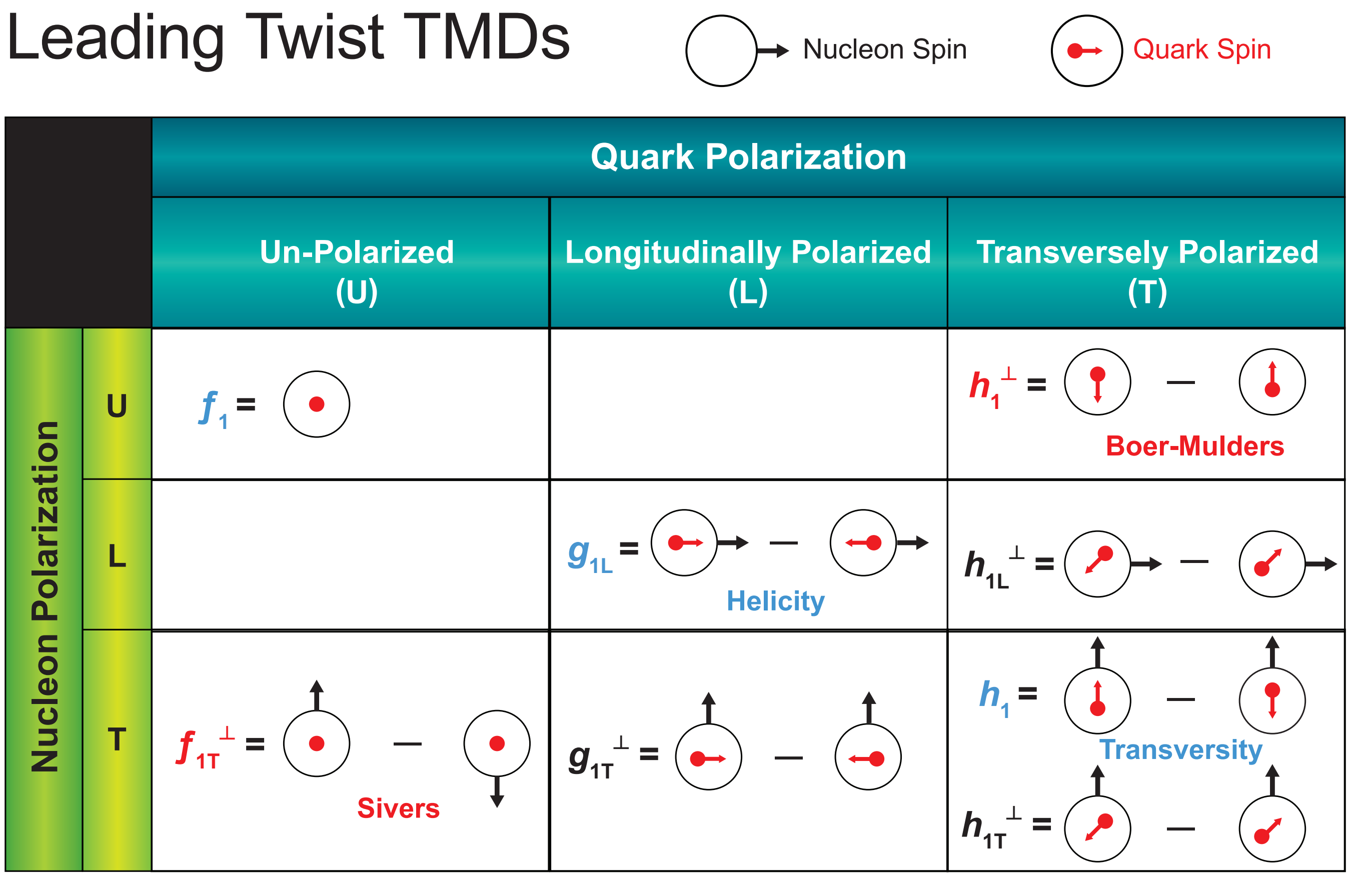

- For now, we will concentrate on the region where *x* is small, but not small enough to include the nonlinear saturation effects.

Unpolarized Nucleon TMDs

Dipole Gluon TMD

- We start with the gluon dipole TMD:

$$f_1^{G\,dip}(x, k_T^2) = \frac{2}{x\,P^+} \int \frac{d\xi^-\, d^2\xi}{(2\pi)^3}\, e^{ixP^+\,\xi^- - i\underline{k}\cdot\underline{\xi}}\, \langle P|\mathrm{tr}\left[F^{+i}(0)\,\mathcal{U}^{[+]}[0,\xi]\;F^{+i}(\xi)\,\mathcal{U}^{[-]}[\xi,0]\right]|P\rangle_{\xi^+=0}$$

- Here $U^{[+]}$ and $U^{[-]}$ are future and past-pointing fundamental Wilson line staples (hence the name `dipole' TMD – it looks like a quark dipole scattering on a proton)
- Dipole gluon TMD enters a number of cross sections: DIS, DY, SIDIS, hadron production in pA.
- Dominguez, Marquet, Xiao, Yuan '11; M. Braun '00; YK, Tuchin '01, Kharzeev, YK, Tuchin '03.

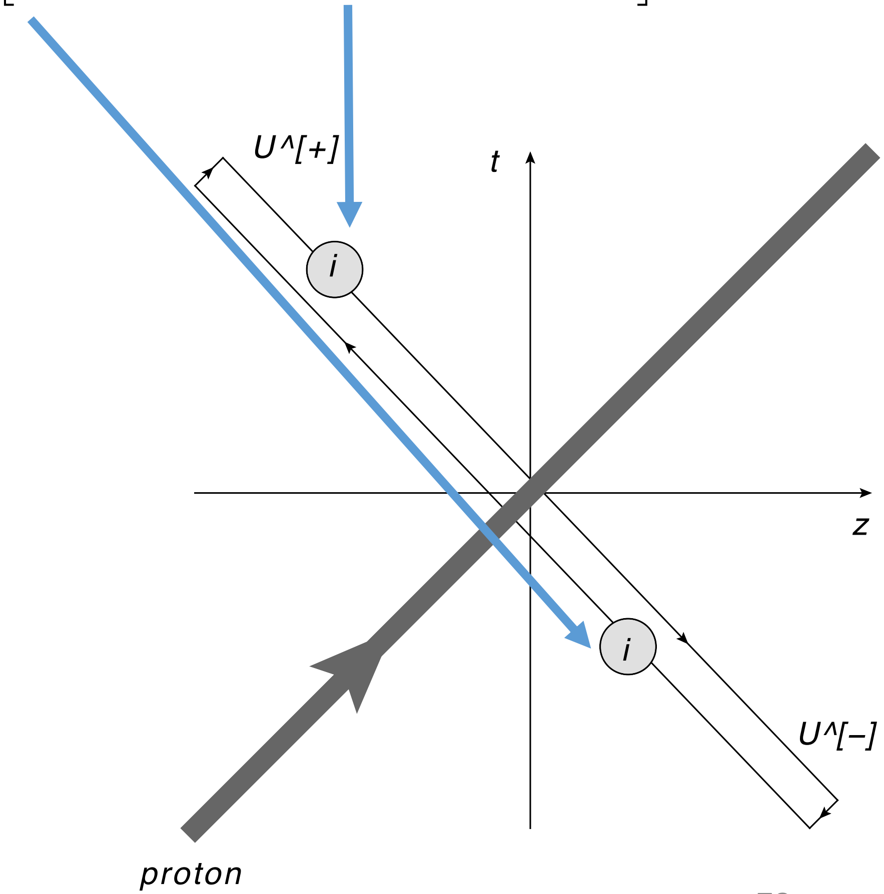

Dipole Gluon TMD

- One can show that the gluon dipole TMD at small *x* is indeed related to the dipole amplitude N= 1-S (Dominguez et al, ’11; M. Braun ’00; YK, Tuchin ‘01, Kharzeev, YK, Tuchin ’03):

$$f_1^{G\,dip}(x, k_T^2) = \frac{k_T^2\, N_c}{(2\pi)^3\, \pi\, \alpha_s\, x} \int d^2b\, d^2r\, e^{-i\vec{k}_\perp \cdot \vec{r}_\perp}\, S(\vec{r}_\perp, \vec{b}_\perp, Y = \ln(1/x))$$
$$= -\frac{k_T^2\, N_c}{(2\pi)^3\, \pi\, \alpha_s\, x} \int d^2b\, d^2r\, e^{-i\vec{k}_\perp \cdot \vec{r}_\perp}\, N(\vec{r}_\perp, \vec{b}_\perp, Y = \ln(1/x))$$

- The resulting small-*x* asymptotics is given by the BFKL evolution,

$$f_1^{G\,dip}(x, k_T^2) \sim \frac{1}{x}\, N(\vec{r}_\perp, \vec{b}_\perp, Y = \ln(1/x)) \sim \left(\frac{1}{x}\right)^{1+\frac{4\,\alpha_s\,N_c}{\pi}\,\ln 2+\mathcal{O}(\alpha_s^2)}$$

- The k_T dependence is also determined by the small-x evolution.

WW Gluon TMD

- Next consider the Weizsacker-Williams gluon TMD:

$$f_1^{G\,WW}(x, k_T^2) = \frac{2}{x\,P^+} \int \frac{d\xi^- \, d^2\xi}{(2\pi)^3} \, e^{ixP^+\,\xi^- - i\underline{k}\cdot\underline{\xi}} \, \langle P|\mathrm{tr}\left[F^{+i}(0)\,\mathcal{U}^{[+]}[0,\xi]\;F^{+i}(\xi)\,\mathcal{U}^{[+]\,\dagger}[\xi,0]\right]|P\rangle_{\xi^+=0}$$

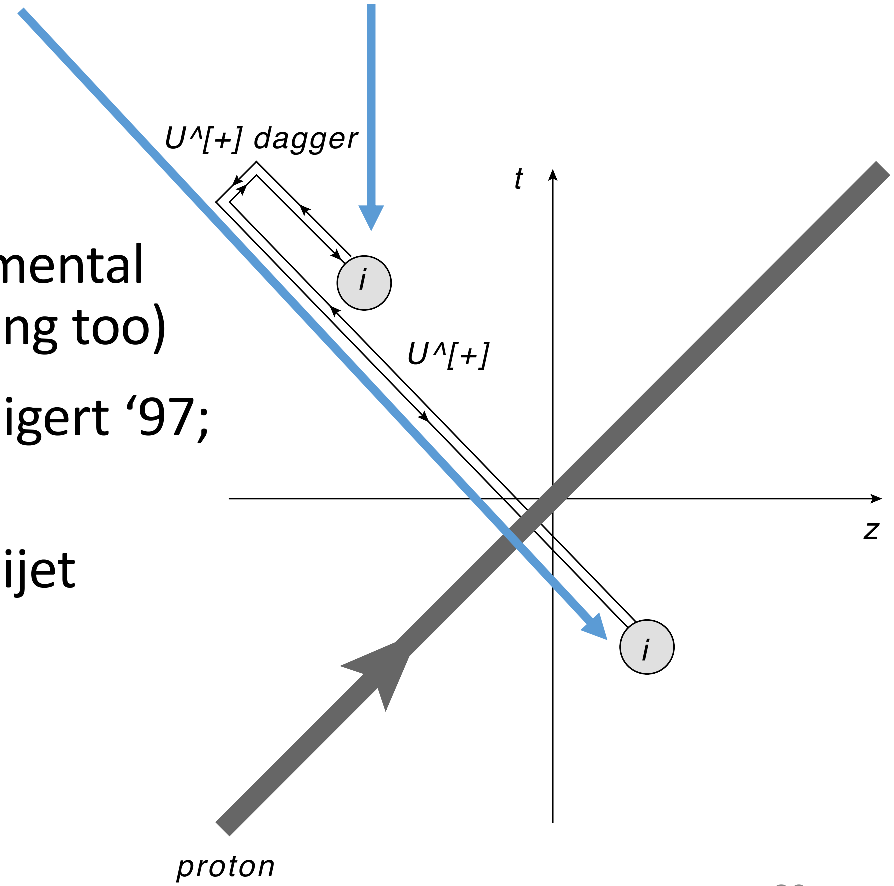

- Here $U^{[+]}$ is the future-pointing fundamental Wilson line staple (can use past-pointing too)
- Jalilian-Marian, Kovner, McLerran, Weigert '97; Dominguez, Marquet, Xiao, Yuan '11.
- WW gluon TMD can be measured in dijet production in DIS and in pA

WW Gluon TMD

- At small *x* the WW gluon TMD is proportional to a different object, now made out of 4 Wilson lines, the quadrupole amplitude Q:

$$Q(x_1, x_2, x_3, x_4) = \frac{1}{N_c} \langle \mathrm{tr}[V_1\, V_2^\dagger\, V_3\, V_4^\dagger] \rangle$$

- Small-*x* evolution for the quadrupole amplitude Q is given by an evolution equation different from BK. (Jalilian-Marian, YK '04; Dominguez, Mueller, Munier, Xiao '11.)

- In the linear regime the dipole amplitude Q obeys BFKL equation, such that the small-*x* asymptotics of the WW gluon TMD is the same as for the dipole gluon TMD:

$$f_1^{G\ WW}(x, k_T^2) \sim \frac{1}{x}\, Q \sim \left(\frac{1}{x} \right)^{1 + \frac{4\, \alpha_s\, N_c}{\pi}\ \ln 2 + \mathcal{O}(\alpha_s^2)}$$

- The difference between the two TMDs is inside the saturation region.

Linearly Polarized Gluon TMD

- If we keep the indices of the two F^{+i} different, we get access to the linearly polarized (WW) gluon TMD $h_1^\perp$ (Metz, Zhou, '11):

$$\frac{1}{P^+} \int \frac{d\xi^- \, d^2\xi}{(2\pi)^3} \, e^{ixP^+ \, \xi^- - i\underline{k}\cdot\underline{\xi}} \, \langle P|\mathrm{tr}\left[F^{+i}(0)\, \mathcal{U}^{[+]}[0,\xi] \, F^{+j}(\xi)\, \mathcal{U}^{[+]\,\dagger}[\xi,0]\right] |P\rangle_{\xi^+=0}$$

$$= \frac{1}{2}\, \delta^{ij} \, x \, f_1^{G\ WW}(x, k_T^2) + \frac{2k^i k^j - k_T^2 \, \delta^{ij}}{4\, k_T^2} \, x \, h_{1,\ WW}^\perp(x, k_T^2)$$

- The linearly polarized WW gluon TMD is thus also related to the color-quadrupole amplitude Q.
- In the linear (BFKL) regime the small-x asymptotics is the same,

$$h_{1,\ WW}^\perp(x, k_T^2) \sim \frac{1}{x} \, Q \sim \left(\frac{1}{x}\right)^{1 + \frac{4\,\alpha_s\, N_c}{\pi}\ \ln 2 + \mathcal{O}(\alpha_s^2)}$$

- For more on small-x evolution of the linear gluon polarization see the work by Dumitru, Skokov '17.

Quark Production in SIDIS at Small-x

- To find the unpolarized-nucleon quark TMDs at small-*x* it is convenient to start by considering the quark production cross section for SIDIS on an unpolarized nucleon.
- The dominant process is due to gluon exchanges, even at the lowest order:

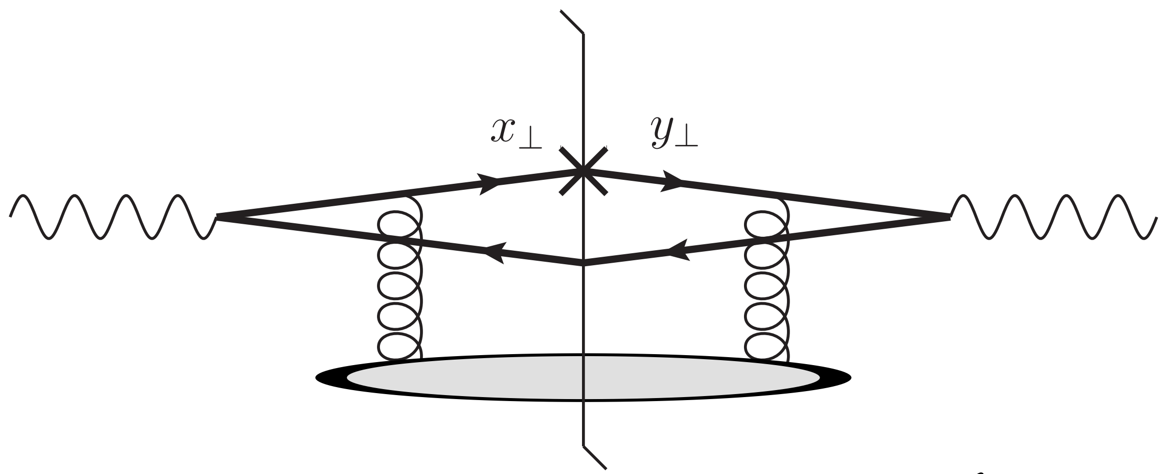

- Compared to the standard LO process, the one above comes in with an extra factor of

$$\sim \frac{\alpha_s}{x}$$

and is dominant at very low *x*.

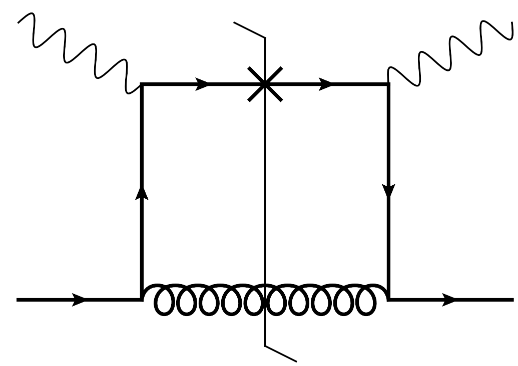

Unpolarized Quark TMD

- We conclude that the small-*x* asymptotics of the unpolarized quark TMD is (Mueller, 2003)

$$f_1^q(x, k_T^2) \sim \frac{1}{x}\, N \sim \left(\frac{1}{x}\right)^{1+\frac{4\,\alpha_s\,N_c}{\pi}\ \ln 2+\mathcal{O}(\alpha_s^2)}$$

Mini-Summary

- All the unpolarized quark and gluon TMDs for an unpolarized nucleon had the same *x*-dependence at small *x*,

$$\mathrm{TMD}^{q,G}_{unpolarized}(x, k_T^2) \sim \left(\frac{1}{x}\right)^{1+\frac{4\,\alpha_s\,N_c}{\pi}\,\ln 2+\mathcal{O}(\alpha_s^2)}$$

Sivers function

Sivers function

- Now let’s consider the Sivers TMD function (for quarks and gluons).

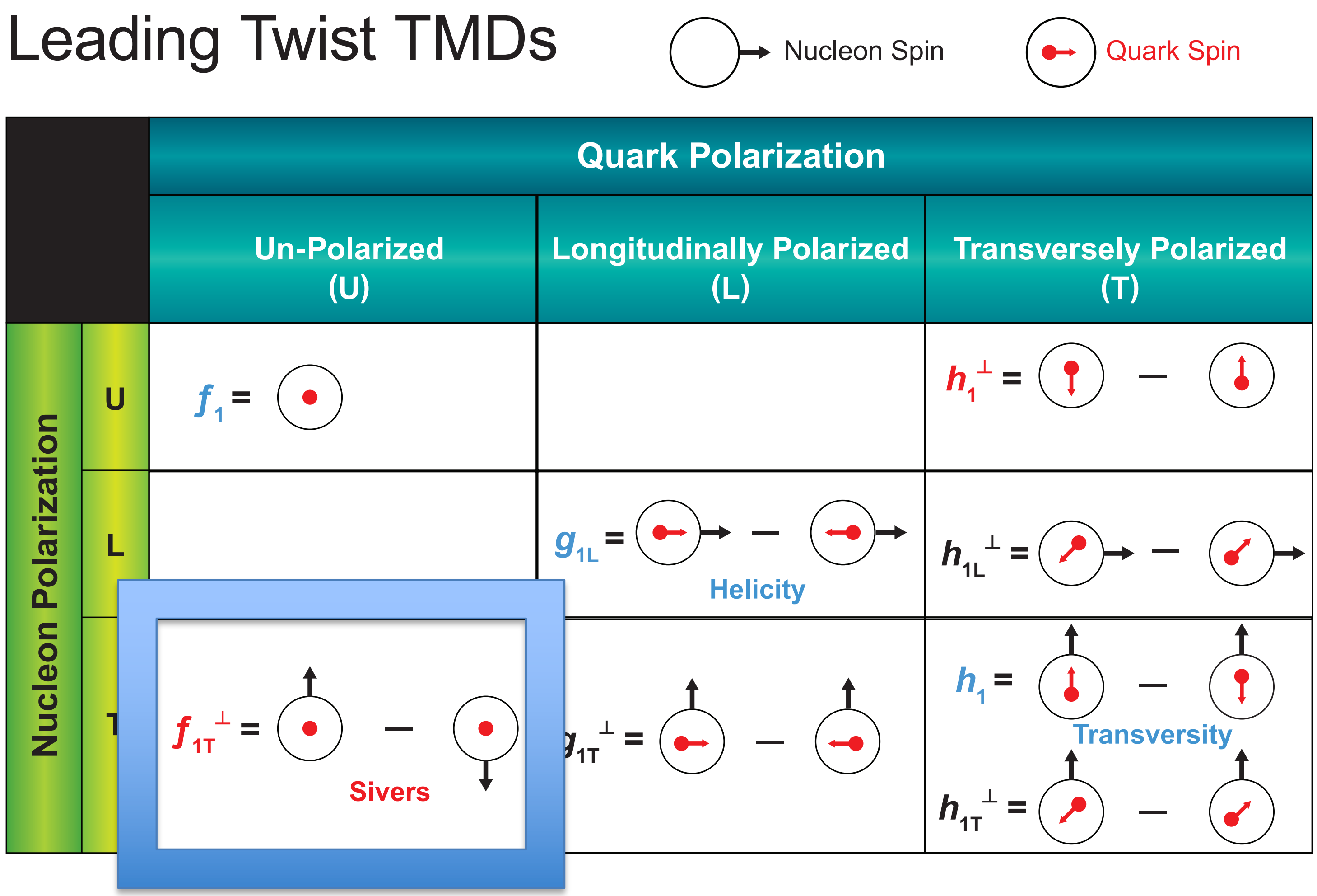

Sivers function

- Another TMD receiving an eikonal contribution is the Sivers function (quark or gluon one).

- Consider the quark Sivers function:

$$f_1^q(x, k_T^2) - \frac{\underline{k} \times \underline{S}_P}{M_P} f_{1\,T}^{\perp\,q}(x, k_T^2) = \int \frac{dr^- d^2 r_\perp}{2\,(2\pi)^3} e^{ik\cdot r} \langle P, S | \bar{\psi}(0) \mathcal{U}[0, r] \frac{\gamma^+}{2} \psi(r) | P, S \rangle$$

- The small-*x* asymptotics of the Sivers function is given by the odderon exchange (Boer, Echevarria, Mulders and Zhou ’15 (gluon); Dong, Zheng, Zhou ‘18; YK, Santiago ’21 (quark))

$$-\frac{\underline{k} \times \underline{S}_P}{M_P} f_{1\,T}^{\perp\,q}(x, k_T^2)\Big|_{\text{eikonal}} = \frac{4i\,N_c\,p_1^+}{(2\pi)^3} \int d^2\zeta_\perp d^2 w_\perp \frac{d^2 k_{1\perp} dk_1^-}{(2\pi)^3} e^{i(\underline{k}_1 + \underline{k})\cdot(\underline{w} - \underline{\zeta})} \theta(k_1^-)$$
$$\times \left[\frac{2\,\underline{k}\cdot\underline{k}_1}{(xp_1^+ k_1^- + \underline{k}_1^2)(xp_1^+ k_1^- + \underline{k}^2)} + \frac{\underline{k}_1^2}{(xp_1^+ k_1^- + \underline{k}_1^2)^2} \right] \mathcal{O}_{\underline{\zeta}\underline{w}}$$

Sivers function at small *x*

To determine the small-x asymptotics of the Sivers function (or any other TMD), one first rewrites its definition as follows, by inserting a complete set of states:

$$f_1^q(x, k_T^2) - \frac{\underline{k} \times \underline{S}_P}{M_P} f_{1\,T}^{\perp\,q}(x, k_T^2) = \frac{2p_1^+}{2(2\pi)^3} \sum_X \int d\xi^- d^2\xi_\perp d\zeta^- d^2\zeta_\perp e^{ik\cdot(\zeta-\xi)} \left[\frac{\gamma^+}{2}\right]_{\alpha\beta} \times \left\langle \bar{\psi}_\alpha(\xi) V_{\underline{\xi}}[\xi^-, \infty] | X \rangle \langle X | V_{\underline{\zeta}}[\infty, \zeta^-] \psi_\beta(\zeta) \right\rangle$$

One can then show that the following diagrams will dominate for the Sivers function (in the "shock wave" picture):

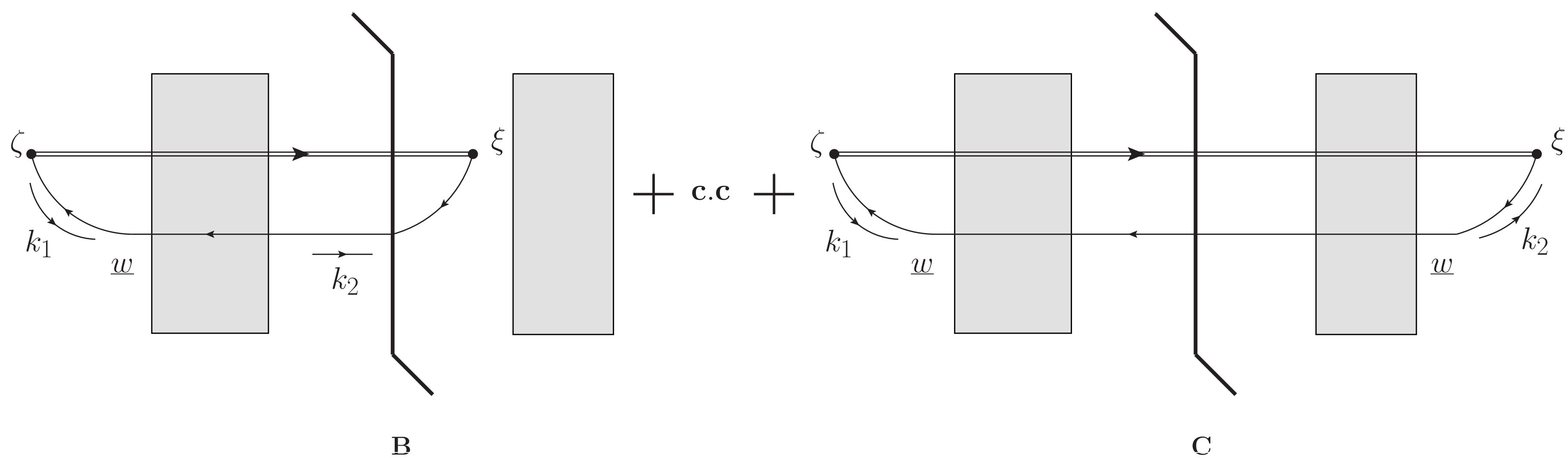

Odderon as a 3-gluon exchange

- In perturbation theory, the *C*-odd exchange can be due to
  - 1-gluon exchange: yes, it is *C*-odd, but not color-singlet, cannot give an elastic amplitude.
  - 2-gluon exchange: can be color-singlet, but not *C*-odd. (Each gluon has C=-1.)
  - 3 gluon exchange: can be both color-singlet and *C*-odd! That's the Odderon at the lowest order.

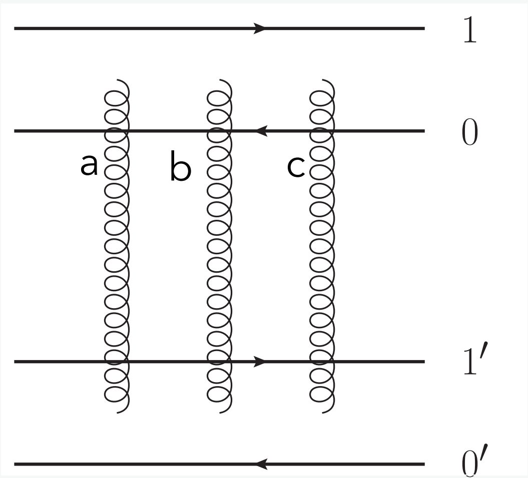

Note that the gluons must be in a symmetric d^{abc} color state ($d^{abc} = 2\,\mathrm{tr}[t^a\,\{t^b, t^c\}]$). If the color group was SU(2), there would be no Odderon.

Disconnected gluon lines imply sum over all possible gluon connections to the quark and anti-quark lines.

The BKP Equation

Bartels (1980),
Kwiecinski&Praszalowicz (1980)

The BFKL equation describes evolution of the 2-reggeized gluon system shown below (a *C*-even exchange)

The BKP equation describes evolution of an n-reggeized gluon system. For 3 reggeized gluons in d^{abc} color state it gives a *C*-odd exchange.

$$Y = \ln(s/\perp^2)$$

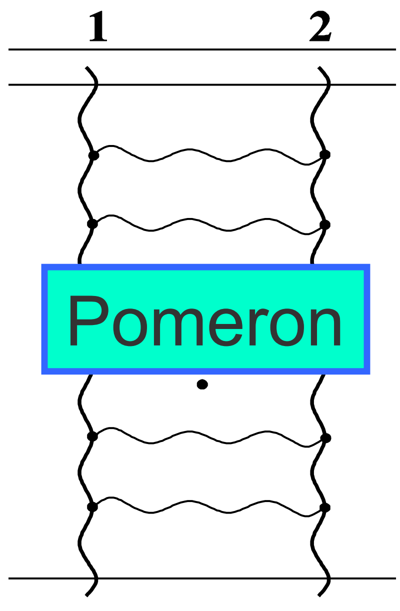

$$\frac{\partial f}{\partial Y} = K_{12} \otimes f$$

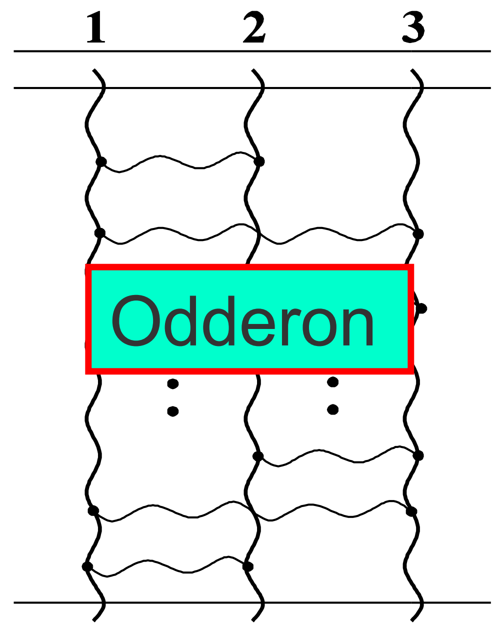

$$\frac{\partial O}{\partial Y} = K_{12} \otimes O + K_{23} \otimes O + K_{31} \otimes O$$

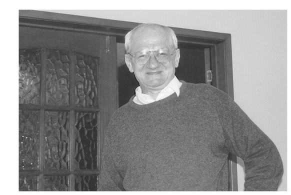

Jan Kwiecinski 1938 - 2003

...absolutely the kindest man I have ever met in my whole life. ....
CERN Courier, Jan-Feb 2004

Odderon Evolution Equation

One can easily write down an evolution equation for the odderon amplitude in the dipole model.

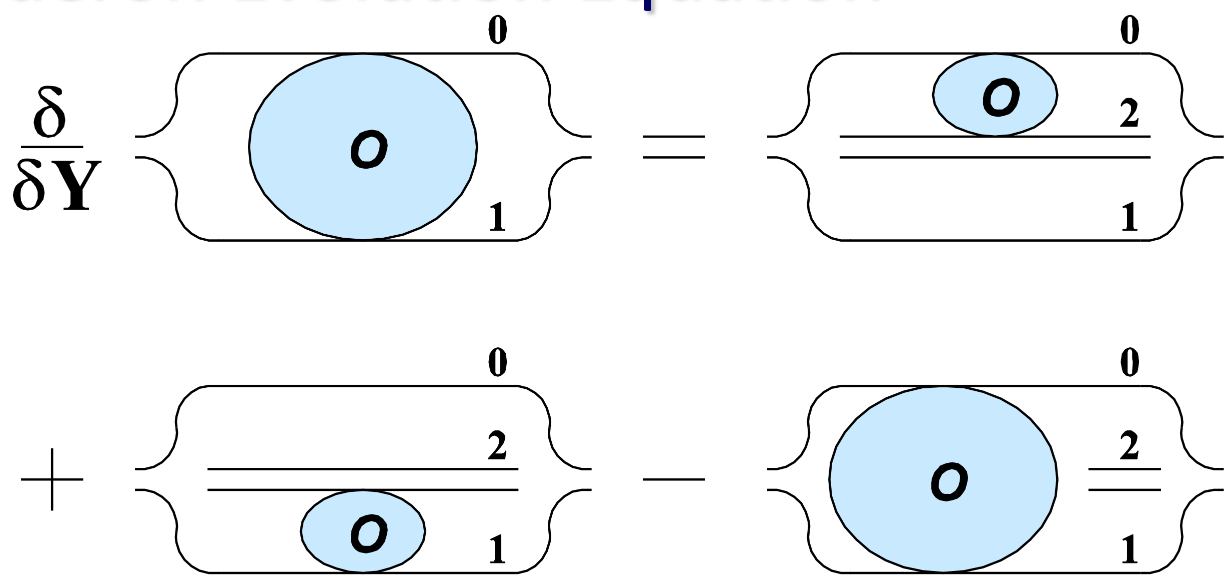

$$\frac{\partial O(\underline{x}_0,\underline{x}_1,Y)}{\partial Y} = \frac{\alpha_S N_C}{2\pi^2}\int d^2x_2\, \frac{x_{01}^2}{x_{02}^2\, x_{12}^2}\left[O(\underline{x}_0,\underline{x}_2,Y)+O(\underline{x}_2,\underline{x}_1,Y)-O(\underline{x}_0,\underline{x}_1,Y)\right]$$

YK, L. Szymanowski, S. Wallon 2003;
Y. Hatta, E. Iancu, K. Itakura, L. McLerran, 2005;
A. Kovner and M. Lublinsky, 2005.

This is the same evolution equation as for the BFKL Pomeron in the dipole model!
The difference is in the C-odd initial conditions for the odderon.

$$\frac{1}{N_c}\left\langle \mathrm{Ttr}[V_{\underline{x}} V_{\underline{y}}^\dagger]\right\rangle = \mathcal{S}_{\underline{x}\underline{y}} + i\,\mathcal{O}_{\underline{x}\underline{y}}$$

Pomeron is C-even: $\mathcal{S}_{\underline{x}\underline{y}} = \mathcal{S}_{\underline{y}\underline{x}}$ Odderon is C-odd: $\mathcal{O}_{\underline{x}\underline{y}} = -\mathcal{O}_{\underline{y}\underline{x}}$

Odderon high-energy asymptotics

$$\mathcal{O}_{10}(s) \sim s^{\alpha_{odd}-1}$$

- BLV solution: $\alpha_{odd} - 1 = \mathcal{O}(\alpha_s^2)$
- At NLO it turns out that the intercept is still zero (YK, 2012; C. Marquet): $\alpha_{odd} - 1 = \mathcal{O}(\alpha_s^3)$
- The intercept is shown to be zero at any order in the coupling at large N_C (S. Caron-Huot, 2013):

$$\alpha_{odd} - 1 = \mathcal{O}\left(\frac{1}{N_c}\right)$$

- In AdS/CFT, several intercepts were found, but zero was still the leading one (R. C. Brower, M. Djuric, and C.-I. Tan, 2009):

$$\alpha_{odd} - 1 = \mathcal{O}\left(\frac{1}{\lambda}\right), \quad \lambda = g^2 N_c$$

- It appears likely that the Odderon intercept is exactly zero in QCD and *N*=4 SYM. Not clear why. Is there a symmetry that protects it?

Small-x asymptotics of the Sivers function

The leading (eikonal) small-x asymptotics is
(Boer, Echevarria, Mulders and Zhou ’15 (gluon); Dong, Zheng, Zhou ‘18 (quark))

$$f_{1\,T}^{\perp\,G}(x, k_T^2) \sim \frac{1}{x} \qquad\qquad f_{1\,T}^{\perp\,q}(x, k_T^2) \sim \frac{1}{x}$$

Sub-eikonal (suppressed by x) correction to the quark Sivers function has been calculated recently (YK, Santiago ‘21). The power (intercept) is also an integer…

$$f_{1\,T}^{\perp\,q}(x, k_T^2) = C_O(x, k_T^2)\,\frac{1}{x} + C_1(k_T^2)\,\left(\frac{1}{x}\right)^0 + \ldots$$

Eikonality

- One can classify various TMDs by their small-*x* asymptotics.
- Eikonal behavior corresponds to (up to ~α_S corrections in the power)

$$f(x, k_T^2) \sim \frac{1}{x}$$

  Examples: unpolarized TMDs, Sivers function for gluons and quarks.
- Sub-eikonal behavior corresponds to

$$g(x, k_T^2) \sim \left(\frac{1}{x}\right)^0 = \text{const}$$

  Example: helicity TMDs.
- Sub-sub-eikonal behavior is $h(x, k_T^2) \sim x$
  Example: transversity.

- We've been calling the leading power of x "eikonality".

Helicity

Observables

- We want to calculate quark helicity PDF and TMD at small x.

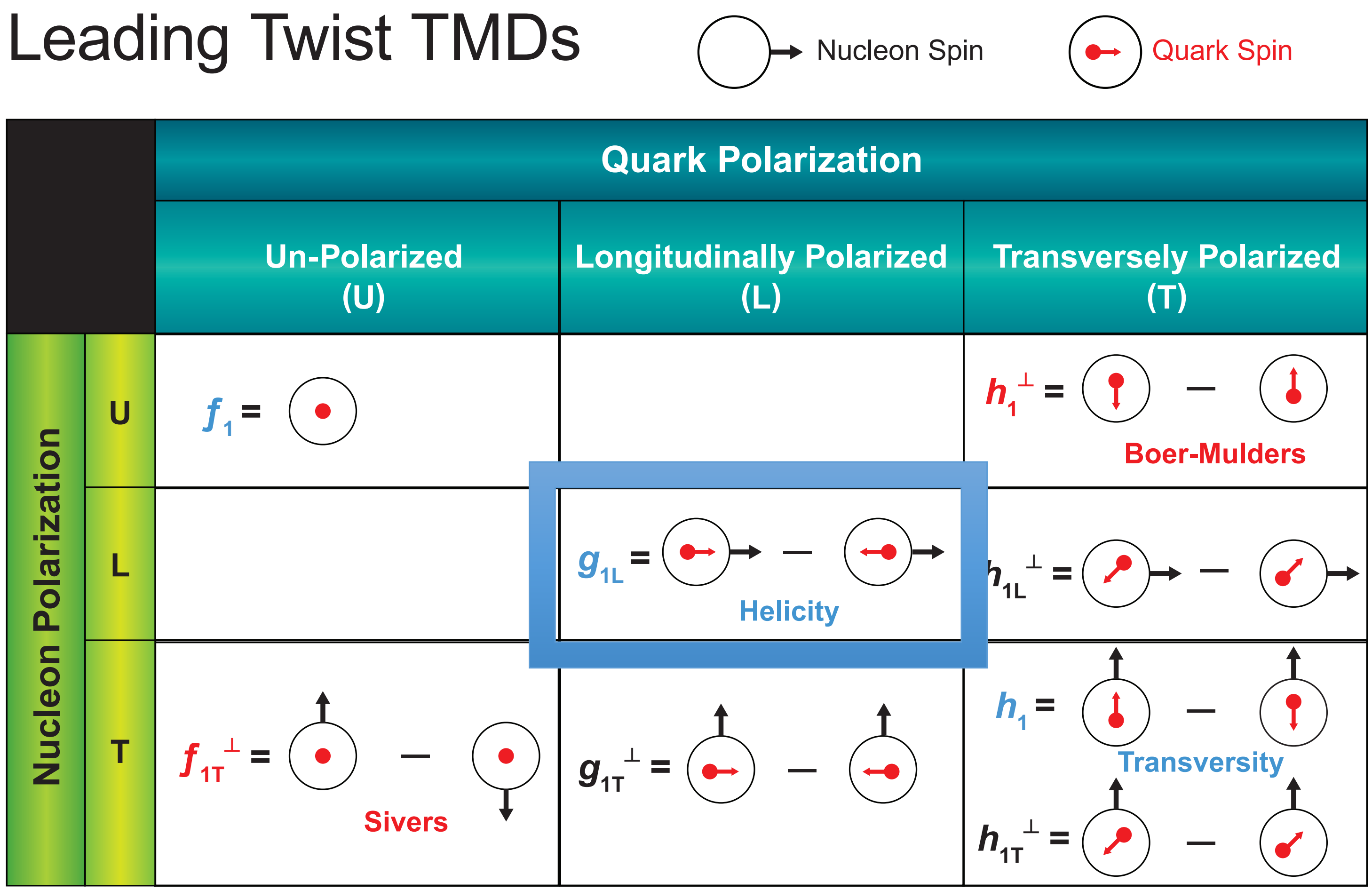

Quark Helicity TMD

- We start with the definition of the quark helicity TMD with a future-pointing Wilson line staple.

$$g_{1L}^q(x, k_T^2) = \frac{1}{(2\pi)^3} \frac{1}{2} \sum_{S_L} S_L \int d^2r\, dr^- \; e^{ik\cdot r} \langle p, S_L | \bar{\psi}(0)\, \mathcal{U}[0, r] \, \frac{\gamma^+ \gamma^5}{2} \, \psi(r) | p, S_L \rangle_{r^+=0}$$

- At small-x, in anticipation of the shock-wave formalism, we rewrite the quark helicity TMD as (in A^-=0 gauge for the + moving proton)

$$g_{1L}^q(x, k_T^2) = \frac{2p^+}{(2\pi)^3} \int d^2\zeta\, d\zeta^- \, d^2\xi\, d\xi^- \; e^{ik\cdot(\zeta-\xi)} \left(\frac{1}{2}\gamma^+\gamma^5\right)_{\alpha\beta} \left\langle \bar{\psi}_\alpha(\xi)\, V_{\underline{\xi}}[\xi^-, \infty] \;\; V_{\underline{\zeta}}[\infty, \zeta^-]\, \psi_\beta(\zeta) \right\rangle$$

where the fundamental light-cone Wilson line is

$$V_{\underline{x}}[b^-, a^-] = \mathrm{P} \exp \left\{ ig \int\limits_{a^-}^{b^-} dx^- \; A^+(x^-, \underline{x}) \right\}$$

Quark Helicity TMD

Space-time representation of the quark helicity TMD definition.

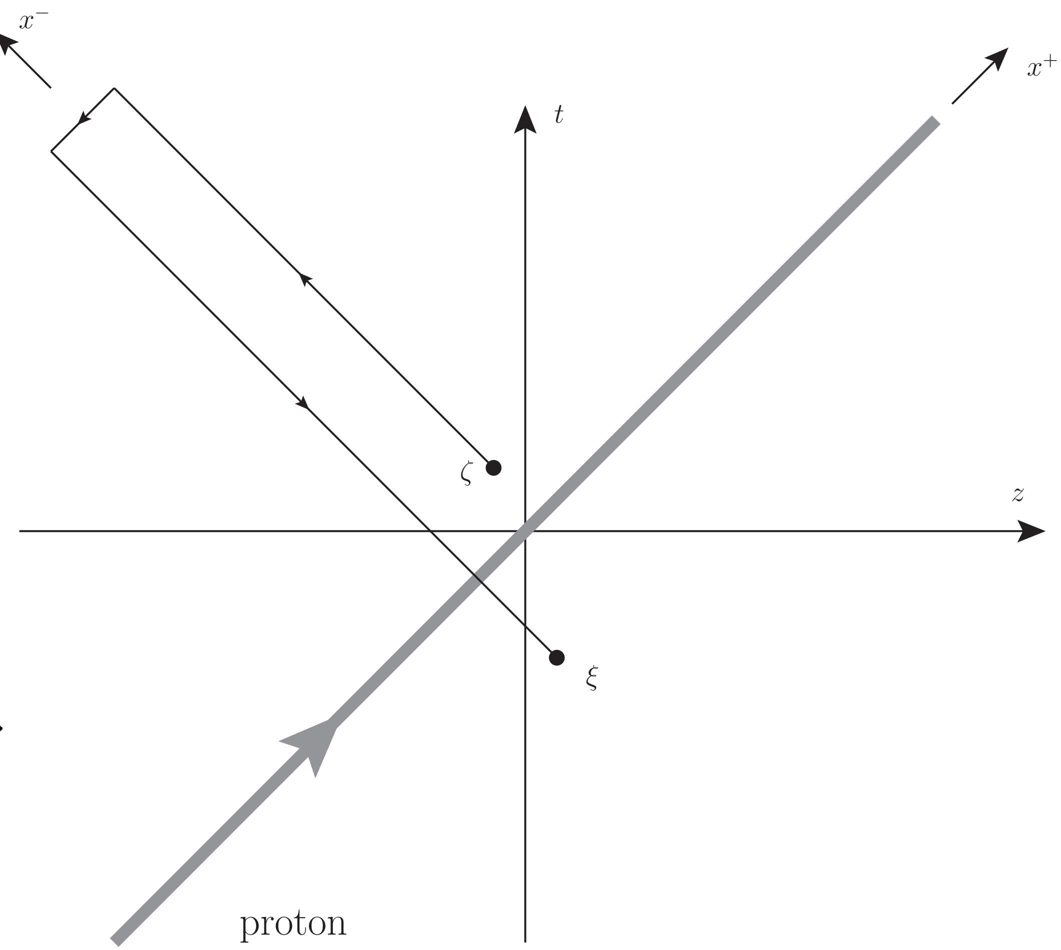

$$V_{\underline{x}}[b^-, a^-] = \mathrm{P}\exp\left\{ ig \int\limits_{a^-}^{b^-} dx^- \, A^+(x^-, \underline{x}) \right\}$$

$$g_{1L}^q(x, k_T^2) = \frac{2p^+}{(2\pi)^3} \int d^2\zeta \, d\zeta^- \, d^2\xi \, d\xi^- \, e^{ik\cdot(\zeta-\xi)} \left(\frac{1}{2}\gamma^+\gamma^5 \right)_{\alpha\beta} \left\langle \bar{\psi}_\alpha(\xi) \, V_{\underline{\xi}}[\xi^-, \infty] \;\, V_{\underline{\zeta}}[\infty, \zeta^-] \, \psi_\beta(\zeta) \right\rangle$$

Quark Helicity TMD at Small x

- At high energy/small-x the proton is a shock wave, and we have the following contributions to the SIDIS quark helicity TMD:

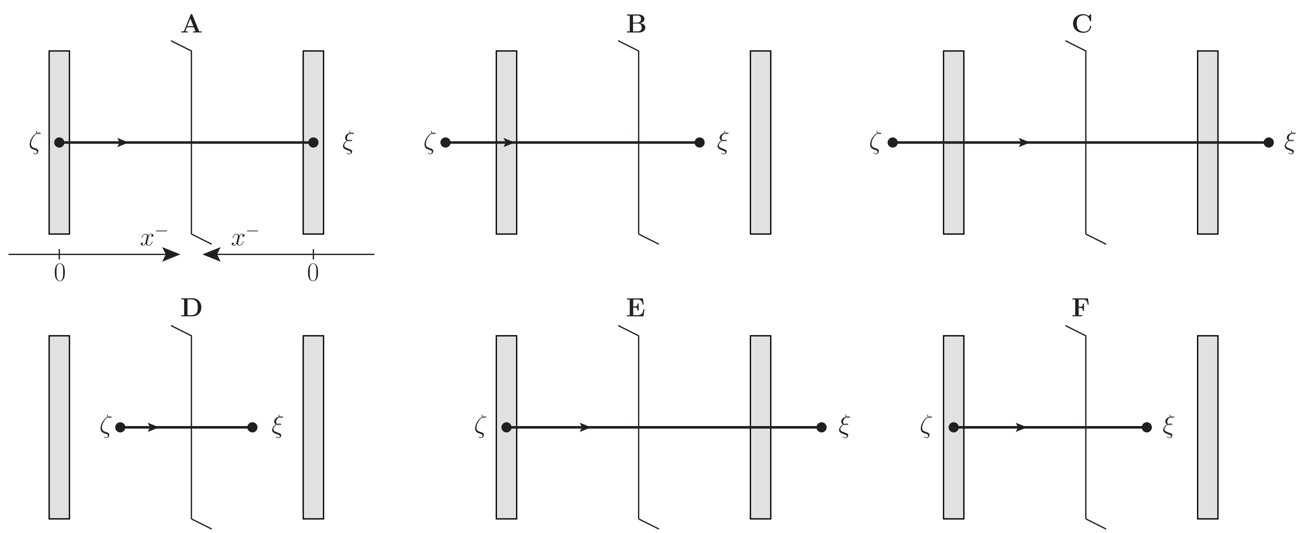

$$g_{1L}^{q}(x,k_T^2)=\frac{2p^+}{(2\pi)^3}\sum_X\int d^2\zeta\,d\zeta^-\,d^2\xi\,d\xi^-\,e^{ik\cdot(\zeta-\xi)}\left(\tfrac{1}{2}\gamma^+\gamma^5\right)_{\alpha\beta}\left\langle\bar{\psi}_\alpha(\xi)\,V_{\underline{\xi}}[\xi^-,\infty]\,|X\rangle\;\langle X|\,V_{\underline{\zeta}}[\infty,\zeta^-]\,\psi_\beta(\zeta)\right\rangle$$

Quark Helicity TMD at Small x

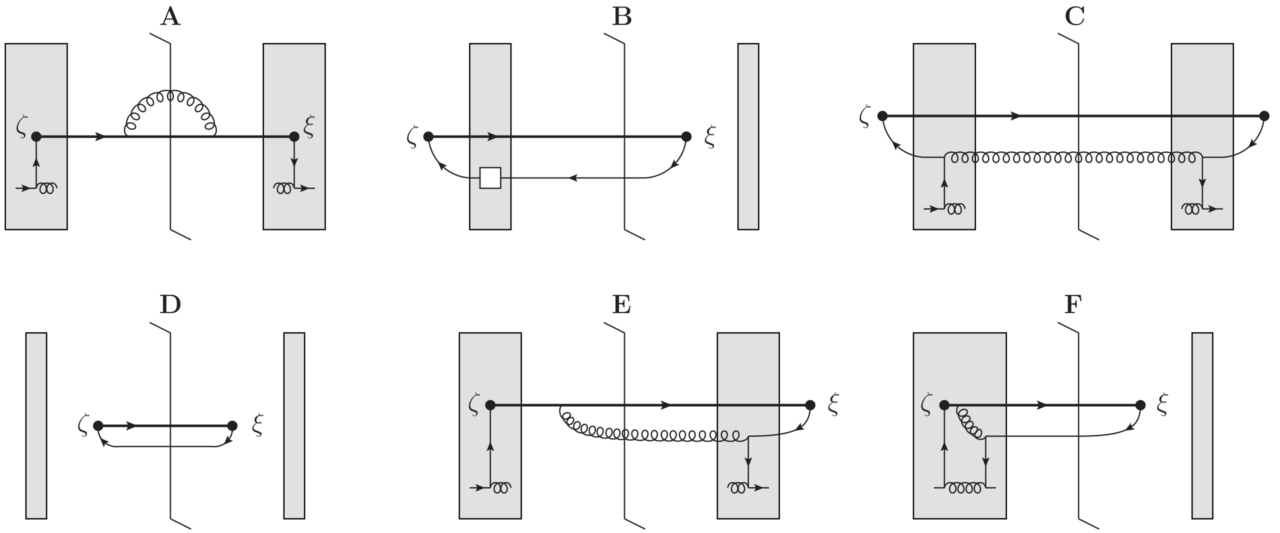

- Diagram D does not transfer spin information from the target. Diagram C is canceled as we move t-channel quarks across the cut.
- Diagram F is energy-suppressed, since the gluon should have no time to be emitted and absorbed inside the shock wave.
- Diagrams of the types A and E++ can be shown to cancel each other at the leading (DLA) order (Ward identity).
- We are left with the diagram B.

Quark Helicity TMD at Small x

- Only one diagram contributes, giving

$$g_{1L}^{q}(x, k_T^2) = \frac{4N_c}{(2\pi)^6} \int d^2\zeta \, d^2w \, d^2y \, e^{-i\underline{k}\cdot(\underline{\zeta}-\underline{y})} \int\limits_{\Lambda^2/s}^{1} \frac{dz}{z} \, \frac{\underline{\zeta}-\underline{w}}{|\underline{\zeta}-\underline{w}|^2} \cdot \frac{\underline{y}-\underline{w}}{|\underline{y}-\underline{w}|^2} \, G_{\underline{w},\underline{\zeta}}(zs)$$

  where $G_{w\zeta}$ is the polarized dipole amplitude (defined on the next slide).

- Here s is the cms energy squared, Λ is some IR cutoff, underlining denotes transverse vectors, z = smallest longitudinal momentum fraction of the probe minus momentum out of those carried by the quark and the antiquark

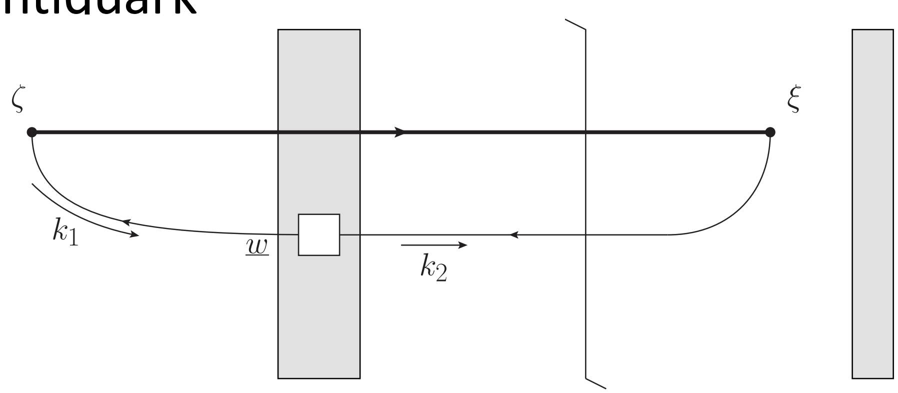

Polarized Dipole

- All flavor-singlet small-x helicity observables depend on one object, "polarized dipole amplitude":

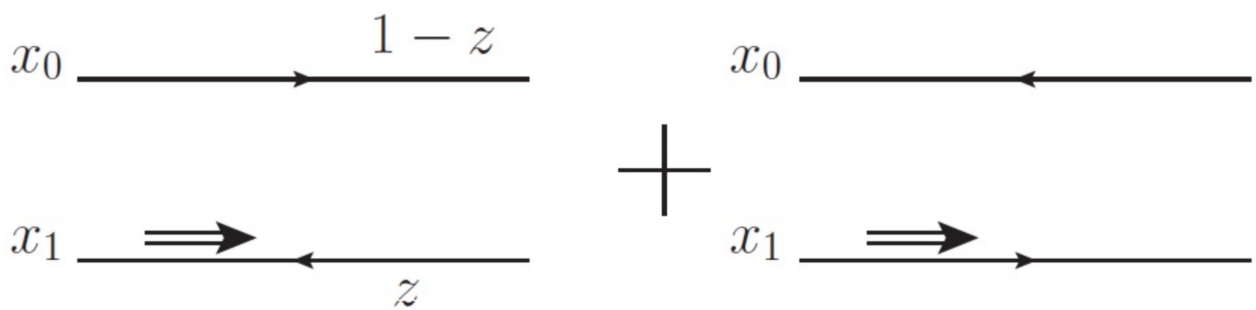

$$G_{10}(z) \equiv \frac{1}{2N_c} \text{Re} \left\langle\!\!\left\langle \text{T tr} \left[V_{\underline{0}} V_{\underline{1}}^{pol\,\dagger} \right] + \text{T tr} \left[V_{\underline{1}}^{pol} V_{\underline{0}}^{\dagger} \right] \right\rangle\!\!\right\rangle (z)$$

unpolarized quark

polarized quark: eikonal propagation, non-eikonal spin-dependent interaction

$$V_{\underline{x}} \equiv \mathcal{P} \exp \left[ig \int\limits_{-\infty}^{\infty} dx^+ \, A^-(x^+, 0^-, \underline{x}) \right]$$

- Double brackets denote an object with energy suppression scaled out:

$$\left\langle\!\!\left\langle \mathcal{O} \right\rangle\!\!\right\rangle (z) \equiv zs \left\langle \mathcal{O} \right\rangle (z)$$

Polarized fundamental "Wilson line"

- To complete the definition of the polarized dipole amplitude, we need to construct the definition of the polarized "Wilson line" V^{pol}, which is the leading helicity-dependent contribution for the quark scattering amplitude on a longitudinally-polarized target proton.

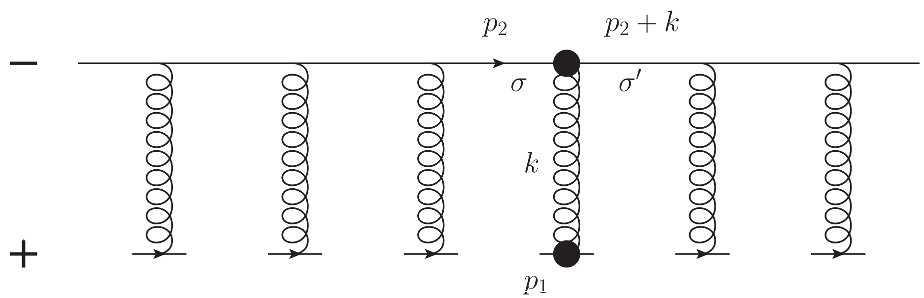

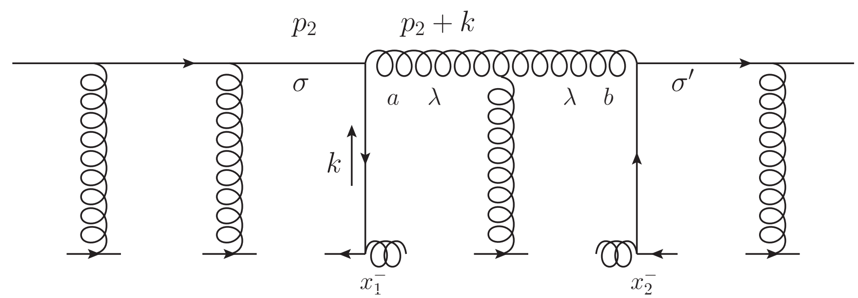

- At the leading order we can either exchange one non-eikonal t-channel gluon (with quark-gluon vertices denoted by blobs above) to transfer polarization between the projectile and the target, or two t-channel quarks, as shown above.

Polarized fundamental "Wilson line"

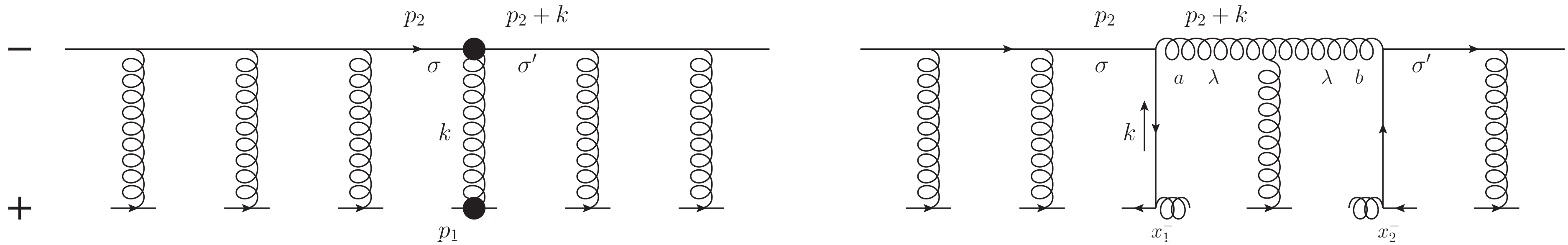

- In the end one arrives at (KPS '17; YK, Sievert, '18; cf. Chirilli '18)

$$V_{\underline{x}}^{pol} = \frac{igp_1^+}{s} \int\limits_{-\infty}^{\infty} dx^- \, V_{\underline{x}}[+\infty, x^-] \, F^{12}(x^-, \underline{x}) \, V_{\underline{x}}[x^-, -\infty]$$

$$- \frac{g^2 \, p_1^+}{s} \int\limits_{-\infty}^{\infty} dx_1^- \int\limits_{x_1^-}^{\infty} dx_2^- \, V_{\underline{x}}[+\infty, x_2^-] \, t^b \, \psi_\beta(x_2^-, \underline{x}) \, U_{\underline{x}}^{ba}[x_2^-, x_1^-] \left[\frac{1}{2} \, \gamma^+ \, \gamma^5\right]_{\alpha\beta} \bar{\psi}_\alpha(x_1^-, \underline{x}) \, t^a \, V_{\underline{x}}[x_1^-, -\infty].$$

- We have employed an adjoint light-cone Wilson line

$$U_{\underline{x}}[b^-, a^-] = \mathcal{P} \exp \left[ig \int\limits_{a^-}^{b^-} dx^- \, \mathcal{A}^+(x^+ = 0, x^-, \underline{x}) \right]$$

- Note the simple physical meaning of the first term:

$$-\vec{\mu} \cdot \vec{B} = -\mu_z \, B_z = \mu_z \, F^{12}$$

Polarized Dipole Amplitude

- The polarized dipole amplitude is then defined by

$$\sim F^{12}$$

$$G_{10}(z) \equiv \frac{1}{4N_c} \int\limits_{-\infty}^{\infty} dx^- \left\langle \text{tr} \left[V_{\underline{0}}[\infty, -\infty] V_{\underline{1}}[-\infty, x^-] \, (-ig) \, \underline{\nabla} \times \underline{\tilde{A}}(x^-, \underline{x}) \, V_{\underline{1}}[x^-, \infty] \right] + \text{c.c.} \right\rangle (z)$$

with the standard light-cone Wilson line

$$V_{\underline{x}}[b^-, a^-] = \text{P} \exp \left\{ ig \int\limits_{a^-}^{b^-} dx^- \, A^+(x^-, \underline{x}) \right\}$$

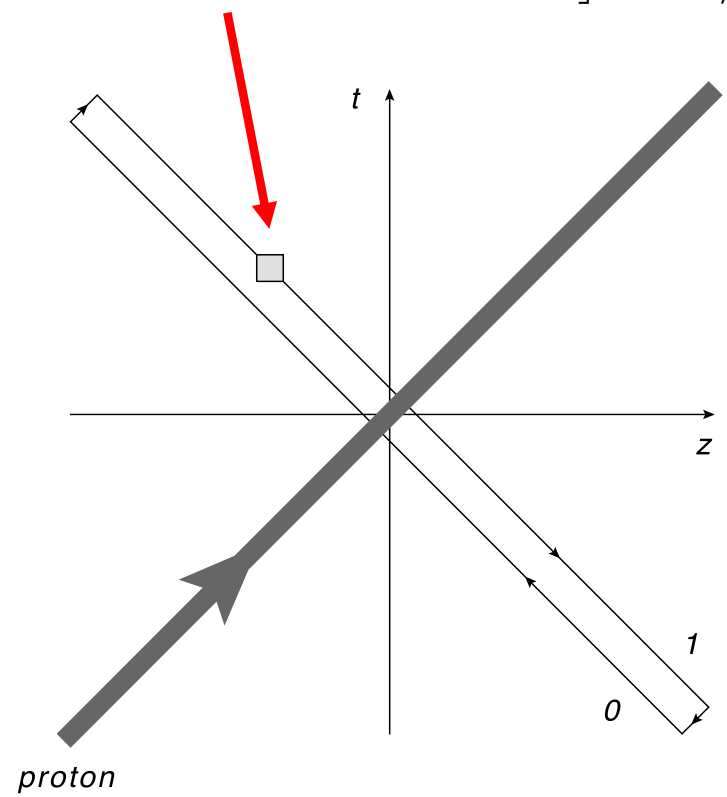

Polarized adjoint “Wilson line”

- Quarks mix with gluons. Therefore, we need to construct the adjoint polarized Wilson line --- the leading helicity-dependent part of the gluon scattering amplitude on the longitudinally polarized target.

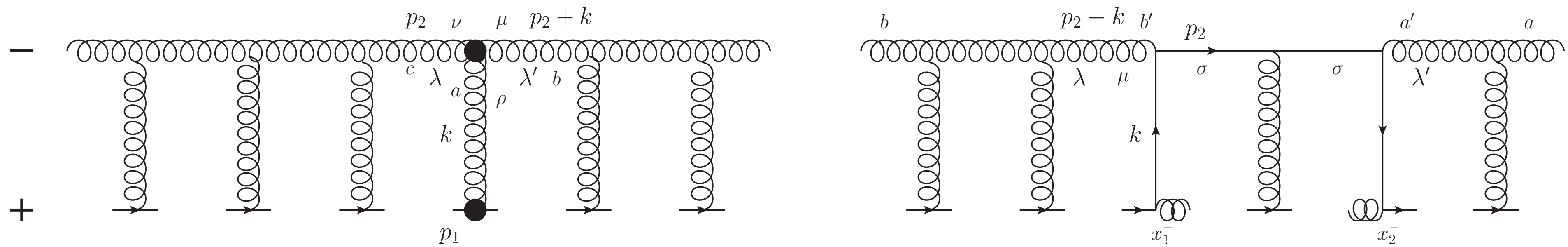

- The calculation is similar to the quark scattering case.
It yields (YK, Sievert, ‘18; cf. Chirilli ‘18)

$$(U_{\underline{x}}^{pol})^{ab} = \frac{2i\, g\, p_1^+}{s} \int\limits_{-\infty}^{+\infty} dx^- \ \left(U_{\underline{x}}[+\infty, x^-]\, \mathcal{F}^{12}(x^+ = 0, x^-, \underline{x})\, U_{\underline{x}}[x^-, -\infty] \right)^{ab}$$

$$- \frac{g^2\, p_1^+}{s} \int\limits_{-\infty}^{\infty} dx_1^- \int\limits_{x_1^-}^{\infty} dx_2^-\, U_{\underline{x}}^{aa'}[+\infty, x_2^-]\, \bar{\psi}(x_2^-, \underline{x})\, t^{a'}\, V_{\underline{x}}[x_2^-, x_1^-]\, \frac{1}{2}\, \gamma^+ \gamma_5\, t^{b'}\, \psi(x_1^-, \underline{x})\, U_{\underline{x}}^{b'b}[x_1^-, -\infty] - \text{c.c.}$$

Evolution for Polarized Quark Dipole

One can construct an evolution equation for the polarized dipole:

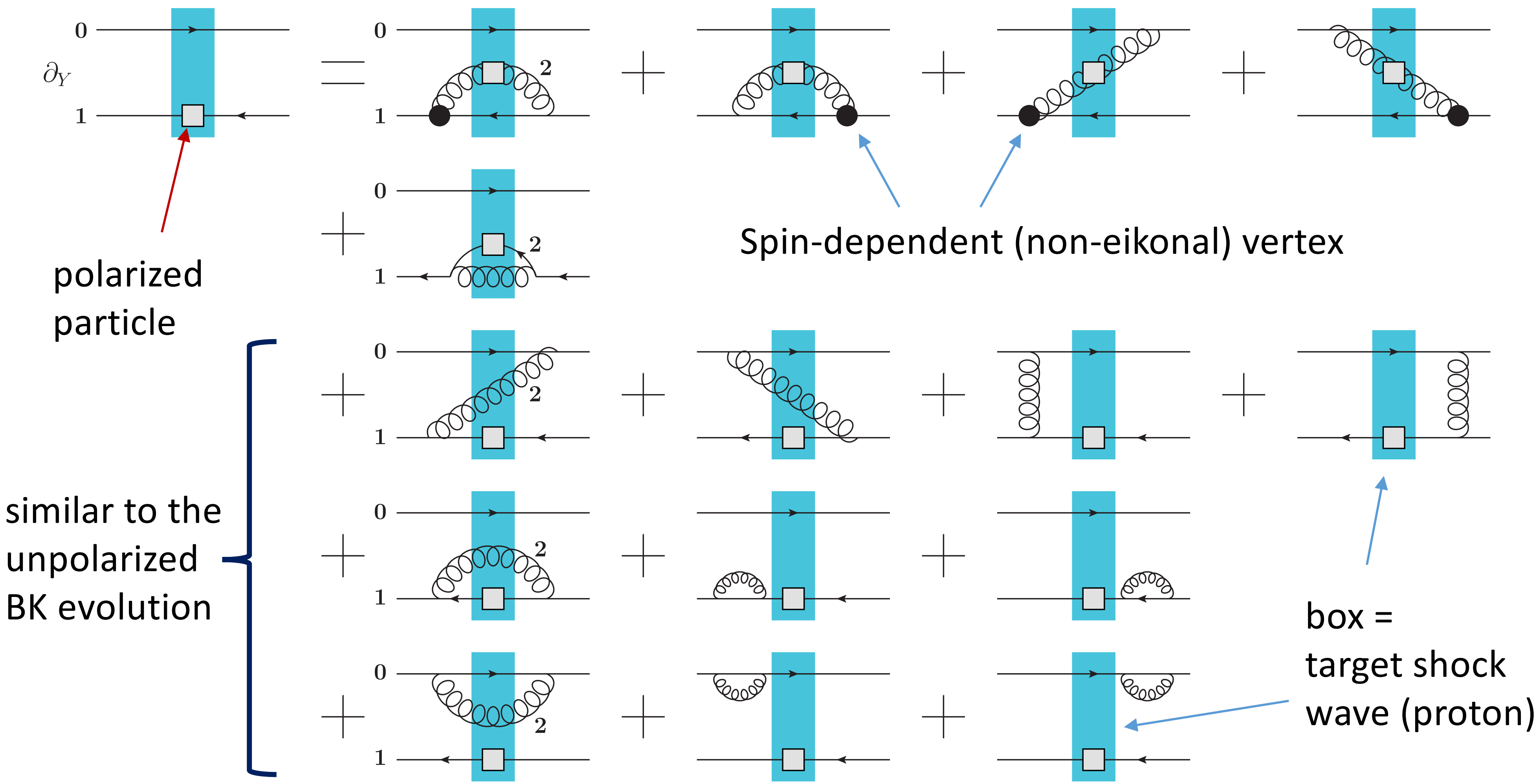

Evolution for Polarized Quark Dipole

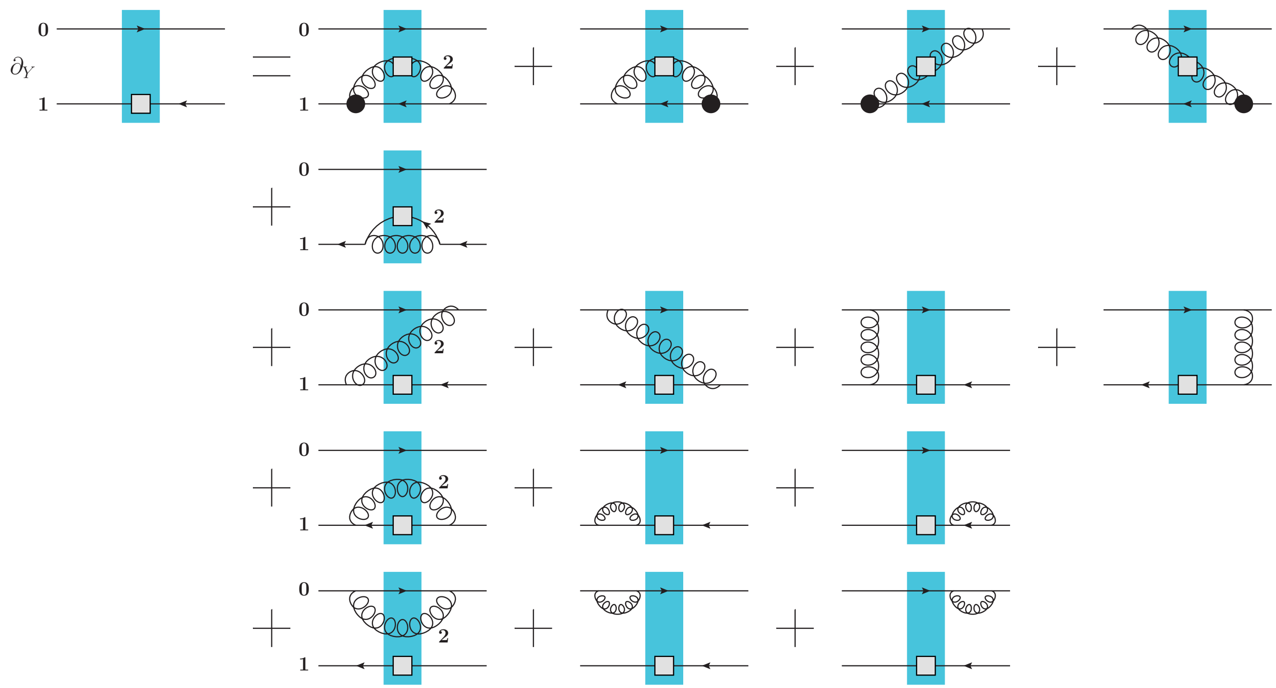

$$\langle\langle \ldots \rangle\rangle = \frac{1}{z\, s} \langle \ldots \rangle$$

$$\rho'^{\,2} = \frac{1}{z'\, s}$$

$$\frac{1}{N_c} \left\langle\!\!\left\langle \mathrm{tr}\left[V_0^{unp}\, V_1^{pol\,\dagger} \right] \right\rangle\!\!\right\rangle (z) = \frac{1}{N_c} \left\langle\!\!\left\langle \mathrm{tr}\left[V_0^{unp}\, V_1^{pol\,\dagger} \right] \right\rangle\!\!\right\rangle_0 (z) + \frac{\alpha_s}{2\pi^2} \int\limits_{z_i}^{z} \frac{dz'}{z'} \int\limits_{\rho'^2} \frac{d^2 x_2}{x_{21}^2}$$

$$\times \Bigg\{ \theta(x_{10} - x_{21})\, \frac{2}{N_c} \left\langle\!\!\left\langle \mathrm{tr}\left[t^b\, V_0^{unp}\, t^a\, V_1^{unp\,\dagger} \right] \, U_2^{pol\; ba} \right\rangle\!\!\right\rangle (z')$$

$$+ \theta(x_{10}^2 z - x_{21}^2 z')\, \frac{1}{N_c} \left\langle\!\!\left\langle \mathrm{tr}\left[t^b\, V_0^{unp}\, t^a\, V_2^{pol\,\dagger} \right] \, U_1^{unp\; ba} \right\rangle\!\!\right\rangle (z')$$

$$+ \theta(x_{10} - x_{21})\, \frac{1}{N_c} \left[\left\langle\!\!\left\langle \mathrm{tr}\left[V_0^{unp}\, V_2^{unp\,\dagger} \right] \, \mathrm{tr}\left[V_2^{unp}\, V_1^{pol\,\dagger} \right] \right\rangle\!\!\right\rangle (z') - N_c \left\langle\!\!\left\langle \mathrm{tr}\left[V_0^{unp}\, V_1^{pol\,\dagger} \right] \right\rangle\!\!\right\rangle (z') \right] \Bigg\}$$

Equation does not close!

Polarized Dipole Evolution in the Large-N_c Limit

In the large-N_c limit the equations close, leading to a system of 2 equations:

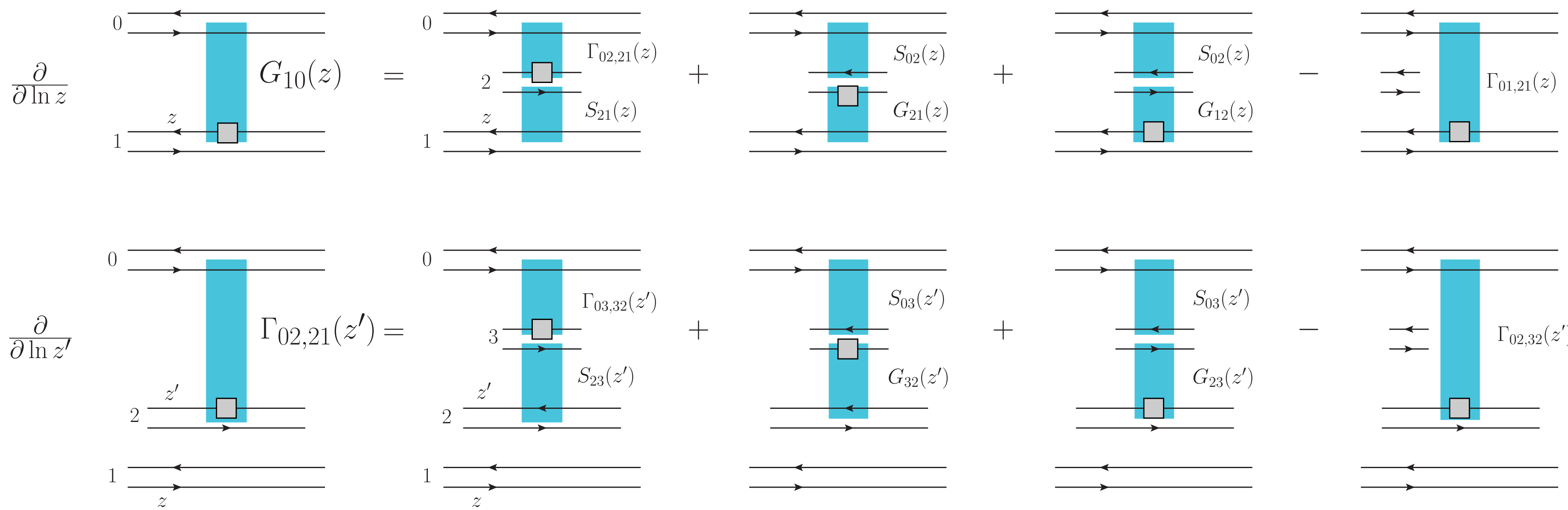

$$G_{10}(z) = G_{10}^{(0)}(z) + \frac{\alpha_s N_c}{2\pi} \int\limits_{z_i}^{z} \frac{dz'}{z'} \int\limits_{\rho'^2}^{x_{10}^2} \frac{dx_{21}^2}{x_{21}^2} \left[2\,\Gamma_{02,\,21}(z')\, S_{21}(z') + 2\, G_{21}(z')\, S_{02}(z') + G_{12}(z')\, S_{02}(z') - \Gamma_{01,\,21}(z') \right]$$

$$\Gamma_{02,\,21}(z') = \Gamma_{02,\,21}^{(0)}(z') + \frac{\alpha_s N_c}{2\pi} \int\limits_{z_i}^{z'} \frac{dz''}{z''} \int\limits_{\rho''^2}^{\min\{x_{02}^2, x_{21}^2\, z'/z''\}} \frac{dx_{32}^2}{x_{32}^2} \left[2\,\Gamma_{03,\,32}(z'')\, S_{23}(z'') + 2\, G_{32}(z'')\, S_{03}(z'') + G_{23}(z'')\, S_{03}(z'') - \Gamma_{02,\,32}(z'') \right]$$

S = found from BK/JIMWLK, it is LLA

"Neighbor" dipole

- There is a new object in the evolution equation – **the neighbor dipole**.
- This is specific for the DLA evolution. Gluon emission may happen in one dipole, but, due to transverse distance ordering, may `know' about another dipole:

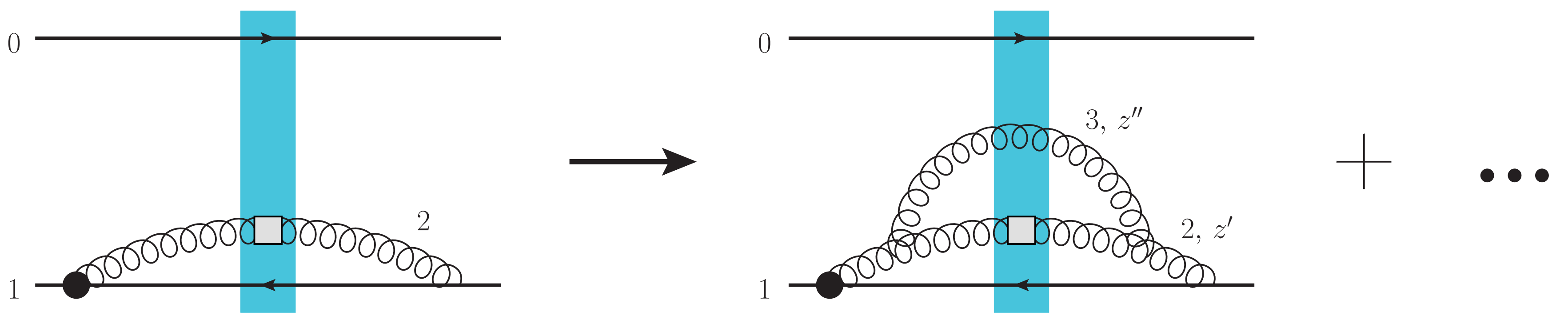

$$x_{21}^2\, z' \gg x_{32}^2\, z''$$

- We denote the evolution in the neighbor dipole 02 by $\Gamma_{02,\,21}(z')$

Resummation Parameter

- For helicity evolution the resummation parameter is different from BFKL, BK or JIMWLK, which resum powers of leading logarithms (LLA)

$$\alpha_s \ \ln(1/x)$$

- Helicity evolution resummation parameter is double-logarithmic (DLA):

$$\alpha_s \ \ln^2 \frac{1}{x}$$

- The second logarithm of x arises due to transverse momentum (or transverse coordinate) integration being logarithmic both in the UV and IR.

- This was known before: Kirschner and Lipatov ’83; Kirschner ’84; Bartels, Ermolaev, Ryskin ‘95, ‘96; Griffiths and Ross ’99; Itakura et al ’03; Bartels and Lublinsky ‘03.

Helicity and OAM asymptotics

- At large N_c we have obtained the following small-x asymptotics:

$$\Delta q(x, Q^2) \sim \left(\frac{1}{x}\right)^{\alpha_h^q} \quad \text{with} \quad \alpha_h^q = \frac{4}{\sqrt{3}} \sqrt{\frac{\alpha_s N_c}{2\pi}} \approx 2.31 \sqrt{\frac{\alpha_s N_c}{2\pi}}$$

$$\Delta G(x, Q^2) \sim \left(\frac{1}{x}\right)^{\alpha_h^G} \quad \text{with} \quad \alpha_h^G = \frac{13}{4\sqrt{3}} \sqrt{\frac{\alpha_s N_c}{2\pi}} \approx 1.88 \sqrt{\frac{\alpha_s N_c}{2\pi}}$$

$$L_{q+\bar{q}}(x, Q^2) = -\Delta\Sigma(x, Q^2) \sim \left(\frac{1}{x}\right)^{\frac{4}{\sqrt{3}} \sqrt{\frac{\alpha_s N_c}{2\pi}}},$$

$$L_G(x, Q^2) \sim \Delta G(x, Q^2) \sim \left(\frac{1}{x}\right)^{\frac{13}{4\sqrt{3}} \sqrt{\frac{\alpha_s N_c}{2\pi}}}$$

- At large N_c & N_f we have obtained

$$\Delta\Sigma(x, Q^2)\Big|_{\text{large-}N_c\&N_f} \sim \left(\frac{1}{x}\right)^{\alpha_h^q} \cos\left[\omega_q \ln\frac{1}{x} + \varphi_q\right]$$

with

$$\omega_q \approx \frac{0.22 N_f}{1 + 0.1265 N_f} \sqrt{\frac{\alpha_s N_c}{2\pi}}$$

Transversity

Quark Transversity

- We want to calculate quark transversity TMD at small x:

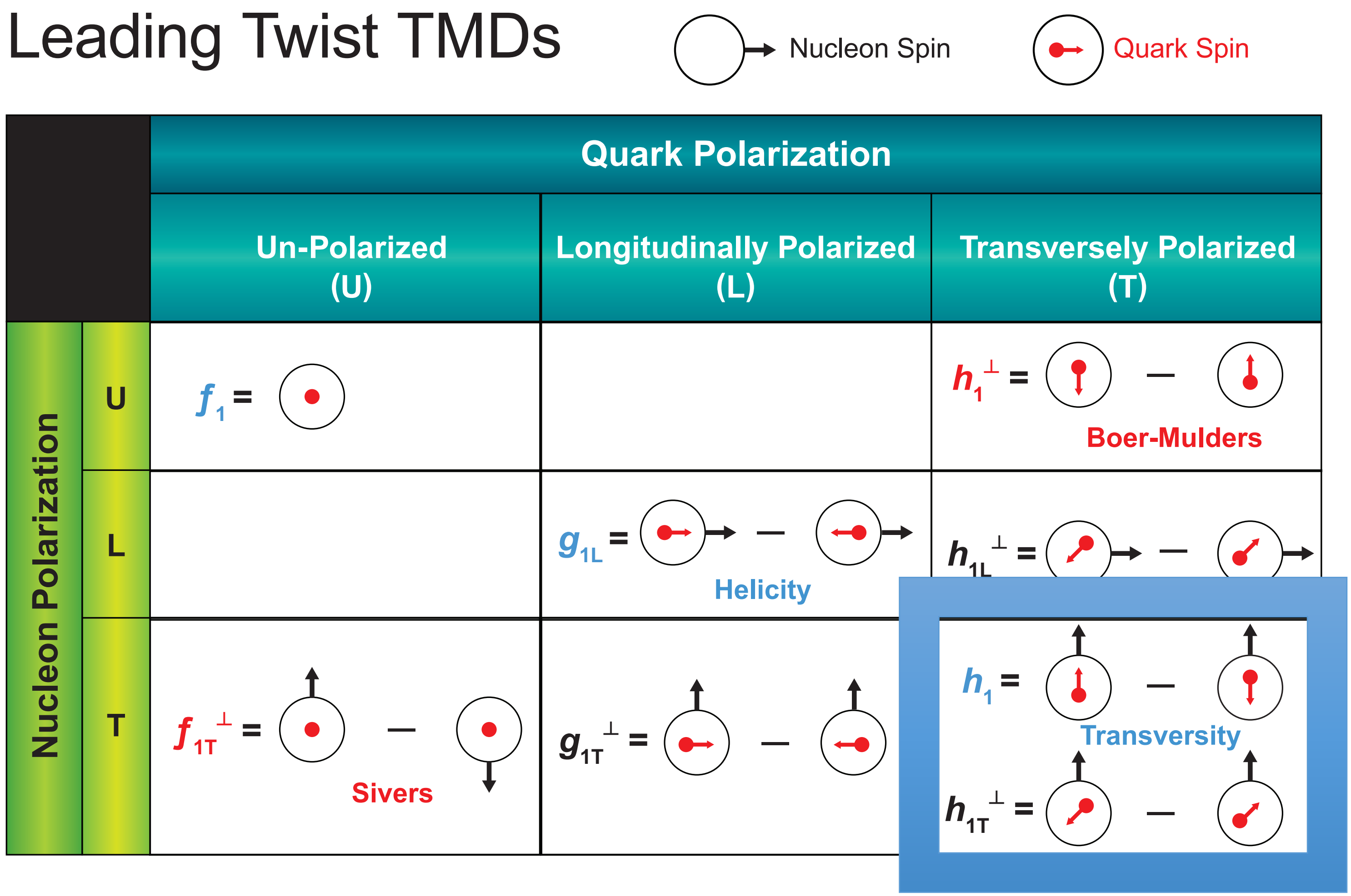

Small-x Asymptotics of Quark Transversity

- The small-x asymptotics of quark transversity is (cf. Kirschner et al, 1996)

$$h_{1T}^{q}(x, k_T^2) \sim h_{1T}^{\perp\, q}(x, k_T^2) \sim \left(\frac{1}{x}\right)^{\alpha_t^q} \quad \text{with} \quad \alpha_t^q = -1 + 2\sqrt{\frac{\alpha_s\, C_F}{\pi}}$$

- Note the suppression by x^2 compared to the unpolarized quark TMDs.
- For $\alpha_s = 0.3$ we get

$$h_{1T}^{q}(x, k_T^2) \sim h_{1T}^{\perp\, q}(x, k_T^2) \sim x^{0.286}$$

- This certainly satisfies the Soffer bound, but is not likely to produce much tensor charge from small x.

$$\delta q(Q^2) = \int_0^1 dx\, h_1(x, Q^2)$$

Conclusions

- In recent decades we have seen a lot of progress in our understanding of QCD in high energy collisions/ at small *x*.
- Multiple rescattering have been summed up at small-x (GGM/MV).
- Non-linear small-x evolution equations have been derived, unitarizing the BFKL evolution, while predicting and quantifying gluon saturation. They led to a lot of successful phenomenology at HERA, RHIC, and LHC, providing possible evidence for gluon saturation (not discussed here).
- Application of the small-*x* / saturation formalism to TMDs has been under development in recent years: while there are many new results, some TMDs at small *x* are yet to be explored. Stay tuned for further developments!

Backup Slides

Black Disk Limit

- Start with basic scattering theory: the final and initial states are related by the S-matrix operator,

$$|\psi_f\rangle = \hat{S}\,|\psi_i\rangle$$

- Write it as
$$|\psi_f\rangle = |\psi_i\rangle + \left[\hat{S} - 1\right]\,|\psi_i\rangle$$

- The total cross section is

$$\sigma_{tot} \propto \left|\left[\hat{S} - 1\right]\,|\psi_i\rangle\right|^2 = 2 - S - S^*$$

where the forward matrix element of the S-matrix operator is

$$S = \langle\psi_i|\,\hat{S}\,|\psi_i\rangle$$

and we have used unitarity of the S-matrix

$$\hat{S}\,\hat{S}^\dagger = 1$$

Black Disk Limit

- Now, since $|\psi_f\rangle = |\psi_i\rangle + \left[\hat{S} - 1\right] |\psi_i\rangle$

  the elastic cross section is

$$\sigma_{el} \propto \left| \langle \psi_i | \left[\hat{S} - 1\right] |\psi_i\rangle \right|^2 = |1 - S|^2$$

- The inelastic cross section can be found via

$$\sigma_{tot} = \sigma_{inel} + \sigma_{el}$$

- In the end, for scattering with impact parameter b we write

$$\sigma_{tot} = 2 \int d^2 b \, [1 - \mathrm{Re}\, S(b)]$$

$$\sigma_{el} = \int d^2 b \, |1 - S(b)|^2$$

$$\sigma_{inel} = \int d^2 b \left[1 - |S(b)|^2\right]$$

Unitarity Limit

- Unitarity implies that

$$1 = \langle\psi_i|\,\hat{S}\,\hat{S}^\dagger\,|\psi_i\rangle = \sum_X \langle\psi_i|\,\hat{S}|X\rangle\,\langle X|\hat{S}^\dagger\,|\psi_i\rangle \geq |S|^2$$

- Therefore

$$|S| \leq 1$$

leading to the unitarity bound on the total cross section

$$\sigma_{tot} = 2\int d^2b\;[1 - \mathrm{Re}\,S(b)] \leq 4\int d^2b = 4\pi R^2$$

- Notice that when S=-1 the inelastic cross section is zero and

$$\sigma_{tot} = 2\int d^2b\,[1 - \mathrm{Re}\,S(b)]$$

$$\sigma_{tot} = 4\pi R^2 = \sigma_{el}$$

$$\sigma_{el} = \int d^2b\,|1 - S(b)|^2$$

This limit is realized in low-energy scattering!

$$\sigma_{inel} = \int d^2b\left[1 - |S(b)|^2\right]$$

Black Disk Limit

- At high energy inelastic processes dominate over elastic. Imposing

$$\sigma_{inel} \geq \sigma_{el}$$

we get

$$\mathrm{Re}\, S \geq 0$$

- The bound on the total cross section is (aka the **black disk limit**)

$$\sigma_{tot} = 2\int d^2b\,[1 - \mathrm{Re}\, S] \leq 2\int d^2b = 2\pi R^2$$

- The inelastic and elastic cross sections at the black disk limit are

$$\sigma_{inel} = \sigma_{el} = \pi R^2$$

$$\sigma_{tot} = 2\int d^2b\,[1 - \mathrm{Re}\, S(b)]$$

$$\sigma_{el} = \int d^2b\,|1 - S(b)|^2$$

$$\sigma_{inel} = \int d^2b\left[1 - |S(b)|^2\right]$$

Notation

- At high energies $$\mathrm{Im}\, S \approx 0$$

  while the dipole amplitude N is the imaginary part of the T-matrix (S=1+iT), such that $$\mathrm{Re}\, S = 1 - N$$

- The cross sections are

$$\sigma_{tot} = 2 \int d^2b\, N(x_\perp, b_\perp)$$

$$\sigma_{el} = \int d^2b\, N^2(x_\perp, b_\perp)$$

$$\sigma_{inel} = \int d^2b \left[2\, N(x_\perp, b_\perp) - N^2(x_\perp, b_\perp) \right]$$

- We see that N=1 is the black disk limit. Hence $N \leq 1$ as we saw above.